5-2011

A NOVEL FUNCTION FOR AURORA B KINASE IN THE REGULATION OF P53 BY PHOSPHORYLATION

chris p. gully

A NOVEL FUNCTION FOR AURORA B KINASE IN THE REGULATION OF P53 BY PHOSPHORYLATION

by

Christopher Patrick Gully, B.S., M.S.

APPROVED:

_____
Mong-Hong Lee, Ph.D.
Supervisory Professor

_____
Min Gyu Lee, Ph.D.

_____
Randy J. Legerski, Ph.D.

_____
Hui-Kuan Lin, Ph.D.

_____
Sai-Ching Yeung, M.D., Ph.D.

APPROVED:

_____
George M. Stancel, Ph.D.
Dean, The University of Texas
Graduate School of Biomedical Sciences at Houston

A NOVEL FUNCTION FOR AURORA B KINASE IN THE REGULATION OF P53 BY PHOSPHORYLATION

A

DISSERTATION

Presented to the Faculty of

The University of Texas

Health Science Center at Houston

and

The University of Texas

M. D. Anderson Cancer Center

Graduate School of Biomedical Sciences

in Partial Fulfillment

of the Requirements

for the Degree of

DOCTOR OF PHILOSOPHY

by

Christopher Patrick Gully, B.S., M.S.
Houston, Texas

May 2011

Dedication

To my wife and best friend Shirl,

for all her patience and support.

I couldn't have done this without you.

Acknowledgements

It is my sincerest wish to convey my utmost gratitude to the many people who have aided me throughout my Ph.D. studies. Without their encouragement, support and advice, the completion of this dissertation would not have been possible.

I would like to thank in particular, my mentor, Dr. Mong-Hong Lee for his guidance, wisdom, expertise and kindness over the course of my career in graduate school. He has been a model of integrity and honesty and brought to me a great enthusiasm for success in furthering scientific advances. He is also a kindred spirit in his respect for all life and the pursuit of the highest ethical standards to which we must all aspire in scientific research. His devotion has given me the knowledge and desire to succeed and I hope I can repay this debt by being a committed scientist who makes meaningful contributions to our field. I would also especially like to thank Dr. Sai-Ching "Jim' Yeung for our many productive, thoughtful discussions and his guidance on my academic path. Dr. Yeung's work ethic and ability to incorporate clinical vision in our work serves as an inspiration for many of us in our lab. My interaction with him has been at all times fruitful and informative. I appreciate all he has done for me and our group at MD Anderson. Many thanks also go to my other committee members Dr. Hui-Kuan Lin, Dr. Randy Legerski, Dr. Min Gyu Lee, Dr. Dos Sarbassov, Dr. Pierre McCrae and Dr. Lalitha Nagajaran for their time and effort in giving me thoughtful

critiques, thought provoking discussion and a rigorous candidacy exam. My gratitude also goes to Dr. Ralph Arlinghaus for allowing me to rotate in his lab.

I truly appreciate all my colleagues including Guermarie Velazquez-Torres for her dedication to our lab and all of her efforts in making it a place where we can all work efficiently and effectively, Dr. Jian Chen for his guidance, training and unwavering willingness to serve as a sounding board for scientific ideas and Dr. Enrique Fuentes-Mattei for his expertise and calm under-pressure confidence through stressful times. I would also like to thank many other colleagues for their support and expertise over the course of my project: Edward Wang, Colin Carlock, Ji-Hyun Shin, James Yeung, Daniel Rothenberg, Hyun-Ho Choi, Chun-Hui Su, Sergei Guma, Hank Adams, Dr. Jerry Teng, Fanmao Zhang and Ben Chou.

For all of the material support I have received during my time at MD Anderson, I would like to thank the people who provided reagents, plasmids, antibodies or direct training, Elsa Flores, Randy Legerski, Jill Schumacher, Wendy Schober, Gordon Mills, Subrata Sen, Hiroshi Katayama, Zenbo Han, Bert Vogelstein, Cheng-Ming Chian, Hui-Kuan Lin, Zeev Ronai, Gigi Lozano, Jeffrey Wahl, Edward Yeh and Jiangdong Chen.

My most humble and sincere appreciation also goes to the forty laboratory mice who gave their lives in the interest of human health. It is my hope that their sacrifice will serve to further the field of cancer research and I will do my best to ensure that the data collected will be used to its fullest potential to do so.

Last, I would like to thank my my wife Shirl for her support, patience and caring over the past four years. She has served as my inspiration and greatest advocate. She shared my successes and setbacks along the way and without her, the completion of my Ph.D. would not have been possible.

Abstract

The mitotic kinase Aurora B plays a pivotal role in mitosis and cytokinesis and governs the spindle assembly checkpoint which ensures correct chromosome segregation and normal progression through mitosis. Aurora B is overexpressed in breast and other cancers and may be an important molecular target for chemotherapy. Tumor suppressor p53 is the guardian of the genome and an important negative regulator of the cell cycle. Previously, it was unknown whether Aurora B and p53 had mutual regulation during the cell cycle. A small molecule specific inhibitor of Aurora B, AZD1152, gave us an indication that Aurora B negatively impacted p53 during interphase and mitosis. Here, we show the antineoplastic activity of AZD1152 in six human breast cancer cell lines, three of which overexpress HER2. AZD1152 specifically inhibited Aurora B kinase activity, thereby causing mitotic catastrophe, polyploidy and apoptosis, which in turn led to apoptotic death. Further, AZD1152 administration efficiently suppressed tumor growth in orthotopic and metastatic breast cancer cell xenograft models. Notably, it was found that the protein level of Aurora B kinase declined after inhibition of Aurora B kinase activity. Investigation of the underlying mechanism suggested that AZD1152 accelerated the protein turnover of Aurora B by enhancing its ubiquitination.

As a consequence of inhibition of Aurora B, p53 levels were increased in tissue culture and murine models. This hinted at a possible direct interaction between p53 and Aurora B. Indeed, it was found that p53 and Aurora B exist in complex and interact directly during interphase and at the centromere in mitosis.

Further, Aurora B was shown to phosphorylate p53 at several serine/threonine residues in the DNA binding domain and these events caused downregulation of p53 levels via ubiquitination mediated by Mdm2. Importantly, phosphorylation of threonine 211 was shown to reduce p53's transcriptional activity while other phosphorylation sites did not. On a functional level, Aurora B was shown to reduce p53's capacity to mediate apoptosis in response to the DNA damaging agent, cisplatin. These results define a novel mechanism for p53 inactivation by Aurora B and imply that oncogenic hyperactivation or overexpression of Aurora B may compromise p53's tumor suppressor function.

TABLE OF CONTENTS

DEDICATION III

ACKNOWLEDGEMENTS IV

ABSTRACT VII

TABLE OF CONTENTS IX

LIST OF FIGURES XIII

LIST OF TABLES XVII

LIST OF ABBREVIATIONS XVIII

CHAPTER 1. INTRODUCTION 1

1.1 The Aurora Kinase Family 1

1.2 Aurora B Kinase Activation and the Chromosome Passenger Complex 6

1.3 Function of Aurora B Kinase 9

1.4 Aurora B Kinase and its Role in Cancer 13

1.5 Tumor Suppressor p53- "Guardian of the Genome" 16

1.6 p53 Transcriptional Activity 20

1.7 Phosphorylation of p53 22

1.8 Specific Aurora B Kinase Inhibitor AZD1152 25

1.9 Aurora Kinases and p53 28

1.10 Rationale and Hypothesis 29

CHAPTER 2. MATERIALS AND METHODS 30

2.1 Tissue Culture 31

2.2 Drugs, Reagents, Antibodies 31

2.3 Proliferation and IC_{50} Determination 36

2.4 Colony Forming Assays 36

2.4.1 Adherent Culture. 36

2.4.2 Suspension Culture 37

2.5 Immunofluorescence 37

2.6 Immunoblotting and Immunoprecipitation 38

2.7 Fluorescence Sorting 39

2.7.1 Cell Cycle analysis 39

2.7.2 Measurement of Apoptotic Cells 40

2.8 Cell Cycle Synchronization 40

2.8.1 Double Thymidine Block 40

2.8.2 Thymidine-Nocodazole block 41

2.9 Dual Luciferase Reporter Assays 41

2.10 Nude Mouse Xenograft Assays 42

2.10.1 Orthotopic Xenograft Model 42

2.10.2 Metastatic Xenograft Model 43

2.11 Construction of Mutants 43

2.12 *In Vitro* Kinase/Binding Assays 47

2.13 Ubiquitination Assays 48

2.14 Quantitative Real Time PCR 48

2.15 Venus Fusion Interaction Assays 50

2.16 Statistical Analyses 50

CHAPTER 3. RESULTS 51

3.1 Inhibition of Aurora B kinase Causes Antineoplastic Effects in Breast Cancer. 51

3.1.1 AZD1152 inhibits breast cancer growth regardless of Her2 status.....51

3.1.2 AZD1152-HQPA induces mitotic defects, G2/M arrest and polyploidy in breast cancer cells. 52

3.1.3 AZD1152-HQPA induces apoptosis and reduces tumorigenic phenotype in breast cancer cells. 63

3.1.4 AZD1152 inhibits growth of breast cancer xenografts in vivo. 71

3.1.5 AZD1152 inhibits metastases in breast cancer. 80

3.1.6 Poly-ubiquitination and degradation of Aurora B via the proteasome are increased by AZD1152-HQPA 86

3.1.7 Inhibition of Aurora B with AZD1152 in human xenografts, increases p53 level. 94

3.2 Aurora B downregulates p53 via phosphorylation in the DNA binding domain. 96

3.2.1 Aurora B and p53 interact directly. 96

3.2.2 Aurora B and p53 interact during interphase and mitosis.....97

3.2.3 Aurora B phosphorylates p53.....118

3.2.4 Aurora B phosphorylates multiple serine/threonine residues in the DNA binding domain of p53. 123

3.2.5 Aurora B destabilizes p53 via the ubiquitination-proteasome system. .131

3.2.6 p53 transcriptional activity and oligomerization are decreased by Aurora B. 142

3.2.7 Phosphorylation of threonine 211 in p53's DNA binding domain reduces transcriptional activity and increases turnover. 148

3.2.8 Inhibition of Aurora B stabilizes p53 and increases p53 target genes in tumors and tissue culture.....154

3.2.9 Aurora B reduces p53 mediated apoptosis. 158

CHAPTER 4. DISCUSSION 161

APPENDIX A 177

APPENDIX B 178

APPENDIX C 179

APPENDIX D 180

APPENDIX E 181

CHAPTER 6. REFERENCES 182

CHAPTER 7. VITA 219

List of Figures

		Page
1	Aurora kinase family schematic representation	5
2	Overview of kinetochore-microtubule orientation types	12
3	Domains of the p53 protein	19
4	AZD1152 and AZD1152-HQPA	27
5	AZD1152 inhibits breast cancer cell growth in Her2 negative cell lines	54
6	AZD1152 inhibits breast cancer cell growth in Her2 overexpressing cell lines	56
7	AZD1152 cell growth inhibition in Her18 by direct cell count	58
8	AZD1152-HQPA induces mitotic defects in Her18 breast cancer cells	59
9	Polyploidy is induced by AZD1152-HQPA treatment	61
10	Apoptosis is induced by AZD1152-HQPA in Her18 cells	65
11	Apoptosis is induced by AZD1152-HQPA in MB-MDA-231 cells	66
12	AZD1152-HQPA induces PARP cleavage in Her18 and MB-MDA-231 cells	67
13	Colony formation is reduced by AZD1152-HQPA	68
14	Anchorage-independent colony formation is inhibited by AZD1152-HQPA	70
15	AZD1152 inhibits Aurora B activity *in vivo*	73

16	Her18 tumor mass is inhibited by AZD1152 *in vivo*	75
17	AZD1152 inhibits Aurora B activity *in vivo*	77
18	Immunohistochemical analysis of Her18 xenografts	78
19	Lung weight and metastases are reduced by AZD1152 in a breast cancer model	82
20	Lung lobe photographs from MB-MDA-231 metastatic xenograft model	84
21	Immunohistochemical staining of lung tissue from MB-MDA-231 xenografts	85
22	AZD1152 reduces Aurora B protein level in steady state	89
23	AZD1152 increases the turnover rate of Aurora B kinase	90
24	Aurora B degradation via the ubiquitin-proteasome pathway is increased by AZD1152	91
25	AZD1152 mediated degradation of Aurora B is through the Anaphase Promoting Complex (APC).	93
26	P53 is induced in Her18 xenografts by AZD1152	95
27	Aurora B and p53 exist in complex	100
28	Aurora B and p53 interact directly	101
29	Aurora B binds both the DNA binding domain and the C-terminus of p53	103
30	Hct116 cells synchronized with double-thymidine block	105
31	Aurora B and p53 interact during late S and G2/M phases of the cell cycle	106

32	Endogenous p53 and Aurora B colocalize during mitosis	107
33	Schematic diagram of the Venus-fusion protein system	109
34A,B,C	Aurora B and p53 interact directly in interphase and mitosis	110
35	p53 and Aurora B interaction localizes to the DNA during mitosis	114
36	Venus system interaction also occurs in Hct116 cells	116
37	Controls for Venus fusion system showing Aurora B and p53 direct colocalization	117
38	Aurora B phosphorylates p53 *in vitro*	119
39	Aurora B, but not kinase dead Aurora B, phosphorylates p53	121
40	Aurora B phosphorylation of p53 is inhibited by AZD1152-HQPA	122
41	p53 deletion constructs	125
42	Aurora B phosphorylates p53 in the DNA binding domain	126
43	Putative Aurora B phosphorylation sites in the p53 DNA binding domain	128
44	Putative Aurora B phosphorylation sites in p53 and their NetPhos scores	129
45	Aurora B phosphorylates four serine/threonine residues in the p53 DNA binding domain	130
46	Aurora B reduces p53 steady state level	134
47	Aurora B increases the turnover rate of p53	135
48	Aurora B mediates turnover of p53 via the proteasome	137

49	Mdm2 ubiquitination of p53 is increased by Aurora B	138
50	Aurora B affects p53 at the post-translational level	140
51	Overexpression of Aurora B decreases p53 transcriptional activity	144
52	Knockdown of Aurora B increases p53 transcriptional activity	145
53	P53 oligomerization is decreased by Aurora B phosphorylation	147
54	Aurora B reduces p53 transcriptional activity by phosphorylating threonine 211 in p53's DNA binding domain	150
55	Phosphorylation site mutants are stabilized in the presence of Aurora B	151
56	p21 mRNA is not efficiently reduced by Aurora B in the presence of the p53 AAA mutant	152
57	AZD1152 increases p53 level in Her18 xenografts	155
58	p53 and p53 targets are induced *in vivo* by AZD1152	156
59	AZD1152-HQPA stabilizes p53 and induces p53 targets *in vitro*	157
60	Aurora B reduces p53 mediated apoptosis	159
61	Aurora B reduces p53 mediated apoptosis- representative samples	160
62	Model of regulation of Aurora B kinase by AZD1152	164
63	Model of regulation of p53 by Aurora B kinase	165

List of Tables

		Page
Table 1	Aurora B Substrates	8
Table 2	Types of Cancer with Aurora B overexpression	15
Table 3	p53 phosphorylation sites	24
Table 4	Antibody List	33
Table 5	Plasmid List	45
Table 6	rtPCR Primer List	49

List of Abbreviations

ABL1	Abelson murine leukemia viral oncogene homolog 1
ALL	Acute lymphocytic leukemia
AML	Acute myelogenous leukemia
AMPK	AMP-activated protein kinase
Apaf-1	Apoptosis activating factor 1
APC	Anaphase promoting complex
ATCC	American type culture collection
ATM	Ataxia telangiectasia mutated
ATR	Ataxia telangiectasia mutated and rad3-related
AZD1152-HQPA	AZD1152 (2-(3-((7-(3-(ethyl(2-hydroxyethyl) amino) propoxy) quinazolin-4-yl) amino)-1H-pyrazol-5-yl)-N-(3- fluorophenyl) acetamide)
Bcl-2	B cell lymphoma 2
BSA	Bovine serum albumin
CBP	Creb binding protein
Cdc20	Cell division cycle 20
CDC25B	Cell division cycle homolog B
CDDP	Cisplatin
CDK1	Cyclin dependent kinase 1
CENP-A	Centromere protein A
Chk1/2	Checkpoint kinase 1/2

CI	Protease cocktail inhibitor
CK1	Casein kinase 1
CML	Chronic myeloid leukemia
COP1	Constitutive Photomorphogenic 1
CPC	Chromosome passenger complex
DAPI	4,6-diamidno-2-phenylindole
DMSO	Dimethyl sulfoxide
DNA	Deoxyribonucleic acid
DNA-PK	DNA activated protein kinase
GFP	Green fluorescent protein
GPX1	Glutathione peroxidase 1
GSK3B	Glycogen synthase kinase 3 Beta
GTP	Guanosine triphosphate
HA	Hemaglutinin
HR	Homologous recombination
IC_{50}	Inhibitory concentration 50%
INCENP	Inner centromere protein
Jnk1	c-Jun n-terminal protein kinase 1
Mad1/2	Mitotic spindle assembly checkpoint 1/2
Mdm2	Murine double minute 2
miRNA	Micro ribonucleic acid
MMR	Mismatch repair
mRNA	Messenger ribonucleic acid

MTOR	Mammalian target of rapamycin
MTT	3-(4,5-Dimethylthiazol-2-Yl)-2,5-Diphenyltetrazolium Bromide
NaF	Sodium fluoride
NaV	Sodium orthovanadate
NER	Nucleotide excision repair
NSCLC	Non small cell lung cancer
P53RE	P53 response element
PAGE	Polyacrylamide gel electrophoresis
PARP	Poly ADP ribose polymerase
PBS	Phosphate buffered saline
PCNA	Proliferating cell nuclear antigen
PCR	Polymerase chain reaction
p-HH3	Phospho Histone H3
PI	Propidium iodide
PirH2	P53 induced RING-H2
PP1/2	Protein phosphatase 1/2
Pten	Phosphatase and tensin homolog
Ras	Rat Sarcoma
ROS	Reactive oxygen species
rtPCR	Real time PCR
SAC	Spindle assembly checkpoint
SCO2	Synthesis cytochrome oxidase 2
SDS	Sodium dodecyl sulfate

shRNA	Short hairpin RNA
siRNA	Short interfering RNA
SOD2	Superoxide dismutase 2
SV40	Simian virus 40
TAD	Transactivating domain
TIGAR	TP50 induced glycolysis and apoptosis regulator
TLK1	Tousled-like kinase 1
UV	Ultra violet
XPC	Xeroderma Pigmentosa group C

Chapter 1. Introduction

1.1 The Aurora Kinase Family

The Aurora family of mitotic kinases are a group of evolutionarily conserved serine/threonine kinases (Vas and Clarke, 2008) which share approximately 70% homology in their kinase domains (Katayama et al., 2003; Tao et al., 2008; Yang et al., 2007) (Figure 1). The Auroras are so named because of the discovery of Aurora A in *Drosophila*, a mutation of which caused aberrations at the spindle poles mimicking a likeness of the aurora borealis (Glover et al., 1995). The Auroras are essential in cell cycle control and are crucial regulators from mitotic entry to cytokinesis ensuring that daughter cells receive the correct number of chromosomes (Carmena et al., 2009; Ducat and Zheng, 2004; Fu et al., 2007; Kaitna et al., 2002; Katayama et al., 2003; Lens and Medema, 2003; Petersen and Hagan, 2003; Satinover et al., 2006; Vagnarelli and Earnshaw, 2004). Mammals have three Aurora family members, A, B and C, while *Drosophila*, *Xenopus* and *C. elegans* have two. The budding yeast, *S. cerevisiea*, has only one Aurora, Ipl1P (Sugiyama et al., 2002; Vas and Clarke, 2008). Aurora kinases in humans range from 309 to 403 amino acids with Aurora B at the medium length of 343. Each of the kinases contain an N-terminal regulatory domain, a catalytic domain and a variable C-terminal domain. The genes encoding the Auroras reside on 20q13.2, 17p13.1 and 10q13 for A, B and C respectively (Bernard et al., 1998; Bischoff et al., 1998; Kimura et al., 1998).

Although the Aurora kinases are expressed at maximum levels during mitosis, the two main players, Aurora A and Aurora B, have distinct subcellular localizations and serve differing functions during mitosis. All Aurora kinases have been observed to be overexpressed or amplified in human cancer (Fu et al., 2007; Keen and Taylor, 2004; Nadler et al., 2008) and contribute to tumorigenesis via their link to invasive disease and their ability to cause genomic instability (Bischoff et al., 1998; Carmena and Earnshaw, 2003; Ducat and Zheng, 2004). Auroras A and B have also been found to be overexpressed in many cancer cell lines (Katayama et al., 1999; Sasai et al., 2004; Tatsuka et al., 1998; Zhou et al., 1998) and their inhibition has shown tumor regression in xenografted tumors (Harrington et al., 2004).

Aurora A kinase resides primarily at the centrosomes and at the spindle pole ends during mitosis and has functions in centrosome maturation, mitotic entry and bipolarity of spindles (Adams et al., 2001; Carmena and Earnshaw, 2003; Nigg, 2001). The function of Aurora A depends upon its ability to bind microtubules and its localization at the spindle poles where it phosphorylates and activates CDC25B at serine 353, which leads to activation of Cyclin B/CDK1 (Cazales et al., 2005; Dutertre et al., 2004). Another well known substrate of Aurora A is TPX2 which is a strong binding partner and activator of Aurora A (Eyers and Maller, 2004). Aurora A also plays a role in the activation of PLK1 which further contributes to Cyclin B/CDK1 activation (Macurek et al., 2008; Seki et al., 2008).

Auroras A and B are very similar to each other in their kinase domains and their regulation is largely governed by localization and activation by binding partners. Further, Auroras A and B share some substrates (Histone H3, INCENP and Survivin (Fu et al., 2009; Hans et al., 2009)), which could become important were these kinases to be overexpressed or mislocalized. Also, a point mutant of Aurora A (G198N) displays localization similar to Aurora B, can partially restore loss of Aurora B function and is known to exist in complex with other Chromosome Passenger Complex (CPC) members (Fu et al., 2009; Hans et al., 2009). Nevertheless, Auroras A and B have distinct mitotic functions.

Human Aurora B is also known as Aurora-1, AIRK2, ARK2, Aik2, STK-12 while mouse Aurora B is known as STK-1 and rat as AIM-1 (Sugiyama et al., 2002). Aurora B is the enzymatically active member of the CPC (Carmena et al., 2009) which resides at the inner centromere during early mitosis and relocates to the spindle midzone during anaphase and telophase (Ruchaud et al., 2007; Vader and Lens, 2008). The CPC is composed of Aurora B and its substrates, INCENP, Survivin and Borealin (Carmena et al., 2009). Aurora B's main functions are to govern the correct attachment of spindle fibers during chromosome alignment as well as govern the spindle assembly checkpoint (SAC).

The third member of the Aurora kinase family in humans is Aurora C. Very little is known about Aurora C except that it is very similar to Aurora B in percent identity and function and is known to be a member of the CPC involved

in assembly of meiotic spindles during spermatogenesis (Carmena and Earnshaw, 2003; Carmena et al., 2009).

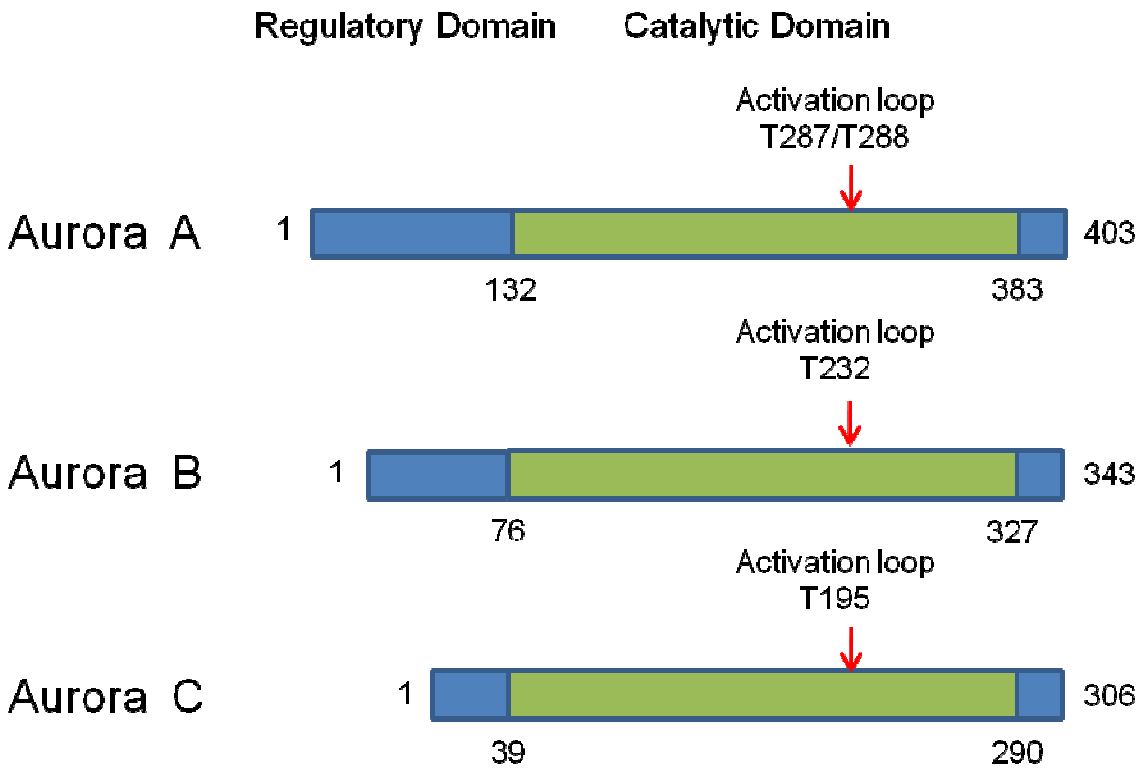

Figure 1. Schematic representation of the domains of the three members of the human Aurora kinase family.

1.2 Aurora B Kinase Activation and the Chromosome Passenger Complex

In addition to Aurora B's function as the major kinase that governs the turnover of kinetochore-microtubule interactions and manages the spindle assembly checkpoint, it also functions in chromatid cohesion, spindle stability and cytokinesis (Ruchaud et al., 2007) and is therefore a multifunctional player during mitotic progression.

Localization and activation of Aurora B requires the other CPC members as binding partners and substrates (Adams et al., 2000; Gassmann et al., 2004; Terada et al., 1998; Uren et al., 2000; Wheatley et al., 2001). (See Table 1 for a complete list of Aurora B substrates.) A 1:1:1 complex can be formed by the binding of the N-terminus of both INCENP and Borealin to the C-terminus of Survivin. This complex is stable and is able to localize to the inner centromere where Aurora B binds via the IN-Box of INCENP (Adams et al., 2000). The binding of Aurora B to INCENP increases the basal kinase activity which allows Aurora B to both autophosphorylate its T-loop and phosphorylate INCENP at a TSS motif near the C-terminus (Bishop and Schumacher, 2002; Carmena et al., 2009; Sessa et al., 2005). The phosphorylation of INCENP by Aurora B has been shown to be necessary for full Aurora B activation (Kelly et al., 2007).

In addition to Aurora B's kinase activity being necessary for its activation, several other mitotic kinases are known to aid in Aurora B's activation. Tousled-like kinase (TLK-1) was found to be a substrate activator of Aurora B (Han et al., 2005) as well as Chk1 which phosphorylates Aurora B and increases its activity

(Zachos et al., 2007). Further, Mps1, yet another mitotic kinase that is required for a proper spindle assembly checkpoint, controls spindle fiber-kinetochore attachments by phosphorylating Borealin, which in-turn increases the activation of Aurora B (Jelluma et al., 2008). And lastly, an integral part of the spindle assembly checkpoint itself, kinase BubR1 resides at the kinetochore and acts as a negative feedback regulator of Aurora B (Ditchfield et al., 2003; Hauf et al., 2003; Lampson and Kapoor, 2005; Morrow et al., 2005).

In the opposite way that many mitotic kinases act to activate Aurora B, there are phosphatases that act as negative regulators. Protein Phosphatase 1 (PP1) and PP2A both bind and inhibit Aurora B by dephosphorylation (Sugiyama et al., 2002; Sun et al., 2008). During anaphase, plus-end microtubule binding protein EB1 blocks Aurora B's T-loop from dephosphorylation by PP2A (Sun et al., 2008). It is through a delicate balance of phosphorylation and dephosphorylation of Aurora B or its substrates, that the activation of Aurora B is managed.

Another mechanism for the regulation of Aurora B comes from its degradation by the E3 ligase, Anaphase Promoting Complex (APC) together with its substrate recognition subunits Cdh1 and Cdc20. At the onset of anaphase APC facilitates the ubiquitination of Aurora B which requires the A-Box and KEN box found in the first 65 amino acids (Nguyen et al., 2005). Aurora B is then rapidly degraded via the ubiquitin-proteasome pathway.

Table 1. List of Aurora B Substrates

Substrate	Amino Acid	Reference
Histone H3	S10, S28	(Crosio et al., 2002; Goto et al., 2002)
CENP-A	S7	(Zeitlin et al., 2001b)
GFAP	T7, S13, S38	(Kawajiri et al., 2003)
Desmin	S59	(Kawajiri et al., 2003)
INCENP	T893, S894, S895	(Bishop and Schumacher, 2002)
MgcRacGAP	S387, S410	(Minoshima et al., 2003)
REC-8	T625, S626	(Rogers et al., 2002)
Vimentin	S72	(Goto et al., 2003)
Survivin	T117	(Wheatley et al., 2004)
MCAK	S161, T162, S177, S196, T229, S253	(Lan et al., 2004)
Hec1/Ndc80	Multiple N-term	(DeLuca et al., 2006)
Topoisomerase II		(Morrison et al., 2002)
Tousled-like kinase	S634	(Han et al., 2005)

1.3 Function of Aurora B Kinase

As discussed previously, Aurora B and the CPC have multiple roles to play in mitosis and these can be separated into roughly two categories, a role at the centromere during early mitosis (prophase-metaphase) and a role at the midbody during late mitosis and cytokinesis (anaphase-telophase). Upon mitotic entry, Aurora B and the CPC are localized at the chromosome arms and are mainly apparent at the centromere (Beardmore et al., 2004). After metaphase and with the onset of anaphase, Aurora B and the CPC relocate to the midbody/spindle midzone.

During early mitosis, Aurora B as well as the CPC recruit many effector proteins to the kinetochore and the inner centromere. Kinetochore proteins recruited by the CPC include Bub1, BubR1, Mad1, Mad2, Mps1 and Cenp-E (Ditchfield et al., 2003; Lens et al., 2003; Vigneron et al., 2004). Kinetochore-microtubule interaction proteins include Cenp-E, Ndc80, Kn11, Mis12, Zwilch MCAK, PLK1 and Dam1 (Andersson et al., 1989; Emanuele et al., 2008; Goto et al., 2006; Lan et al., 2004; Ohi et al., 2004; Pouwels et al., 2007). Inner centromere proteins recruited include MCAK, Sgo1 and Sgo2 (Goto et al., 2006; Kawashima et al., 2007; Pouwels et al., 2007). It has been shown that if the CPC does not function properly, syntelic and merotelic attachments (Cimini et al., 2006; Ditchfield et al., 2003; Hauf et al., 2003) will result most likely due to improper attachments failing to be resolved (Figure 2) (Lampson et al., 2004; Tanaka et al., 2002). Phosphorylation of some of these proteins is thought to destabilize incorrect attachments and facilitate correct reattachment. Likewise,

both Aurora B and the CPC are found to be more abundant at incorrect attachments (Knowlton et al., 2006). Some reports have also concluded that Aurora B phosphorylation occurs less during metaphase than prophase suggesting that at metaphase, some correct attachments already exist and do not need to be released (Andrews et al., 2004; Lan et al., 2004; Zeitlin et al., 2001a).

Although the actual function of Aurora B and the CPC with regard to how they regulate correct spindle fiber attachments is unknown, one promising model suggests that via phosphorylation, Aurora B continually destabilizes microtubule-kinetochore interaction until a correct attachment results in tension pulling across both kinetochores, which in-turn pulls Aurora B's substrates away from its local zone of influence (Tanaka et al., 2002). This would lead to stabilized attachments and satisfaction of the spindle assembly checkpoint. Other studies confirmed this by noting the levels of phosphorylated MCAK in correct versus incorrect attachment scenarios and found that MCAK has reduced phosphorylation when attachments were incorrect and no tension was present (Andrews et al., 2004; Lan et al., 2004). Another study further confirmed this by tethering Aurora B to the inner centromere and found that when tethered, Aurora B could not fully disrupt interactions. Conversely, when Aurora B was linked to the kinetochore, it could disrupt attachments and stable biorientation could not occur (Liu et al., 2009). In addition to MCAK as an effector substrate of Aurora B, Hec1/Ndc80, an important component of the microtubule binding KMN

network, is known to be phosphorylated by Aurora B thereby decreasing the affinity of Hec1 for microtubules (Cheeseman et al., 2006; DeLuca et al., 2006).

The spindle assembly checkpoint (SAC) is a mechanism that prevents the completion of mitosis (anaphase onset) until all chromosomes have biorientation and tension across their kinetochores. The yeast Aurora kinase Ip11 has been shown to be required for SAC function when no tension is present (Biggins and Murray, 2001; Pinsky et al., 2006). Also, as seen in vertebrates, by inhibition of Aurora B with small molecule inhibitors, it was shown that Aurora B is necessary for a proper SAC in response to taxol, a microtubule stabilizing agent (Kallio et al., 2002).

As mentioned previously, after the onset of anaphase, Aurora B and the CPC change localization to the midbody and carry out an entirely different function in cytokinesis. This change of localization was found to be essential for late mitotic events to progress (Carmena and Earnshaw, 2003; Ruchaud et al., 2007; Vader and Lens, 2008; Vagnarelli and Earnshaw, 2004). Indeed the position of the cleavage furrow is determined by a RhoA microtubule dependent zone induced by Aurora B phosphorylation of the central spindlin complex proteins MKLP1/ZENK and the GTPase activating protein 1 (MgcRacGAP) (Bement et al., 2005; Minoshima et al., 2003; Mishima et al., 2002; Wadsworth, 2005).

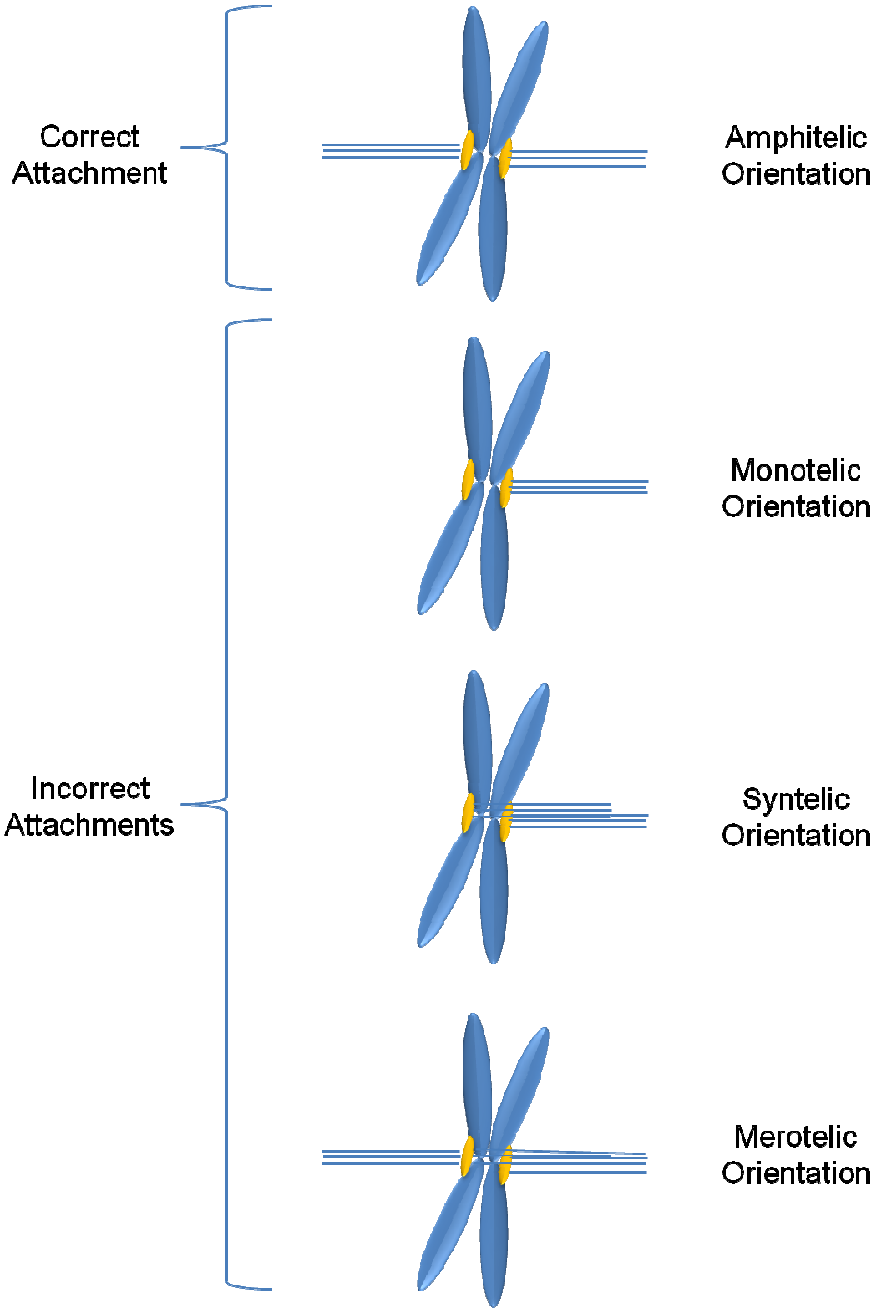

Figure 2. Overview of Kinetochore-Microtubule Orientation Types. From Top, Amphitelic, correct attachment, microtubules connected to corresponding kinetochores from each pole. Monotelic, microtubules from only one pole connected to corresponding kinetochore. Syntelic, microtubules from one pole connected to both kinetochores. Merotelic, microtubules from both poles connected to one kinetochore.

1.4 Aurora B Kinase and its Role in Cancer

Although it has been well established that Aurora A is overexpressed in many cancer types and is considered to be a high value target for new and developing chemotherapy agents, Aurora B is not quite so well known as an oncogene and the evidence for such a claim is still not conclusive. Despite this, there are many reports that show that Aurora B is overexpressed in many cancer types (Table 2) such as colorectal cancer (Katayama et al., 1999), oral cancers (Qi et al., 2007), breast cancer (Tchatchou et al., 2007) and hepatocellular carcinoma (Lin et al.).

It makes sense, however, that Aurora B could function as a classical oncogene given its diverse roles in governing mitosis and handling of proper genome fidelity such as spindle checkpoint function, cytokinesis and chromosome segregation. Without Aurora B or with perturbation of Aurora B levels, genomic fidelity could be altered in a way so as to create aneuploidy and genomic instability.

One report found that when resected tumors from human patients were analyzed by Western blotting, Northern blotting and *in situ* hybridization, Aurora B overexpression or amplification correlated with colon cancer progression (Katayama et al., 1999). Further, in colorectal cancer cell lines, increased levels of Aurora B correlated to increased phosphorylation of Histone H3 and aneuploidy (Ota et al., 2002). Aurora B levels were also found to be increased along with anaplasia in thyroid carcinoma (Sorrentino et al., 2005).

Aurora B has been shown to be effective in transformation phenotypes. Murine embryo fibroblasts, in which Aurora B was overexpressed, were not only shown to be transformed but significantly, they were able to form invasive tumors in mice. Also, Aurora B overexpression was shown to enhance the tumorigenic phenotype of Ras-V12 transformed cells (Kanda et al., 2005).

Clearly, Aurora B has been shown to contribute to tumorigenesis and progression in several cancer and cell types, including, breast cancer. Aurora B overexpression was not found to correlate to survival in human cases in contrast to Aurora A (Nadler et al., 2008). Therefore, although there is some evidence that Aurora B's function as a classical oncogene seems apparent, this could be possibly due to the closely related natures of Aurora A and B function, and possibly due to direct overlap of some substrates.

Table 2. Cancer Types Overexpressing Aurora B Kinase

Cancer Type	Reference
Colon cancer	(Katayama et al., 1999)
Thyroid cancer	(Sorrentino et al., 2005)
Oral cancer	(Qi et al., 2007)
NSCLC	(Smith et al., 2005)
Breast cancer	(Tchatchou et al., 2007)
Seminoma	(Chieffi et al., 2004)
Glioma	(Araki et al., 2004)
Hepatoma	(Lin et al.)

1.5 Tumor Suppressor p53- "Guardian of the Genome"

p53 is perhaps the most important gene in relation to cancer since it is mutated or lost in 50% of all cancer types (Soussi and Wiman, 2007). p53 has been described as the "Guardian of the Genome" (Lane, 1992) and is a key transcription factor governing the integrity of the genome through multiple pathways. p53 was first described as a protein that was bound to the large T antigen of the SV40 virus (DeLeo et al., 1979; Kress et al., 1979; Lane and Crawford, 1979; Linzer and Levine, 1979; Melero et al., 1979) and was first thought to be an oncogene since it was found to be present in large amounts in tumor cells. Later, p53 was found to be mutated in these cells and was actually a tumor suppressor (Baker et al., 1989). Not only can mutated p53 contribute to the formation of cancer, but this can also happen through the disruption of many of the regulatory pathways that govern the activation of p53 (Oren, 2003).

The p53 protein is organized into four domains, the Transactivating domain (TAD), the DNA binding domain, the Oligomerization domain and the Basic domain (Figure 3). The Transactivating domain is broken up into three parts: AD1, AD2 and the proline-rich region. AD1 and AD2 are on the N-terminal end and are where many of the myriad posttranslational modifications of p53 occur as well as the binding of p53's major negative regulator Mdm2 and the two acetyltransferases, p300 and CBP (Espinosa and Emerson, 2001; Gu et al., 1997; Stommel and Wahl, 2004). The proline rich region of the TAD contains five copies of a PXXP motif, the function of which has not been well characterized but which has been implicated in mediation of apoptosis and

growth repression (Baptiste et al., 2002; Sakamuro et al., 1997; Walker and Levine, 1996; Zhu et al., 1999). The DNA binding domain spans amino acids 102-292 and functions to bind to p53 response elements in DNA. Amino acids 323-356 make up the oligomerization domain, responsible for dimerization and which also contains a nuclear export sequence (Nicholls et al., 2002). Last, the Basic domain at the C-terminal end contains two nuclear localization sequences (Shaulsky et al., 1990; Weinberg et al., 2004).

p53 is a member of the p53 gene family which includes the related genes p63 and p73 (Kaghad et al., 1997; Yang et al., 2002). p63 and p73 both have significant homology to p53 and can indeed function in the same way to activate transcription of some of the same gene targets as p53. Knockdown mouse models of each member of the p53 gene family produced distinct phenotypes, indicating that while they can overlap in their target genes, they serve functionally distinct purposes (Murray-Zmijewski et al., 2006). Just as p63 and p73 are known to have many isoforms (p63=6, p73=35), p53 also has alternate splice variants and more than one internal promoter which results in various isoforms. Intron 9 and Intron 2 can be spliced alternate ways and intron 2 contains an alternate promoter which leads to the expression of 9 isoforms of p53 (Bourdon et al., 2005).

p53 is activated in response to many types of stress and mediates the cellular responses of cell cycle arrest, apoptosis and senescence thereby preventing a genomically unstable cell from proliferating. p53's ability to mediate

these responses is through its ability to bind DNA and regulate the transcription of many target genes. p53 tetramerizes and binds p53 response elements (p53REs) in DNA sequences (Bourdon et al., 1997; el-Deiry et al., 1992; Funk et al., 1992). Major gene targets of p53 include: p21, GADD45, Bax, Puma, Noxa 14-3-3σ and Mdm2 (Vousden and Prives, 2009). p53 also has functions independent of its transcriptional activity, one of which is its ability to translocate to the mitochondria and promote apoptosis (Mihara et al., 2003).

Activation of p53 is mediated through several different types of cellular stress including UV exposure (Maltzman and Czyzyk, 1984), DNA double strand breaks due to ionizing radiation (Kastan et al., 1991) and replication stress induced by oncogene expression (Bartkova et al., 2005; Gorgoulis et al., 2005). In the latter example, oncogenes cause DNA replication errors inducing stalled replication forks which trigger the DNA damage response in which kinases ATM and Chk2 cause accumulation of p53. The N-teminus of p53 contains many residues that are modified by acetylation, sumoylation, methylation, ubiquitination and in the case of ATM and Chk2, phosphorylation (Harris and Levine, 2005). These posttranslational modifications generally prevent the binding of p53 to Mdm2 leading to p53 accumulation and activation (Lavin and Gueven, 2006). In this way p53 forms a blockade against nascent tumor cells by mediating their death through apoptosis and senescence.

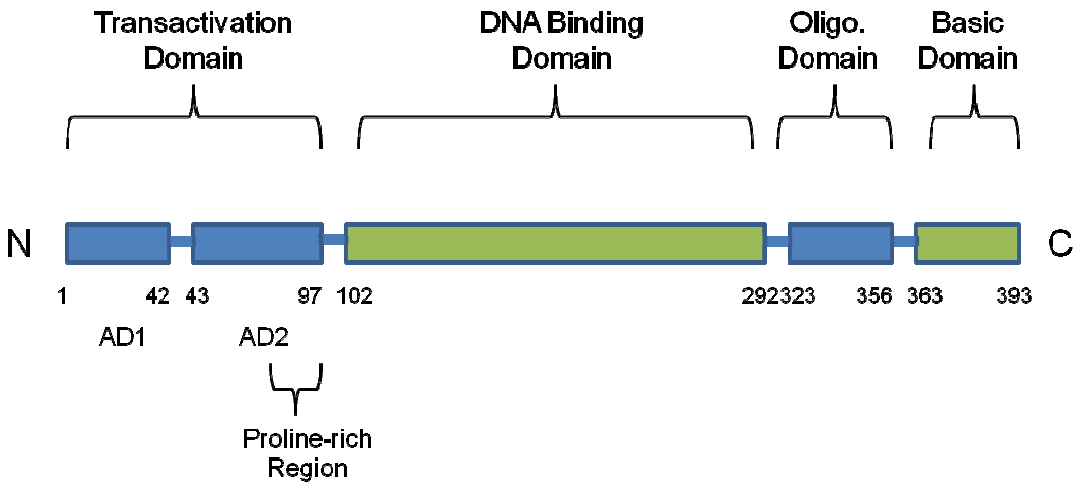

Figure 3. Protein domains of the tumor suppressor p53

1.6 p53 Transcriptional Activity

p53 regulates its transcriptional activities by first sensing cellular stresses from sensor proteins in various cellular processes. Several examples of this are DNA dependent protein kinase (DNA-PK), which senses DNA strand breaks, ATM, which senses ionizing radiation induced DNA damage, REDD-1, which monitors ROS levels, AMPK, which detects nutrient deprivation and ATR, which responds to UV induced DNA damage (Levine et al., 2006). Signaling from these sensors triggers post-translational modification of p53, which results in changes in p53 target gene expression. Generally, transcriptional activity is regulated by direct binding of p53 to the promoter or first intron of the target genes (Horvath et al., 2007; Wei et al., 2006), although gain of function and p53 transcriptional repression are also be investigated actively.

p53 effector genes fall into several distinct functional categories, cell cycle, DNA repair, reactive oxygen species (ROS), apoptosis, miRNA, autophagy, metabolism and autoregulation. These broad functional categories underscore the number of genes p53 can affect. So far, there are 60 genes with validated p53REs and no doubt many more to be discovered (Horvath et al., 2007). Global mapping of the human genome for p53REs revealed 582 REs and identified 98 previously unknown effector genes (Wei et al., 2006).

p53's function in DNA damage repair is one of the most studied and important of its many capacities. Effector genes with p53REs have been found to effect homologous recombination (HR), mismatch repair (MMR) and

nucleotide excision repair (NER). For example, in nucleotide excision repair, p53 upregulates Xeroderma Pigmentosa group C (XPC) and DDB2 (Adimoolam and Ford, 2002; Hwang et al., 1999; Tan and Chu, 2002; Tang et al., 2000). These genes encode proteins that recognize DNA damage and induce NER.

In its caretaker of the genome role, p53 upregulates two genes that are involved in ROS scavenging to prevent oxidative damage to proteins, DNA and lipids. Glutathione Peroxidase 1 (GPX1) and Superoxide Dismutase 2 (SOD2) both act as effectors in this case scavenging reactive oxygen species (Horvath et al., 2007; Hussain et al., 2004; Tan et al., 1999).

Should DNA damage be too great to overcome, p53 can mediate programmed cell death by upregulating genes like Bax, Puma and Noxa. Bax codes for a proapoptotic Bcl-2 family gene that stimulates release of cytochrome C from the mitochondria (Oltvai et al., 1993). Puma and Noxa are also p53 target genes as well as Bcl-2 family members and help to mediate cell death through the Cytochrome C/APAF-1 pathway (Nakano and Vousden, 2001; Oda et al., 2000). p53 increases Puma expression through two REs in its promoter (Wang et al., 2007; Yu et al., 2003).

Another central function of p53 transcriptional control is arrest of the cell cycle. This occurs mainly via regulation of cyclin dependent kinases or PCNA by p21, resulting in G1/S arrest (Gibbs et al., 1997). p21 is a major target of p53 and contains six p53 REs in its promoter (Chen et al., 1995; Chin et al., 1997; Hollander et al., 1993; Horvath et al., 2007; Wei et al., 2006). Similarly, G2/M

arrest is controlled by p53 via GADD45 which has a p53 RE in its third intron (Chen et al., 1995; Chin et al., 1997; Hollander et al., 1993). GADD45 exerts control of the cell cycle by modulating the activity of Cyclin B1.

Autophagy has recently been described as an area of p53 transcriptional control. p53 has been found to increase autophagy by controlling PTEN expression which downregulates the mTOR pathway, a major negative autophagic regulator (Feng et al., 2005). p53 has also recently been implicated in metabolism and energy production as a regulator of Synthesis of Cytochrome C Oxidase (SCO2) (Matoba et al., 2006).

A further regulation of metabolism by p53 is the discovery of TIGAR as a p53 target. TIGAR lowers levels of fructose 2,6-bisphosphate, a substrate of 6-phospho-1-kinase which is a promoter of glycolysis (Bensaad et al., 2006).

To maintain the balance of p53 in the cell, p53 also effects its own regulation in an autoregulatory feedback loop with several E3 ubiquitin ligases. Targets of p53 regulation that can facilitate p53 ubiquitination include Mdm2, Pirh2 and Cop1(Millau et al., 2009).

1.7 Phosphorylation of p53

Phosphorylation of p53 is generally thought to increase accumulation of p53 and increase p53 transcriptional activity, (Bode and Dong, 2004; Hupp and Lane, 1994) and so far more than 20 phosphorylation sites have been found (Table 3). Many of these events occur in the N-terminal TAD domain of p53,

while some occur in the C-terminal Basic domain (Bode and Dong, 2004; Gatti et al., 2000). There is some overlap in that some kinases share phosphorylation sites and distinct kinases can phosphorylate more than one residue of p53. This redundancy is not surprising considering the importance of p53 as a tumor suppressor. The complicated picture of p53 phosphorylation can be explained by the sheer number of genes p53 activates or represses. For many of these genes, a simple on/off switch won't do and this complex array of phosphorylation sites may help to explain this. For example, a different and unique number of phosphorylation events could be used to activate a certain subset of genes in response to a certain cellular stress. Another model could be that a certain combination of phosphorylations could recruit other p53 post translational modifications to coordinate p53 binding to genes. A third way to think about it is that all these phosphorylation sites could just be a failsafe mechanisim since loss of regulatory control by p53 could be catastrophic (Meek and Anderson, 2009).

While most phosphorylation events that modify p53 result in activation of p53 transcriptional activity, this is somewhat dependent on the domain being modified. There is at least one kinase known to phosphorylate p53 in the DNA binding domain thus interfering with p53's ability to bind response elements.

Table 3. p53 Phosphorylation Sites

Kinase	Site(s)	Domain	Reference
ABL1			(Agami et al., 1999; Gonfloni et al., 2009; Gong et al., 1999; Yuan et al., 1999)
ATM	S15	TAD	(Huang et al., 2008)
CDK2	S315	NLS	(Gaiddon et al., 2003; Huang et al., 2008)
Chk1/2	S20	TAD	(Gonzalez et al., 2003)
Gsk3β	S315	NLS	(Patturajan et al., 2002)
HIPK2	S46	TAD	(Kim et al., 2002)
JNK1	S20, T81	TAD	(Jones et al., 2007)
P38	S33, S46, S392	TAD, Basic	(Koida et al., 2008; Mantovani et al., 2007; Papoutsaki et al., 2005)
PLK1			(Koida et al., 2008)
Aurora A	S215, S315	DBD, NLS	(Katayama et al., 2004; Liu et al., 2004)
CK1	S6, S9, T18	TAD	(Dumaz et al., 1999; Sakaguchi et al., 2000)

1.8 Specific Aurora B Kinase Inhibitor AZD1152

Since the discovery of the Aurora kinases in the 1990s, they have been considered excellent potential targets of cancer therapy due to both their central role in mitosis and their overexpression in a variety of tumor types (Kitzen et al.). Many Aurora kinase inhibitors have been developed in recent years, with a few becoming candidates for clinical trials. One such inhibitor is the Aurora B inhibitor, AZD1152. AZD1152 is a specific Aurora B kinase inhibitor developed by Astra Zeneca (Mortlock et al., 2007). It is specific for Aurora B kinase at a K_i=0.36 nM versus Aurora A kinase, K_i=1369 nM (Wilkinson et al., 2007). AZD1152 is an acetanilide-substituted pyrazole-aminoquinazoline prodrug that is converted quickly to the active drug AZD-1152 hydroxy-QPA (AZD1152-HQPA) in human plasma (Mortlock et al., 2007; Wilkinson et al., 2007)(Figure 4). Consistent with inhibition of Aurora B, AZD1152 causes improper cytokinesis, polyploidy, cell cycle arrest, apoptosis, chromosome mis-segregation and chromosome misalignment.

AZD1152 has been evaluated in several preclinical studies in the last few years and has been shown effective in a variety of tumor types including colorectal, hepatocellular carcinoma, lung, multiple myeloma and several hematologic malignancies. Human colorectal SW620 cells showed dose dependent inhibition of p-HH3 at serine 10 when treated with AZD1152. Impressively, in SW620 nude mouse xenografts, one dose of AZD1152 at 150 mg/kg/day reduced mean tumor volume by 80% (Wilkinson et al., 2007). AZD1152 was also shown effective in lung and hematologic cancers. Doses of

10-150 mg/kg/day were able to reduce tumor growth in A549, HL-60 and Calu-6 xenografts (Cheung et al., 2009). Consistently, AZD1152 was shown effective in inhibiting the cell growth of AML, ALL, biphenotypic leukemia, acute eosinophilic leukemia, blast stage CML (Yang et al., 2007) and multiple myeloma (Evans et al., 2008) cell lines. Further, radiosensitivity was shown to be increased with AZD1152 treatment in Hct116 cell xenografts (Tao et al., 2008). AZD1152 is currently being investigated in patients with advanced solid malignancies and is in use in a phase I clinical trial for relapsed AML (Boss et al.).

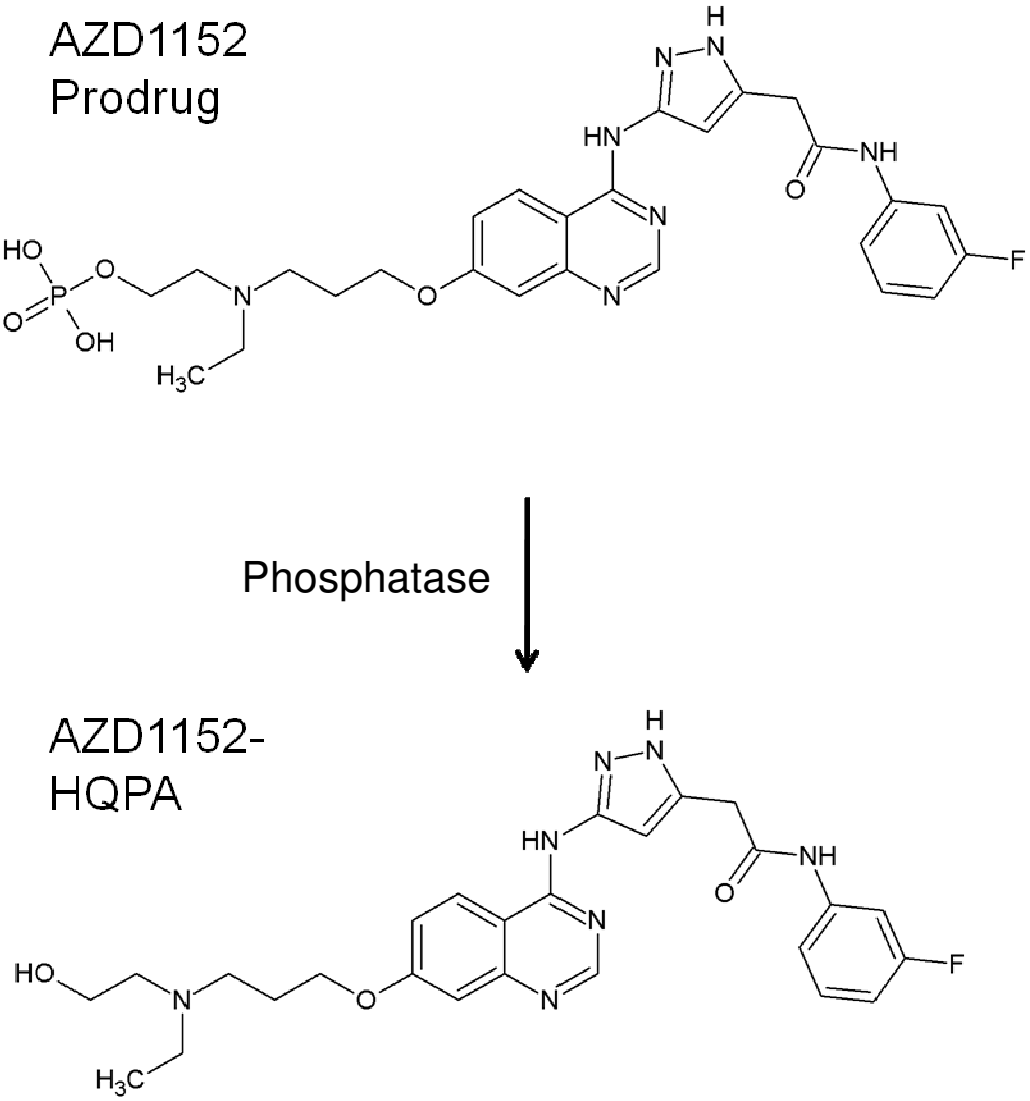

Figure 4. Specific Aurora B kinase inhibitor AZD1152 (2-(3-((7-(3-(ethyl(2-hydroxyethyl)amino)propoxy)quinazolin-4-yl)amino)-1H-pyrazol-5-yl)-N-(3-fluorophenyl)acetamide) prodrug is converted to the active metabolized form AZD1152-HQPA.

1.9 Aurora Kinases and p53

Since p53 is not known to have a function in mitosis, and the Aurora kinases are generally thought to have mitotic-specific functions, there have been few studies that have evaluated the interaction or potential phosphorylation of p53 by Auroras. However, Aurora A kinase has been linked to p53 phosphorylation by at least two separate studies. The first, in 2003, described the phosphorylation of p53 by Aurora A at serine 315 which resulted in decreased p53 level and transcriptional activity due to subsequent p53 destabilization and degradation mediated by Mdm2 (Katayama et al., 2004). In contrast, a previous study found that this phosphorylation site increased p53 activity and was linked to DNA damage induced by UV radiation. The authors also described the phosphorylation being inhibited by the cdk inhibitor Roscovitine (Blaydes et al., 2001). A subsequent study of Aurora A phosphorylation of p53 found an additional site at serine 215 and indicated that this site, and not serine 315, was important for p53 stability and transcriptional activity (Liu et al., 2004). Consistent with the findings that p53 is phosphorylated by Aurora A, it was found that p53 also localizes to the centrosome in an ATM dependent manner (Tritarelli et al., 2004).

Although several studies have linked Aurora A to phosphorylation of p53, the picture remains cloudy due to conflicting reports of which sites are important and whether they activate or suppress p53 function. Additionally, to date no study has found p53 phosphorylation by either Aurora B or Aurora C.

1.10 Rationale and Hypothesis

It is known that Auroras A and B are both overexpressed in breast cancer (Fu et al., 2007; Keen and Taylor, 2004) and several studies have evaluated the importance of the Auroras in breast cancer. Consistently, Aurora A overexpression was shown to induce breast tumor formation in mouse epithelium (Wang et al., 2006). Further, it was found that polymorphisms in the Aurora A gene were closely tied to increased risk of breast cancer (Cox et al., 2006; Fletcher et al., 2006) and that this increased risk was more dangerous in women with prolonged exposure to estrogen (Dai et al., 2004). Two small studies found Aurora A overexpression in 94% of invasive ductal carcinoma (Tanaka et al., 1999) and 64% of breast cancer cases by mRNA analysis (Miyoshi et al., 2001).

Less data is available for Aurora B's importance in breast cancer although Aurora B was shown to be induced by estrogens resulting in cellular proliferation in preclinical models (Ruiz-Cortes et al., 2005) and a specific polymorphism of the Aurora B gene (885A>G) has been shown to increase the risk for breast cancer in these individuals (Tchatchou et al., 2007). Given the known overexpression of Aurora kinases in breast cancer and that Aurora A kinase phosphorylates p53 resulting in decreased p53 activity, it stands to reason that inhibition of Aurora B with a specific kinase inhibitor could produce anti-tumorigenic effects in breast cancer by inhibiting possible phosphorylation of p53 by Aurora B.

Hypothesis: Inhibition of Aurora B kinase reduces tumorigenesis in breast cancer by increasing p53 protein level and transcriptional activity.

Chapter 2. Materials and Methods

2.1 Tissue Culture

HER18 cells, which are Her2 stable transfectants of MCF7 breast cancer cells, are described previously (Laronga et al., 2000). They were cultured in DME/F12 (Sigma, St. Louis, MO) supplemented with either 5% or 10% fetal bovine serum (Gemini, West Sacramento, CA). MDA-MB-468, MDA-MB-435, MDA-MB-361, BT-474 and MDA-MB-468 were obtained from the ATCC (Manassas, VA, USA). MDA-MB-231, MDA-MB-435 and MDA-MB-468 cells were maintained in Leibovitz's L15 media (Cellgro, Manassas, VA) with 10% fetal bovine serum. BT-474, MDA-MB-361, 293T, H1299, MCF7 and Hela cells were also obtained from the ATCC and were maintained in DME/F12 media (In house supplier) supplemented with 5% or 10% (v/v) fetal bovine serum. U2OS (ATCC), Hct116 p53 +/+ and Hct116 p53 -/- (a kind gift from Dr. Bert Vogelstein) (Bunz et al., 1998) were cultured in McCoy's 5A media (Hyclone), supplemented with 5% or 10% fetal bovine serum. All cells were incubated with 5% CO_2 and maintained in a humidified 37 ^{o}C incubator with 2 mM L-glutamine (Cellgro, Manassas, VA) and 1% antibiotic-antimycotic solution (Invitrogen, Grand Island, NY).

2.2 Drugs, Reagents, Antibodies

AZD1152 (prodrug) and AZD1152-HQPA (metabolized form) were a kind gift from Dr. Kirsten Mundt (Astra Zeneca, Macclesfield, Cheshire, UK). AZD1152-HQPA (metabolite) was prepared in 100% DMSO at 10 mM concentration, and used as indicated. AZD1152 (prodrug) was prepared in 0.3 M Tris (pH 9.0) (Fisher, Pittsburgh, PA) and 0.2% DMSO (Fisher). AZD1152

solution was made fresh at a maximum of 20 mg/ml for each cycle of injections into nude mice. *De novo* protein synthesis inhibitor, cycloheximide and proteasome inhibitor MG132 were obtained from Sigma (St. Louis, MO) and used at 100 µg/ml and 5 µg/ml respectively. MG341 (Velcade, Bortezomib) was purchased from Millenium Laboratories (San Diego, CA) and used at 70 ng/ml overnight. Cisplatin was purchased from Bedford Laboratories (Bedford, OH) and used as indicated.

Table 4. Antibody List

Antigen	Method	Source	Manufacturer	Cat/Clone
14-3-3σ	IB	Mouse	RDI	1433S01
Actin	IB	Rabbit	Sigma	A2066
Annexin V-FITC	FACS	Mouse	BD Biosciences	556419
Aurora B	WB, IF	Rabbit	Abcam	Ab2254
Bad	IB	Mouse	BD Biosciences	B36420
Bax	IB	Mouse	BD Transduction labs	B73520
Caspase 3	IHC	Rabbit	Cell Signaling	9661
Cyclin A	IB	Rabbit	Santa Cruz	SC751
Cyclin B1	IB	Mouse	Santa Cruz	SC245
Cyclin D	IB	Mouse	Neomarkers	MS-2110
Cyclin E	IB	Mouse	Santa Cruz	SC-247
Flag	IB, IP	Mouse	Sigma	A804-200
GFP	IB, IP	Mouse	Santa Cruz	SC-9996
HA	IB,IP	Mouse	Roche	12CA5
His	IB	Rabbit	Santa Cruz	SC-803
HH3 (p-S10)	IB	Rabbit	Upstate	05-817

Ki-67	IHC	Rabbit	Abcam	Ab66155
Mdm2	IB	Rabbit	Santa Cruz	S3813
Mouse IgG non-immune	IP, IF	Mouse	Sigma	I5381
Mouse IgG (HRP conj.)	IB	Goat	Pierce	32430
Mouse IgG (Alexa 488)	IF	Goat	Molecular Probes	A11029
Mouse IgG (Alexa 568)	IF	Goat	Molecular Probes	A11031
P53	IHC,WB,IP	Rabbit	Santa Cruz	SC-6243
P53	IF	Mouse	BD Biosciences	610183
P53 (p-S315)	IB	Rabbit	Cell Signaling	2528S
PARP	IB	Mouse	BD Biosciences	516639GR
P21	IB	Mouse	Transduction Labs	610233
PUMA	IB	Rabbit	Santa Cruz	SC-28226
Rabbit IgG (Alexa 488)	IF	Goat	Molecular Probes	A1103
Rabbit IgG (Alexa 568)	IF	Goat	Molecular Probes	A11011

Rabbit IgG non-immune	IP, IF	Rabbit	Sigma	R5756
Rabbit IgG (HRP conj.)	IB	Goat	Pierce	32460
Survivin	IF	Rabbit	Cell Signaling	2808
Tubulin	IB	Mouse	Sigma	T5168

2.3 Proliferation and IC_{50} Determination

To determine amount of proliferation and $IC_{50,}$ an MTT (3-(4,5-dimethylthiazol-2-yl)-2,5-diphenyltetrazolium bromide) (Sigma) assay was utilized. Indicated cells were seeded at 5-20% confluence and allowed to attach for 24 hours. AZD1152-HQPA was applied following serial dilutions in appropriate complete media to the indicated concentrations. 96 well Plates were incubated for between 2 and 5 days. After incubation, 20 µl MTT was applied to each well and then incubated for 1 to 5 hours. After incubation, media was replaced with 200 µl 100% DMSO (Fisher). Plates were mixed on a rotary mixer at room temperature and 50 rpm then read using an MRX revolution plate spectrophotometer (Dynex, Technologies, Chantilly, VA) at 570 nm. Averages were plotted from 4 replicates and 50% inhibitory concentration (IC_{50}) was determined based on sigmoidal curve fitting (Sigma plot, Systat Inc.). The MTT method was validated using live counts of Her18 cells plated in a similar fashion in 3.5 cm^2 tissue culture plates. Cells received a similar treatment with AZD1152-HQPA and were counted using a Z1 Coulter particle counter (Beckman Coulter, Fullerton, CA). Average numbers of cells from triplicate plates were plotted against the concentration of AZD1152-HQPA.

2.4 Colony Forming Assays

2.4.1 Adherent Culture.

Adherent colony (foci) forming assays were performed in triplicate by plating indicated cell lines in 6 cm^2 tissue culture dishes. Cells were plated at approximately 5000 cells/plate in complete DME/F12 medium with either 40 nM

AZD1152-HQPA or vehicle (DMSO, Fisher). Plates were maintained in a 37 ℃ incubator for 12 days with 5% CO_2. Colonies (foci) were counted in three representative one cm^2 areas per plate and the number colonies per cm^2 recorded. Differences between the AZD1152-HQPA-treated cells and vehicle treated cells were compared using a Student's t-test.

2.4.2 Suspension Culture

Soft agar colony forming assays were performed in triplicate plates with a base agar of 1X DME/F12 complete medium with 0.5% low melt agar (Fisher) and either DMSO for the control or 80 nM AZD1152-HQPA. Base agar was added to 6 cm^2 Petri dishes and allowed to set. 5000 cells/plate added to 0.35% top agar with control medium or 80 nM AZD1152-HQPA was poured over the bottom agar. The plates were incubated at 37 ℃ with 5% CO_2 for 26 days. Colonies >100 cells were counted using a dissecting microscope, and results were analyzed using the Student's t-test.

2.5 Immunofluorescence

Indicated cell lines were grown in either chamber slides, tissue culture dishes or on cover glasses to 50-75% confluence. Cells were treated with vehicle, 20 nM AZD1152-HQPA or received no treatment for 48 hours. Cells were rinsed 2x with cold PBS (in house) and then fixed with 3% paraformaldehyde (Electron Microscopy Sciences, Hatfield, PA) solution for 15 minutes at room temperature. Cells were then rinsed 3x with cold PBS, 10 minutes each followed by permeabilization with 0.2% Triton X-100 (Sigma). Plates were blocked in either 5% BSA (Sigma) or 5% normal goat serum (a kind

gift from Dr. Elsa Flores) and diluted in PBS for one hour. Fixed and blocked cells were then stained with antibodies (See Table 4), primaries were diluted appropriately in PBS an applied for a period of one hour to overnight. Cells were stained with either DAPI and mounted on microscope slides using Fluoromount G (Southern Biotech, Birmingham, AL) or they were mounted in Prolong Gold (Invitrogen) which contained DAPI. Immunostained cells were visualized with an Olympus IX81 confocal microscope, an Olympus IX70 fluorescent microscope, a PerkinElmer Ultraview ERS spinning disk confocal microscope or a Nikon Ti with a Photometric CoolSnap HQ2 camera driven by Nikon Elements software. Deconvolved images were processed using AutoQuant X2 software from Media Cybernetics software.

2.6 Immunoblotting and Immunoprecipitation

Cells for Western blot or immunoprecipitation were scraped from tissue culture dishes after two rinses with cold PBS. Cells were then centrifuged at low speed for 10 minutes and supernatants discarded. Pellets were then either frozen at -80 ℃ for further processing later or they were lysed with 100-300 µl 1x lysis buffer (0.5 L batch: 7.5g 1 M tris [Fisher], 15 ml 5M NaCl [Fisher], 0.5 ml NP-40 [USB Corp.], 0.5 ml Triton X-100 [Sigma] and 1 ml 0.5M EDTA [Fisher]) for 20 minutes at 4℃. Lysis buffer also contained a cocktail of protease/phosphatase inhibitors: 5 mM NaV, 1 mM NaF, 1 µM DTT, 0.1 mg/ml Pepstatin A, 1 mM PMSF and 1000x Complete Cocktail Protease Inhibitor (Roche). Lysates were centrifuged at high speed for 10 minutes and cell debris discarded. Protein concentration was measured using the Bradford method with

protein assay reagent (Biorad) and read on Powerwave XS (Biotek) spectrophotometer at 595 nm. Protein samples were standardized and mixed with 5x loading dye (100 ml batch: 3.78 g Tris base, 5 g SDS, 25 g sucrose [Sigma] and 0.04 g bromophenyl blue [Sigma], pH adjusted to 6.8) and boiled 5 minutes prior to SDS-gel analysis. SDS-PAGE was performed according to standard procedures. All gels were 10% except: Mdm2 8%, p-HH3 15%, Bax 15%, oligomerization of p53 6% and p21 15%. Transfer of proteins was performed using 1x transfer buffer (1 L batch: 30.3 g tris base, 144 g glycine [Fisher] and 10 g SDS, pH adjusted to 8.3) to PVDF membrane (Millipore). For immunoprecipitations, cell lysates were prepared and standardized as before and 1 mg protein immunoprecipitated with appropriately diluted antibody in lysis buffer overnight. Antibody was then pulled down with 50 µl of either Protein A or G beads (Santa Cruz) for 1 hour. Beads were then centrifuged at low speed for 10 minutes and supernatant discarded. Beads were rinsed 3x in lysis buffer with inhibitors and dried with a 27 gauge needle. Dried beads were mixed with 2x loading dye (5x loading dye diluted 1:2.5) and boiled 5 minutes. Lysates were loaded into gels and SDS-PAGE performed as before.

2.7 Fluorescence Sorting

2.7.1 Cell Cycle Analysis

Cells to be analyzed were plated in 6 well tissue culture dishes and grown to log phase. Appropriate treatments by either transfection of plasmids or treatment with AZD1152-HQPA were performed and allowed to proceed for 24-48 hours. Monolayers were rinsed twice with PBS and cells scraped into

microcentrifuge tubes. Cells were centrifuged at low speed and rinsed once with PBS. Pellets were resuspended in 0.5 ml hypotonic PI solution (50 ml batch: 0.85 mg/ml sodium citrate (Sigma) 0.1 mg/ml RNase A (Qiagen, Valencia, CA), 0.1% Triton X-100, 20 mg/ml PI (Roche) and incubated in the dark for 30 minutes. Cell cycle/PI analysis was performed using a FACScalibur flow cytometer (Becton Dickinson, Franklin Lakes, NJ, USA).

2.7.2 Measurement of Apoptotic Cells

Cells to be analyzed for apoptosis were plated in 10 cm^2 or 6 well tissue culture dishes and allowed to attach for 24 hours. Treatments with AZD1152-HQPA or transfection were allowed to proceed 24-48 hours prior to harvest. At harvest, cells were washed with PBS and collected by scraping. Cells were centrifuged at low speed and washed twice with PBS and resuspended in 0.5 ml binding buffer (Axxora, San Diego, CA) containing 5 µl Annexin V-FITC (BD, San Jose, CA) for 15 minutes at room temperature. Cells were washed once more in PBS, and PI solution with RNAseA (500 mg/ml, Roche) was applied.

2.8 Cell Cycle Synchronization

2.8.1 Double-Thymidine Block

Hct116, Hela or 293T cells were plated in appropriate complete media and grown to 25-30% confluence. 2 mM thymidine (Sigma) was added to the media for 18 hours followed by release by washing 2x with warm PBS and fresh complete media refeed. Cells were allowed to grow 9 hours without block. After 9 hours, cells were again treated with 2 mM thymidine for 17 hours (second

block). After second block, cells were released as before. At this point approximately 90% of cells are synchronized to S phase.

2.8.2 Thymidine-Nocodazole block

Hct116, Hela or 293T cells were synchronized by plating to 40% confluence in normal complete media. 2mM thymidine was added for 24 hours followed by release by washing 2x with warm PBS and refeed with fresh complete media. Cells were released for 3 hours and 100 ng/ml nocodazole (Sigma) was added to the media for 12 hours. Cells were then released again using 2x PBS wash and refed with fresh complete media. At this point, approximately 75% of cells were synchronized to pro-meta phase.

2.9 Dual Luciferase Reporter Assays

Analysis of p53 transcriptional activity was performed by transfecting log phase cells planted in 12 well tissue culture dishes with either a p53 luciferase reporter plasmid containing the 3 copies of the p53 binding sites from the 14-3-3σ or Mdm2 promoters. Cells were also transfected with the Renilla luciferase reporter plasmid. Following transfection, cells were treated with either AZD1152-HQPA or vehicle and incubated for 24 hours. At harvest, cells were collected using 1x passive lysis buffer (Promega) and analyzed according to the manufacturer's protocol with the Dual Luciferase Reporter Assay kit (Promega).

2.10 Nude Mouse Xenograft Assays

2.10.1 Orthotopic Xenograft Model

Female athymic (6-8 weeks of age) nude mice (Experimental Radiation Oncology, MD Anderson Cancer Center) were maintained in AAALAC approved facilities with food and water ad libitum on a 12-hour light/dark cycle. Mice were housed and treated under an approved protocol in compliance with all animal care and use guidelines (AALAS) of our institution. Twenty four nude mice were injected in the mammary fat pad with 8.5 $x10^6$ Her18 human breast cancer cells (McKenzie et al., 2004; Warburton et al., 2004). Weekly subcutaneous estradiol cypionate (Pfizer, NY, NY) injections were administered at 3 mg/kg/week beginning 2 weeks before injections of Her18 cells (Jerome et al., 2006; Wang et al., 2004). Following tumor cell injection, mice were randomly divided into 3 groups. AZD1152 prodrug treatment began when tumors were greater than 50 mm^3. Mice in the control group received IP injections of vehicle (0.3 M Tris pH 9.0), mice in the low dose group received 62.5 mg/kg/day of AZD1152 and high dose mice received 125 mg/kg/day AZD1152. Drug or vehicle was administered on day 1 and 2 of a 7-day repeating cycle which lasted for 3 cycles. Tumor volume estimates were performed by measuring the tumors every 2 to 3 days with calipers and applying the formula: Length x $Width^2$ /2 (Osborne et al., 1985). After 24 days, mice were sacrificed and tumors excised. Some tumor samples were snap-frozen for protein extraction followed by Western blotting and others fixed in formalin and paraffin embedded for immunochemistry analysis. The ABC kit (Vector Labs) was used for IHC staining. Photomicrographs of IHC

sections were taken at 200x magnification using an Olympus IX70 microscope. Images were recorded and processed with Olympus DP controller imaging software (version. 3.2.1.276).

2.10.2 Metastatic Xenograft Model

Nude mice (6-8 weeks of age) were injected with 2 x10^6 MDA-MB-231 cells by tail vein. Prior to injection, cells were suspended in 200 µl complete media. Mice were then randomly separated into 2 groups (control and 125 mg/kg/day AZD1152 prodrug). Injections were performed on day 1 and 2 of a weekly cycle for 4 cycles beginning two days post tumor cell injection. Vehicle (0.3 M Tris pH 9.0) injections were given to control mice. 10 weeks after tumor cell injection, mice were sacrificed and the lungs excised followed by weighing and examination for tumor nodules. Lungs were fixed in formalin and analyzed by IHC staining as before.

2.11 Construction of Mutants

Aurora B and p53 mutants were constructed using a site directed mutagenesis technique. Forward and reverse primers (complementary) that were approximately 30 bases long were used in a PCR reaction with PFU Turbo polymerase (Stratagene) to amplify plasmids in their entirety. The primers were designed to change one or two bases to effect the change in the amino acid sequence. See Table 5 for plasmid list and primers used in this process. After amplification, plasmids were treated with restriction enzyme DpnI (New England

Biolabs) to digest any remaining template. Plasmids were then transformed into DH5α *E. coli* (in house) and selected with appropriate antibiotics.

Table 5. Plasmid List

Plasmid	Source or Primer Sequence
Flag-Aurora B	Subrata Sen
GFP-Aurora B	Subrata Sen
GFP-p53	Jeffrey Wahl (Stommel et al., 1999)
His-p53	Zeev Ronai
P53 (no tag)	Mong-Hong Lee
HA-Ubiquitin	Edward Yeh
GST-p53	Jiandong Chen
GST-p53 (1-160)	Jiandong Chen
GST-p53 (160-393)	Jiandong Chen
GST-p53 (320-393)	Jiandong Chen
Venus C-term	Gordon Mills (Ding et al., 2006)
Venus N-term	Gordon Mills (Ding et al., 2006)
Venus C-term-AurB	For 5' –GTAATAGGCGCGCCATGGCCCAGAAGGAGAA– 3' Rev 5' –CATTAAGAATTCTCAGGCGACAGATTGAA– 3'
Venus N-term-p53	For 5' –GATATTGGCGCGCCATGGAGGAGCCGCAGTC– 3' Rev 5' –CTATAAGAATTCTCAGTCTGAAGTCAGGCC– 3'
Flag-Aurora B K106R	For 5' – TCATCGTGGCGCTCAGGGTCCTCTTCAAGT – 3' Rev 5' – ACTTCAAGAGGACCCTGAGCGCCACGATGA – 3'
GST-p53 S183A GFP-p53 S183A	For 5' –CCATGAGCGCTGCGCAGATAGCGATGGTCT– 3' Rev 5' –AGACCATCGCTATCTGCGCAGCGCTCATGG– 3'

GST-p53 T211A GFP-p53 T211A	For 5' –CACACTATGTCGAAAAGCGTTTCTGTCATC– 3' Rev 5' –GATGACAGAAACGCTTTTCGACATAGTGTG– 3'
GST-p53 S215A GFP-p53 S215A	For 5' –TTCGACATGCTGTGGTGGTGCCCTATGAGC– 3' Rev 5' –GCTCATAGGGCACCACCACAGCATGTCGAA– 3'
GST-p53 S269A GFP-p53 S269A	For 5' –ACTGGGACGGAACGCCTTTGAGGTGCATGT– 3' Rev 5' –ACATGCACCTCAAAGGCGTTCCGTCCCAGT– 3'
GST-p53 T284A GFP-p53 T284A	For 5' –AGAGACCGGCGCGCAGAGGAAGAGAATCTC– 3' Rev 5' –GAGATTCTCTTCCTGTGCGCGCCGGTCTCT– 3'
Renilla-luciferase	Zeev Ronai
P53-luc. (14-3-3σ)	Bert Vogelstein
P53-luc. (Mdm2)	Gigi Lozano
GFP-p53 S183A, S215A	See primers above
GFP-p53 S183A, T211A, S215A	See primers above
shRNA AurB 468	Sigma Mission shRNA (NM_004217.x-468
shRNA AurB 1185	Sigma Mission shRNA (NM_004217.x-1185)
pCMV5	David Russell (Andersson et al., 1989)
His-Ubiquitin	Hui-Kuan Lin

2.12 *In Vitro* Kinase/Binding Assays

IP purified Aurora B (immunoprecipitation described previously) or recombinant Aurora B (Cell Signaling) were incubated in 1x kinase buffer (80 mM MOPS [Sigma], 7.5 mM MgCl [Fisher], pH 7.0) with GST-purified p53 substrates, cold ATP and γ^{32} ATP (Perkin Elmer) at 30 ℃ for 15 minutes. Kinase reactions were mixed with 5x loading dye and analyzed by SDS-PAGE as described before. SDS-PAGE gels were dried and imaged using a phosphoimager cassette (Molecular Dynamics) and a Typhoon Trio variable mode imager. Images were processed using Image Quant 5.1. p53 substrates were produced by growing BL-21 *E. Coli* (in house) containing the GST-p53 plasmid of interest in 250 ml LB for 1 hour followed by induction of expression with 1mM IPTG (Fisher). Cells were grown for 4 hours and harvested by centrifugation. Cells were lysed with NETN buffer (20 mM Tris–HCl pH 8.0, 150 mM NaCl, 1 mM EDTA, 1% (v/v) Nonidet P-40) plus inhibitor cocktail (see Section 2.6) and sonicated 5 minutes. Cell debris was removed by high speed centrifugation and 200 µl GST beads (GE Healthcare) added. Lysates were incubated with beads overnight at 4 ℃. The following day, beads were spun low speed and washed 3 times in NETN plus inhibitors followed by one wash in 1x kinase buffer. p53 substrates for in vitro binding assays were prepared as for kinase assays. Substrates were incubated with IP purified Flag-Aurora B overnight in 1 ml lysis buffer. GST- tagged substrates were pulled down using GST beads and immunoprecipitates analysed by SDS-PAGE followed by Western blotting with anti-flag antibody.

2.13 Ubiquitination Assays

Ubiquitination assays were performed as described in section 2.6 with the exceptions that MG132 was added to transfected cells 6 hours prior to harvest and upon lysis 0.1 µM NEM (N-ethylmaleimide) (Sigma) was added to lysis buffer as well as inhibitors described previously. Standard procedures for Western blotting were then applied.

2.14 Quantitative Real Time PCR

Total RNA was extracted from 293T, Her18 or Hct116 *p53 -/-* cells by TRIzol (Invitrogen) according to the manufacturer's instructions. Reverse transcription was performed according to the manufacturer's instructions using the iScript cDNA synthesis kit (Biorad). 1 µl per reaction of cDNA product was employed in quantitative real-time PCR according to the manufacturer's instructions with the iQ SYBR Green Supermix (Biorad) and iCycler (BioRad) thermocycler. The following cycle was used: 95 ℃ for 10 minutes (1 cycle), 95 ℃ 15 s, 60 ℃ 1 min, 95 ℃ 15 s (40 cycles) and 95 ℃ 15 s, 60 ℃ 1min (1 cycle). Nucleotide sequences of forward and reverse primers are listed in Table 6.

Table 6. qRT-PCR Primers

p53 For.	5’ - CCGCAGTCAGATCCTAGCG - 3’
p53 Rev.	5’ - AATCATCCATTGCTTGGGACG - 3’
Mdm2 For.	5’ - CCTTCGTGAGAATTGGCTTC - 3’
Mdm2 Rev.	5’ - CAACACATGACTCTCTGGAATCA - 3’
p21 For.	5’ – CCTGTCACTGTCTTGTACCCT - 3’
p21 Rev.	5’ – GCGTTTGGAGTGGTAGAAATCT - 3’
Bax For.	5’ - CCCCGAGAGGTCTTTTTCCG - 3’
Bax Rev.	5’ - GGCGTCCCAAAGTAGGAGA - 3’
14-3-3σ For.	5’ – CTCTCCTGCGAAGAGCGAAAC - 3’
14-3-3σ Rev.	5’ – CCTCGTTGCTTTTCTGCTCAA - 3’
PUMA For.	5’ - GACCTCAACGCACAGTACGAG - 3’
PUMA Rev.	5’ - AGGAGTCCCATGATGAGATTGT - 3’
GAPDH For.	5’ – AGAAGGCTGGGGCTCATTTG - 3’
GAPDH Rev.	5’ - AGGGGCCATCCACAGTCTTC- 3’

2.15 Venus Fusion Interaction Assays

Venus plasmids were a kind gift from Gordon Mills and were modified to contain Aurora B and p53 by subcloning. Primers for Aurora B and p53 were designed to contain AscI and EcoRV restriction sites. See Table 5. Cells were transfected by the liposome method with Venus plasmids containing Aurora B, p53 or empty Venus plasmids as appropriate controls. After 24 hours, cells were imaged as described in Section 2.5.

2.16 Statistical Analyses

Statistical analyses including student's t test, one way ANOVA, Tukey, Rank sum and analysis of mixed linear models were performed using SigmaPlot version 11 (Systat Software).

Chapter 3. Results

3.1 Inhibition of Aurora B kinase causes antineoplastic effects in breast cancer.

3.1.1 AZD1152 inhibits breast cancer growth regardless of Her2 status.

To evaluate the effect of specific Aurora kinase inhibitor, AZD1152, in breast cancer, six breast cancer cell lines were treated for between 2 and 5 days. Half of the cell lines tested, MDA-MB-435, MDA-MB-468 and MDA-MB-231 were all normal for Her2 expression, an important marker in breast cancer and indicator of potential treatment. Normal expression of Her2 is considered to be negative since they do not overexpress Her2, as do other breast cancers at high levels. Figure 5 shows that these cell lines are all sensitive to AZD1152-HQPA (prodrug, see Figure 4) activity with IC_{50}s of 125 nM, 14 nM and 105 nM respectively. IC_{50} is the dose of the drug that inhibited 50% of cell growth and was determined by sigmoidal curve fitting of the optical density reading at 570 nm after treatment with MTT. Next, I evaluated the use of AZD1152-HQPA in breast cancer cell lines that overexpressed Her2. Figure 6 shows that three cell lines, BT474, MDA-MB-361 and Her18 (parent line MCF7, described here (Laronga et al., 2000), which all overexpress Her2 also had sensitivity to inhibition of Aurora B kinase. IC_{50}s were comparable to those from non Her2 expressing lines at 8 nM, 70 nM and 20 nM respectively. Further, to validate the MTT assay as an effective method for investigating the proliferation of breast

cancer cell lines, the inhibition curve of AZD1152-HQPA in Her18 cells was repeated and cell numbers were measured directly by cell count. Figure 7 shows that the live cell count IC_{50} agrees with that of the MTT assay for Her18 cells. All cell lines tested displayed typical sigmoidal dose response curves for treatment with AZD1152-HQPA. The IC_{50}s observed are typical of those found for leukemia and other human cancer cells (Wilkinson et al., 2007; Yang et al., 2007). These results indicate that AZD1152-HQPA effectively inhibited growth of human breast cancer cell lines regardless of Her2 status. See APPENDIX A for AZD1152-HQPA dose response curves for other cell types and APPENDIX D for analysis of synergy between AZD1152 and etoposide.

3.1.2 AZD1152-HQPA induces mitotic defects, G2/M arrest and polyploidy in breast cancer cells.

Since Aurora B is an important regulator of mitosis, the effects of AZD1152-HQPA on separation of chromosomes in mitotic Her18 cells was investigated. Cells were treated with 20 nM AZD1152-HQPA for 48 hours followed by staining with DAPI and imaging with a confocal microscope. While normal cells displayed normal morphology, interphase cells treated with AZD1152-HQPA were bi-nucleate, an indicator of mitotic slippage (Figure 8, top panel, arrow). Also with AZD1152-HQPA treatment, micronuclei, indicators of mis-segregated chromosomes, were observed. During mitosis, prophase appeared normal but metaphase and anaphase showed considerable numbers of mitotic defects including misaligned chromosomes, anaphase bridges and mis-

segregation. Quantification of mitotic defects was performed and it was found that 60% of cells treated with AZD1152-HQPA had defects versus 1-2% for control (Figure 8, bottom panel). These results show that AZD1152-HQPA effectively causes mitotic catastrophe in Her18 breast cancer cells and that these observations are consistent with loss of Aurora B activity.

To further analyze mitotic outcome after treatment with AZD1152-HQPA, Her18 cells were treated for up to 48 hours and stained with propidium iodide followed by analysis by FACS for DNA content. The results indicate that the number of 4N cells increased with drug treatment in a time exposure to the drug (Figure 9A). Consistently, the number of 2N cells decreased and at the 48 hour time point, 8N (polyploidy) cells were observed. This in consistent with mitotic slippage caused by a defective spindle assembly checkpoint and is also consistent with loss of Aurora B. Percentage of 2N, 4N and 8N cells from 9A were quantified and are displayed in Figure 9B. It can be seen that as 4N cell percentage increases, there is a decrease in the percentage of 2N cells. Figure 9C shows the fold increase of polyploid 8N cells from 9A. At 48 hours, polyploid cells had increased to 9.7% from 1.35% at 24 hours, a 13 fold increase. These results, together with the mitotic defect data from Figure 8, indicate that cells become polyploid as mitotic catastrophe occurs with treatment of AZD1152-HQPA. See APPENDIX B for analysis of polyploidy induced by AZD1152-HQPA in the Her18 parent cell line, MCF7.

Figure 5

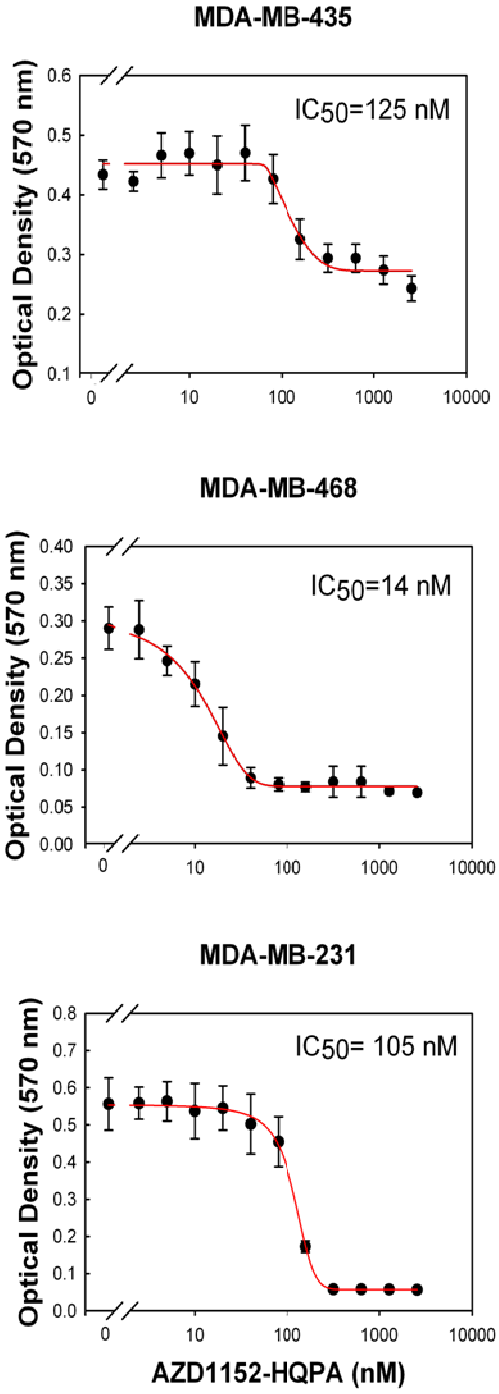

Figure 5. AZD1152-HQPA inhibits breast cancer cell growth in Her2 negative cell lines. Three breast cancer cell lines, MDA-MB-435, MDA-MB-468 and MDA-MB-231 that are all normal for Her2 (considered Her2 negative or not overexpressing) were treated with indicated doses of AZD1152-HQPA for between 2 and 5 days. After drug treatment, cells were treated with MTT and log(dose)-response curves plotted. Data points are means of at least four replicates. IC_{50} was determined by sigmoidal curve fitting. Error bars represent 95% confidence intervals.

Figure 6

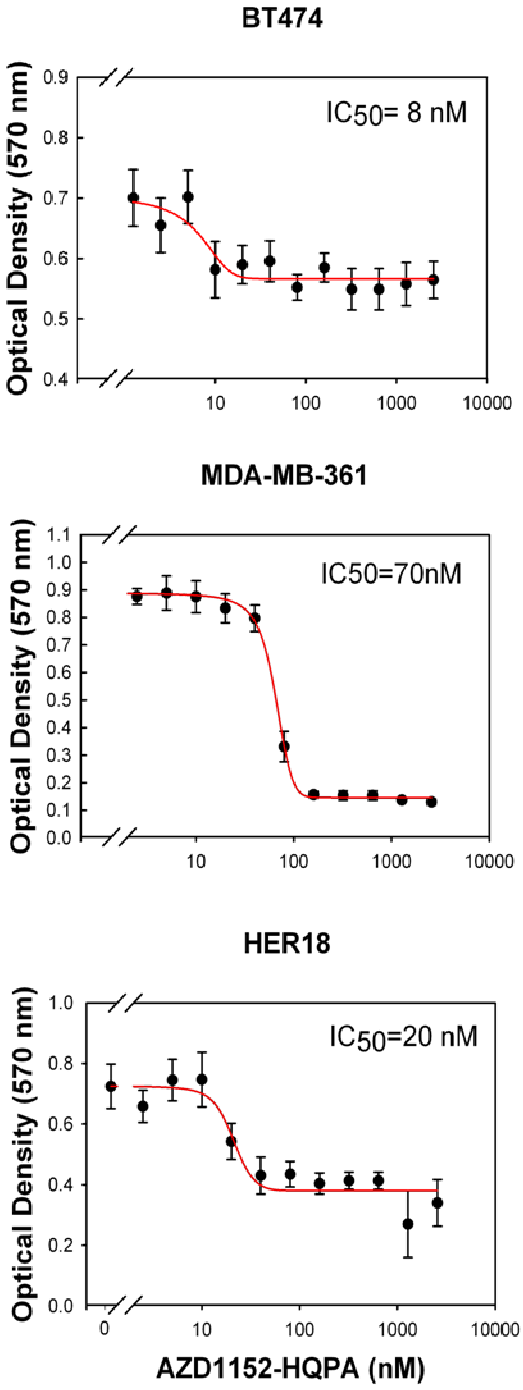

Figure 6. AZD1152-HQPA inhibits breast cancer cell growth in Her2 overexpressing cell lines. Three breast cancer cell lines, BT474, MDA-MB-361 and Her18 that all overexpress Her2 (Her18 is Her2 overexpression by lentivirus infection- parent MCF7) were treated with indicated doses of AZD1152-HQPA for between 2 and 5 days. After drug treatment, cells were treated with MTT and log(dose)-response curves plotted. Data points are means of at least four replicates. IC_{50} was determined by sigmoidal curve fitting. Error bars represent 95% confidence intervals.

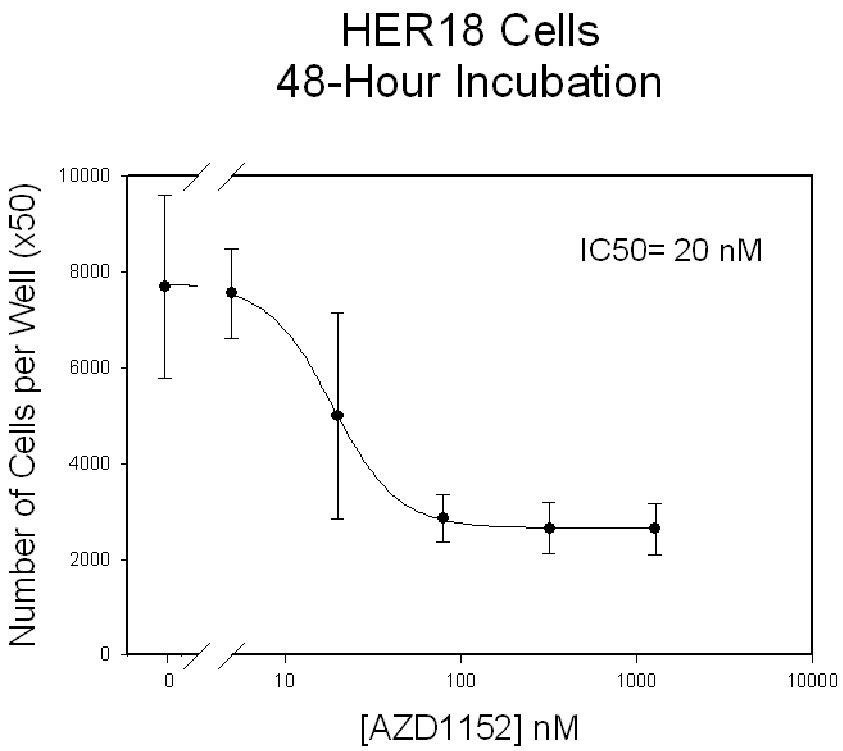

Figure 7. AZD1152-HQPA inhibits breast cancer cell growth in Her18 as measure by live cell count. Her18 cells were plated in 6-well tissue culture dishes and incubated with AZD1152-HQPA for 48 hours. Live cell counts were performed and plotted against dose of drug. Data points represent mean of three replicates. IC_{50} was determined by sigmoidal curve fitting. Error bars represent 95% confidence intervals.

Figure 8

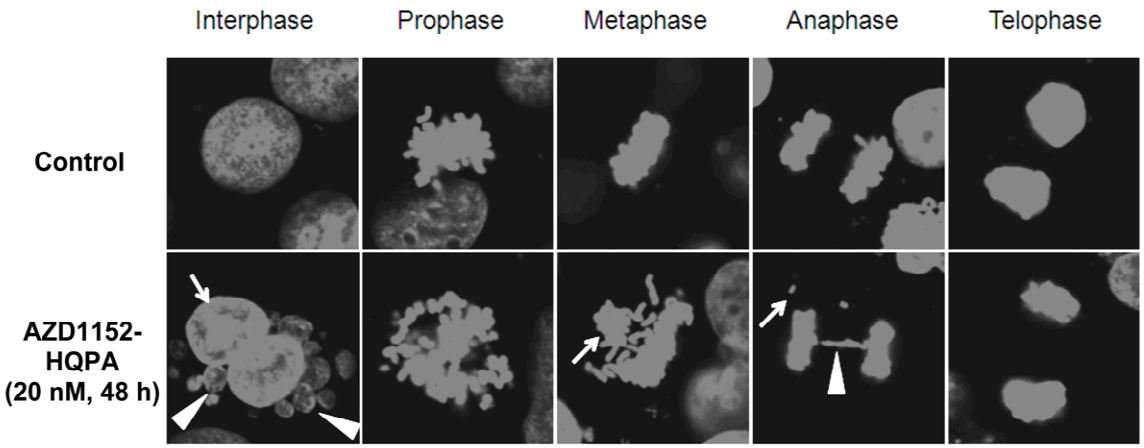

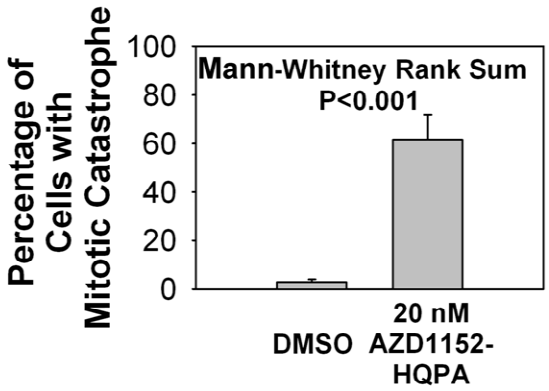

Figure 8. AZD1152-HQPA induces mitotic defects in Her18 breast cancer cells. Top panel. Her18 cells were treated for 48 hours with AZD1152-HQPA or control medium followed by DAPI staining. Fluorescence images of interphase cells show bi-nucleation (arrow) and micronuclei (arrow heads). Misaligned chromosomes are indicated by arrows in metaphase. Anaphase cells show anaphase bridges (arrow head) and mis-segregated chromosomes (arrow). Bottom panel. Percentage of cells displaying mitotic catastrophe (from top panel) are plotted for control and AZD1152-HQPA treated cells. Error bars represent 95% confidence intervals.

Figure 9

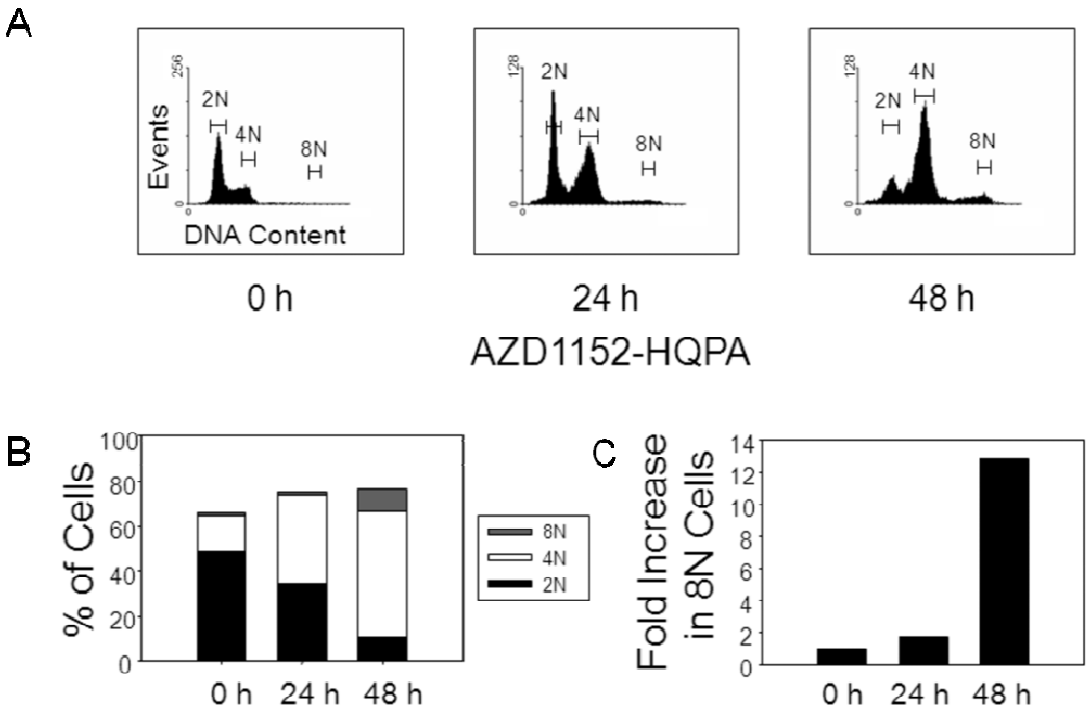

Figure 9. Polyploidy results from treatment of Her18 breast cancer cells with AZD1152-HQPA. A Her18 cells were treated with 100 nM AZD1152-HQPA for 48 hours followed by staining with propidium iodide and FACS analysis for cell cycle profile. Cells are gated for 2N (G1), 4N (G2/M) and 8N (polyploid) DNA content. B Percentage 2N, 4N and 8N cells versus time from A. C Fold increase in 8N cells from A plotted at 0, 24 and 48 hours post treatment with AZD1152-HQPA.

3.1.3 AZD1152-HQPA induces apoptosis and reduces tumorigenic phenotype in breast cancer cells.

To investigate the cell death induced by AZD1152-HQPA , we evaluated apoptosis as a possibility. Her18 cells were treated for up to 48 hours with 100 nM AZD1152-HQPA and stained with Annexin V/PI followed by analysis via FACS for apoptotic cells. Figure 10 shows that control cells had 5.64% apoptotic cells while the treated groups had 9.22% at 24 hours and 15.57% at 48 hours. Lower right and upper right panels were added together for total apoptotic cell percentage. The lower right quadrant indicates early apoptosis and the upper right indicates late apoptosis. Similar observations were made for MB-MDA-231 cells where control showed 3.2% apoptosis while the drug treated groups showed 12.5% and 16.4% apoptosis at 48 and 72 hours respectively (Figure 11). Further evidence for apoptosis in AZD1152-HQPA treated cells can be seen in Figure 12. Both Her18 and MB-MDA-231 cells treated with increasing dose of the drug displayed cleavage of PARP (Poly [ADP-Ribose] Polymerase). Both results agree with the IC_{50}s for these cell lines (Figures 5 & 6) and are confirmation that AZD1152 can kill breast cancer cells by inducing apoptosis.

Given that AZD1152 was causing apoptosis in breast cancer cells and inhibiting their growth, it was investigated if the drug could affect the tumorigenicity of these cell lines by colony forming and soft agar assays. Her18 cells were plated in 6-well tissue culture dishes at 5000 cells /well then treated with 40 nM AZD1152-HQPA or vehicle. Cells were incubated for 12 days and

colonies allowed to develop. Crystal violet staining revealed that AZD1152-HQPA was able to reduce the tumorigenic phenotype by reducing the colony number from approximately 2250 in the control, to under 500 in the treated group (Figure 13, bottom panel). Representative plates are shown in Figure 13, top panel. The difference in mean colony number was significant at $P<0.001$ by student's t test. To investigate the effect of AZD1152-HQPA in anchorage-independent growth of cells, Her18 cells were evaluated in a soft agar colony formation assay. Cells were planted at low density in 3.5 cm Petri dishes with soft agar and treated with 80 nM of drug. Control plates showed a mean of approximately 70 colonies while the drug treatment plates showed <10 colonies. This result was significant ($P<0.001$) and is furher evidence that AZD1152-HQPA can reduce the tumorigenic phenotype observed in Her18 cells in both anchorage-dependent and anchorage-independent environments. See APPENDIX C for colony forming and soft agar assays is response to AZD1152-HQPA in Her18 parent line, MCF7.

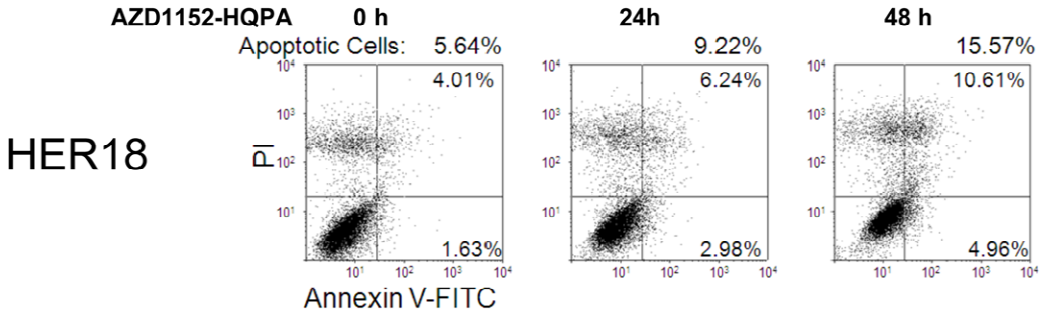

Figure 10. Apoptosis is induced by AZD1152-HQPA in Her18 cells. Her18 breast cancer cells were treated for up to 48 hours with 100 nM AZD1152-HQPA. Cells were stained with Annexin V-FITC and PI followed by analysis via flow cytometry at time 0, 24 and 48 hours.

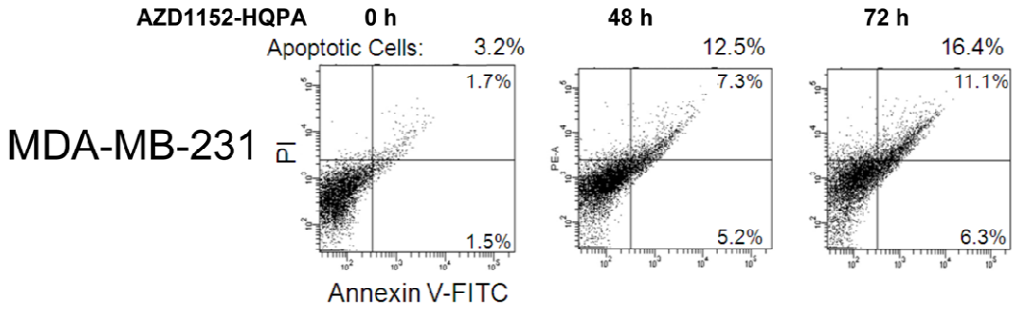

Figure 11. Apoptosis is induced by AZD1152-HQPA in MB-MDA-231 cells. MB-MDA-231 breast cancer cells were treated for up to 72 hours with 100 nM AZD1152-HQPA. Cells were stained with Annexin V-FITC and PI followed by analysis via flow cytometry at time 0, 48 and 72 hours.

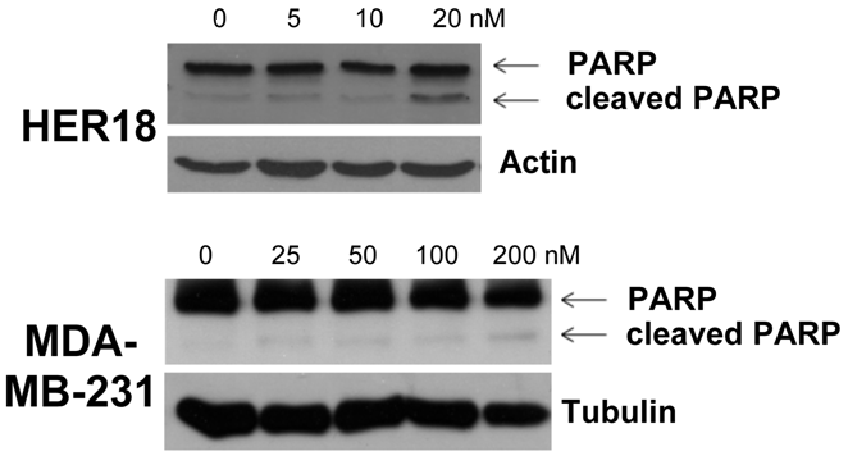

Figure 12. AZD1152-HQPA induces PARP cleavage in Her18 and MB-MDA-231 cells. Her18 and MB-MDA-231 breast cancer cells were treated with increasing dose of AZD1152-HQPA as indicated for 48 hours. Cell lysates were analyzed by immunoblot with anti-PARP antibody. PARP appears at 115 kD and the apoptotic indicator, cleaved PARP, appears at 85 kD.

Figure 13

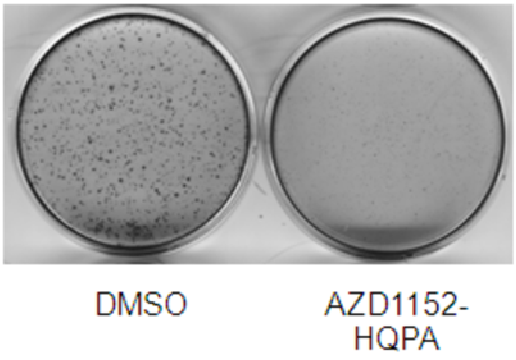

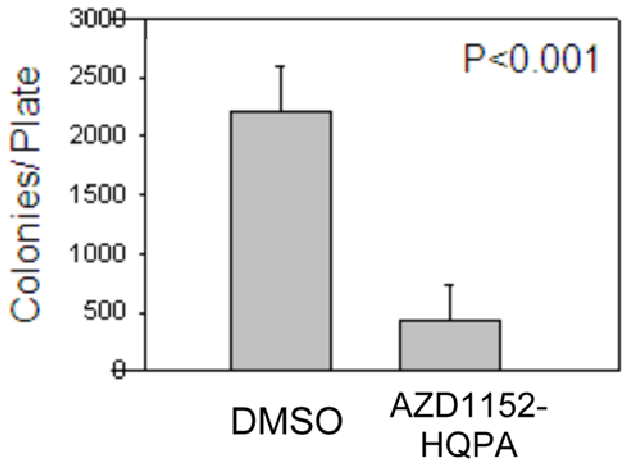

Figure 13. Colony formation is reduced by AZD1152-HQPA. Her18 cells were plated in 6-well tissue culture dishes at 5000 cells/well and allowed to attach for 24 hours followed by treatment with either vehicle or 40 nM AZD1152-HQPA. After 12 days, plates were stained with crystal violet and photographed, top. Bottom panel, colonies per plate are plotted for 3 replicates. Statistical significance was observed using the Student' t test. Error bars: 95% CI.

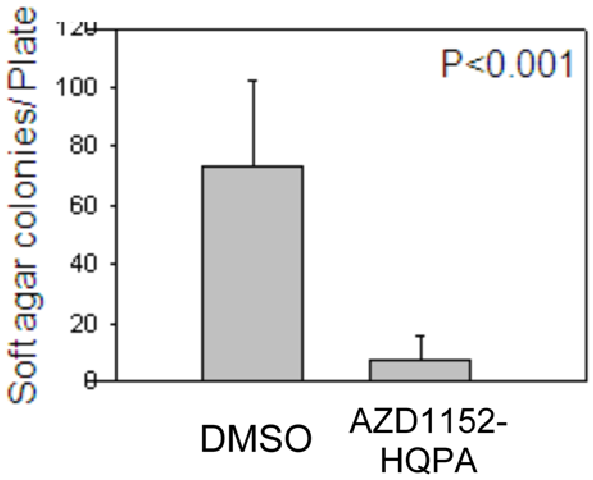

Figure 14. Anchorage-independent colony formation is inhibited by AZD1152-HQPA. Her18 cells were plated at 5000 cells/plate in 3.5 cm Petri dishes in soft agar. Plates were treated with 80 nm AZD1152 and incubated for 26 days. Colonies numbers are plotted for vehicle and treatment groups as means from 3 replicate plates. Significance of $p<0.001$ was observed with the Student's t test. Error bars: 95% CI.

3.1.4 AZD1152 inhibits growth of breast cancer xenografts *in vivo*.

To investigate the potential for AZD1152 to inhibit the growth of aggressive breast cancer *in vivo,* the use of a mammary fat pad xenograft system was employed. 8.5×10^6 Her18 cells were injected subcutaneously into the mammary fat pad of six to eight week old female athymic nude mice. Mice were randomized into three groups: control (0.3 M Tris), low dose AZD1152 (62.5 mg/kg/day) and high dose AZD1152 (125 mg/kg/day). Dose of AZD1152 was based on previous reports that 10-150 mg/kg/day will produce sufficient plasma concentration in nude mice (Mortlock et al., 2007; Wilkinson et al., 2007). AZD1152 prodrug was used rather than the metabolized form, AZD1152-HQPA. Tumor growth was maintained with weekly IP injections of 3 mg/kg estradiol cypionate (estrogen analog) as described here (Jerome et al., 2006; Wang et al., 2004). When tumors reached measureable range (approximately 50 mm^3), treatment began. AZD1152 or control were injected IP on day one and two of a seven day repeating cycle for three weeks. Tumor volumes were estimated every two to three days by caliper measurement and the formula: Length x $Width^2/2$. Figure 15 shows the tumor volume estimates plotted for each group. The high dose group showed significant reduction in tumor volume versus control ($P<0.001$) while the low dose group showed near significant reduction ($P<0.08$) in tumor volume. Figure 16, top panel, shows representative mice from the three treatment groups bearing xenografts. After 24 days, mice were sacrificed and tumors removed and weighed. Figure 16, bottom panel, shows the mean tumor weight plotted for each group. Tumor mass for both low and high dose groups

were significantly reduced compared to control ($P<0.01$). Tumor proteins were extracted and analyzed by immunoblot for Aurora B activity. Figure 17 shows that the major Aurora B substrate (Goto et al., 2002), phosphorylated Histone H3 (serine 10), which is important in Histone H1 dissociation from chromatin during chromatin condensation (Hirota et al., 2005; Wei et al., 1999), is reduced in AZD1152 treated tumors versus untreated controls indicating that AZD1152 was able to reduce Aurora B kinase activity *in vivo*. Tumor samples from all groups were also fixed in formalin and paraffin embedded for immunohistochemical staining. Figure 18 top panels, show H&E staining for control and high dose groups at high magnification. Multinucleate cells can be seen in AZD1152 treated cells (circles) and are consistent with *in vitro* observation of multinucleation in Figure 8. Further immunohistochemical staining of all three treatment groups for Ki-67 and cleaved Caspase-3 indicate that consistent with *in vitro* results (Figures 5, 6 and 10), AZD1152 is able to reduce proliferation and induce apoptosis *in vivo.*

Figure 15

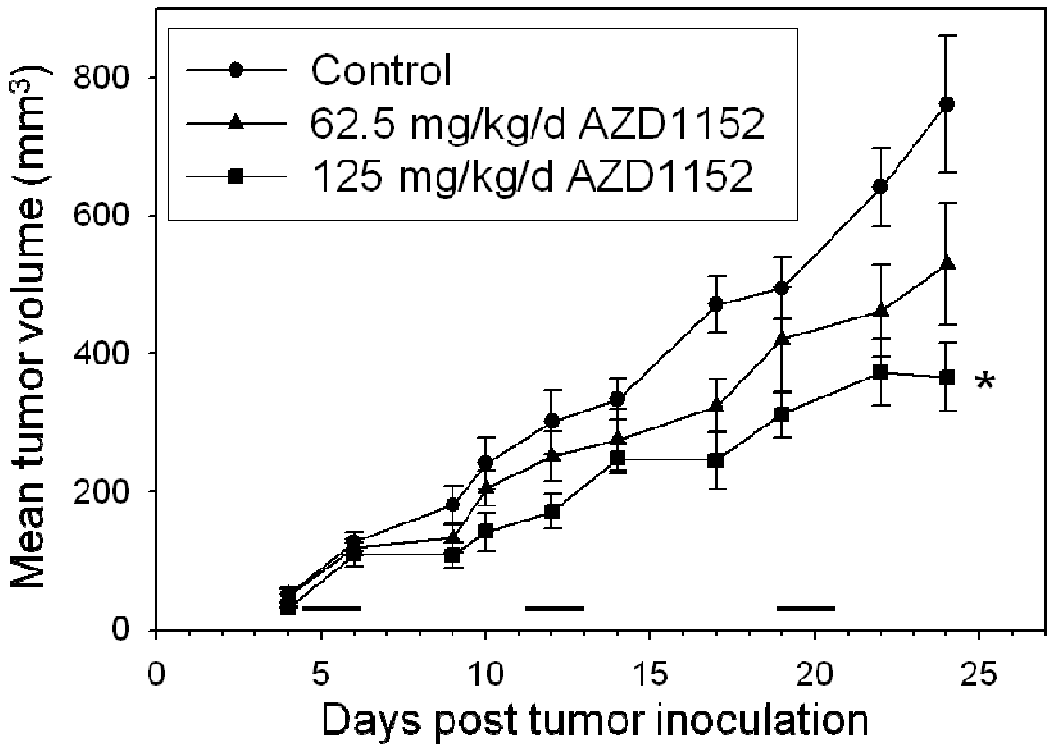

Figure 15. AZD1152 prodrug inhibits growth of breast cancer cells *in vivo.* Six to eight week old athymic nude mice were injected in the mammary fat pad with 8.5 x 10^6 Her18 cells and randomized into 3 treatment groups: Control (0.3 M Tris), low dose (62.5 mg/kg/day) AZD1152 and high dose 125 mg/kg/day AZD1152. All mice received weekly subcutaneous injections of estradiol cypionate (3 mg/kg/week) to support tumor growth beginning two weeks prior to injection with xenografts. Treatment with drug or control began when tumors were measureable (approximately 50 mm^3) and continued for 3 weeks on day 1 and 2 of a 7 day repeating cycle (indicated by horizontal bars). Tumor volumes were measured with calipers and estimates plotted as means of each group. Significance was determined in a mixed linear model: $P<0.001$. Error bars represent standard error.

Figure 16

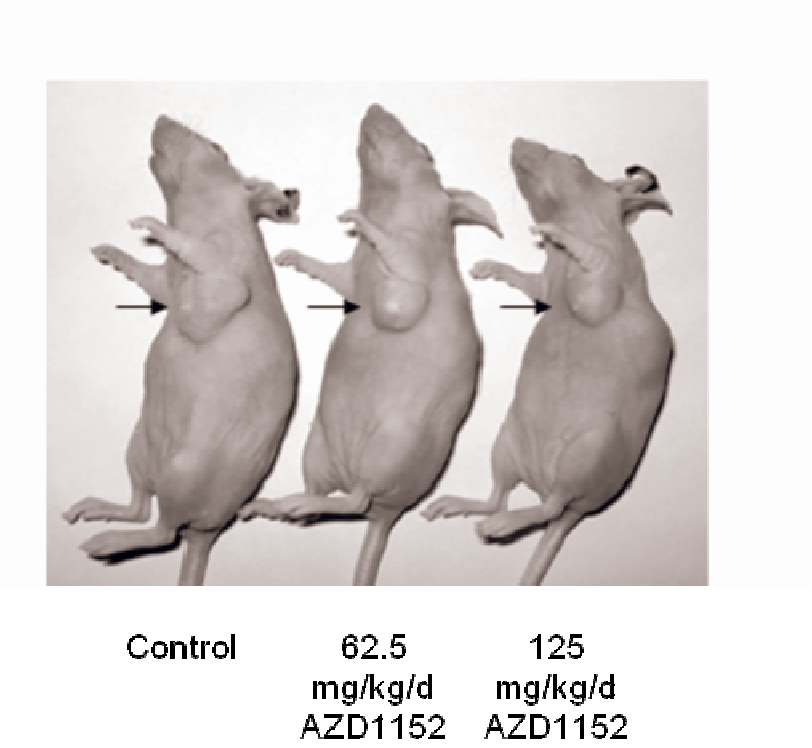

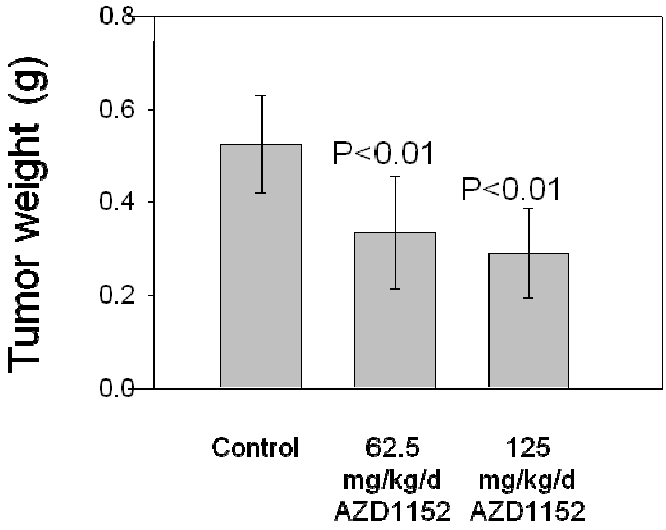

Figure 16. Tumor mass in Her18 xenografts is reduced with AZD1152 treatment. Top panel, representative mice from control, low dose and high dose treatment groups from Figure 15. Arrows indicate xenograft. Bottom panel, excised tumors from control (n=6), low dose (n=8) and high dose (n=6) mice were weighed and are shown plotted as means for each group. P values were calculated as one-way ANOVA. Error bars represent 95% CI.

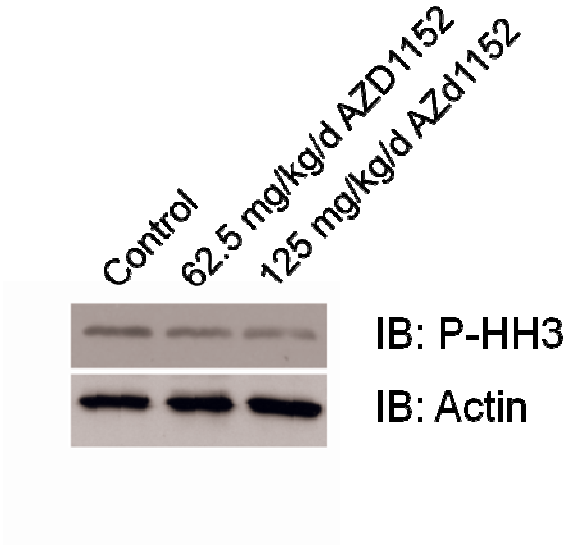

Figure 17. AZD1152 inhibits Aurora B kinase activity *in vivo.* Tumor samples from Her18 xenografted nude mice treated with control, low and high doses of AZD1152 were lysed and proteins analyzed by immunoblot for phospho-Histone H3.

Figure 18

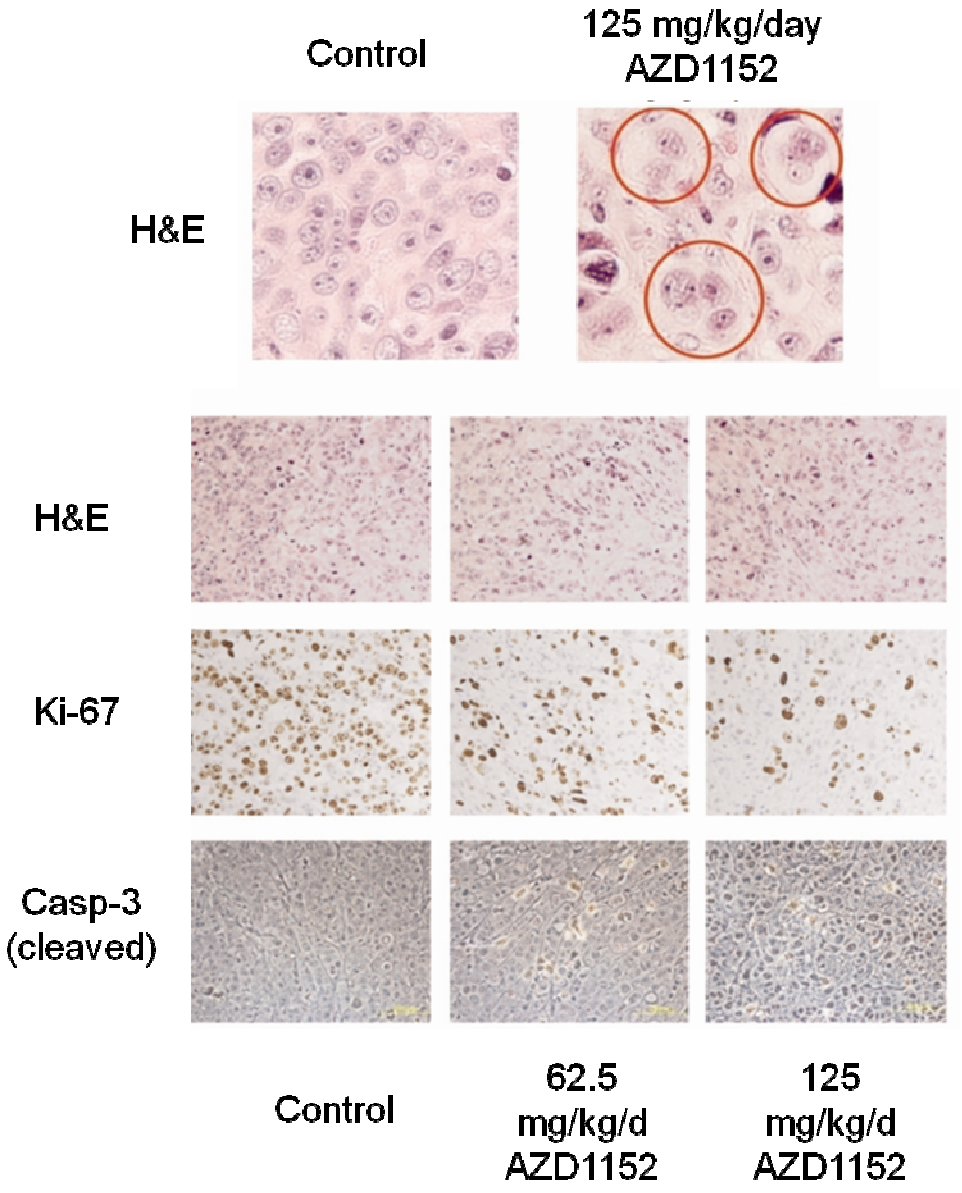

Figure 18. Immunohistochemistry analysis of Her18 xenograft tumor samples. Tumor samples from Her18 xenografted nude mice treated with control, low and high doses of AZD1152 were paraffin embedded and analyzed by Immunohistochemistry. Upper panel, H&E staining of control and high dose samples. Red circles indicate multinucleate cells in high dose treated samples. Lower panels, H&E, Ki-67 and cleaved Caspase-3 staining.

3.1.5 AZD1152 inhibits metastases in breast cancer.

In the previous orthotopic xenograft assay (Figures 15-18) metastasis of tumors in either treatment or control groups was not observed. To address whether AZD1152 could interfere with metastases of breast cancer as well as growth of primary tumors, a model of breast cancer with lung metastasis potential was implemented. Six to eight week-old female athymic *nu/nu* mice were injected with 2 x 10^6 MDA-MB-231 human breast cancer cells via tail vein. Mice were randomly separated into two groups: control and 125 mg/kg/day AZD1152. Treatment with vehicle or drug began two days post IV injection of breast cancer cells. Vehicle or drug were administered IP on days 1 and 2 of a 7-day repeating cycle for 4 weeks. Mice were sacrificed after ten weeks and the lungs removed and weighed. Figure 19 (top) displays mean weight of lungs per mouse. Control mice had significantly ($P < 0.01$, two-tailed t-test) higher lung mass than lungs in the AZD1152 group. Further, the number of gross tumor nodules was found to be significantly higher ($P < 0.008$, two-tailed t-test) in the lungs of control treated mice versus AZD1152 treated mice (Figure 19, bottom panel). Matched lung lobes were photographed for gross anatomic comparison from two representative mice (Figure 20). The drug treated mouse lung lobes are clearly smaller and display no metastatic nodules while control treated lung lobes are very large and bear many nodules. Mouse lungs were fixed in formalin and analyzed by IHC. H&E staining of lung tissues from AZD1152-treated mice showed reduction of tumor burden at the microscopic level (Figure 21). These data show clearly that

AZD1152 is effective in blocking the aggressive and highly metastatic phenotype of MDA-MB-231 cells *in vivo*.

Figure 19

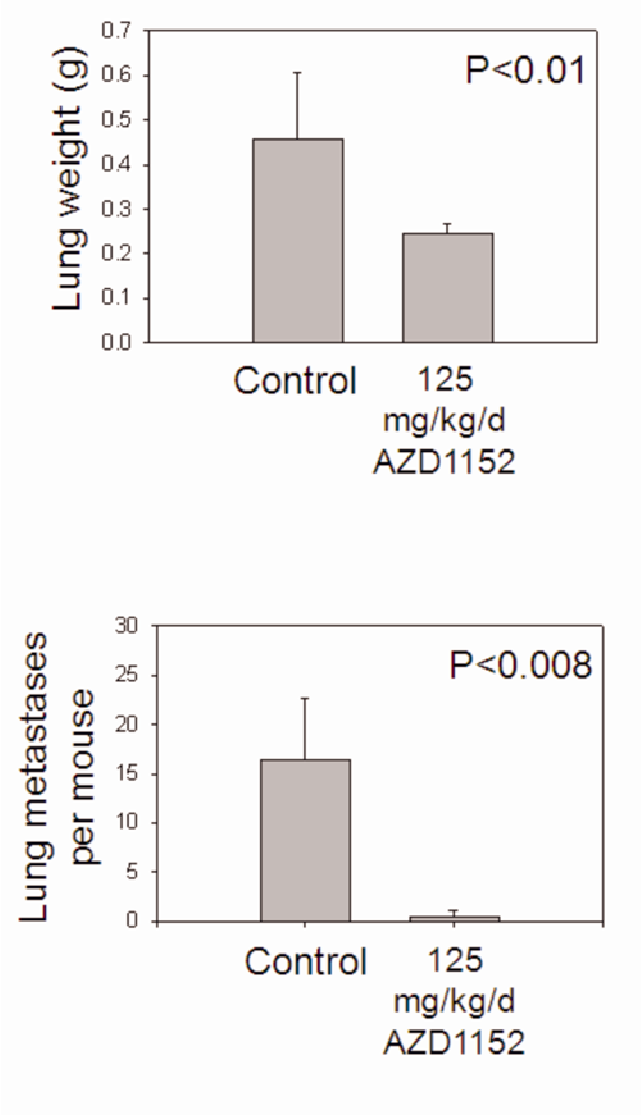

Figure 19. Lung weight and metastases are reduced by AZD1152 in a metastatic breast cancer model. 2.0 x 10^6 MB-MDA-231 breast cancer cells were injected in the tail vein of six to eight week old female athymic nude mice. Two days post injection mice were randomized into two groups: Control (0.3 M Tris) or drug-treated (125 mg/kg/day) AZD1152. Two days post xenograft, control or drug were injected IP on day one and two of a seven day repeating cycle for four cycles. After ten weeks mice were sacrificed and lungs removed for analysis. Lung weights (top) are plotted as the means for each group. Number of metastatic lung nodules per mouse are plotted as means for each treatment group (bottom). P values were calculated by two-tailed t test. Error bars: 95% CI.

Figure 20

Figure 20. Lung lobe photographs from MB-MDA-231 metastatic xenograft model. Matched pairs of lung lobes of representative mice from Figure 19 were photographed for comparison.

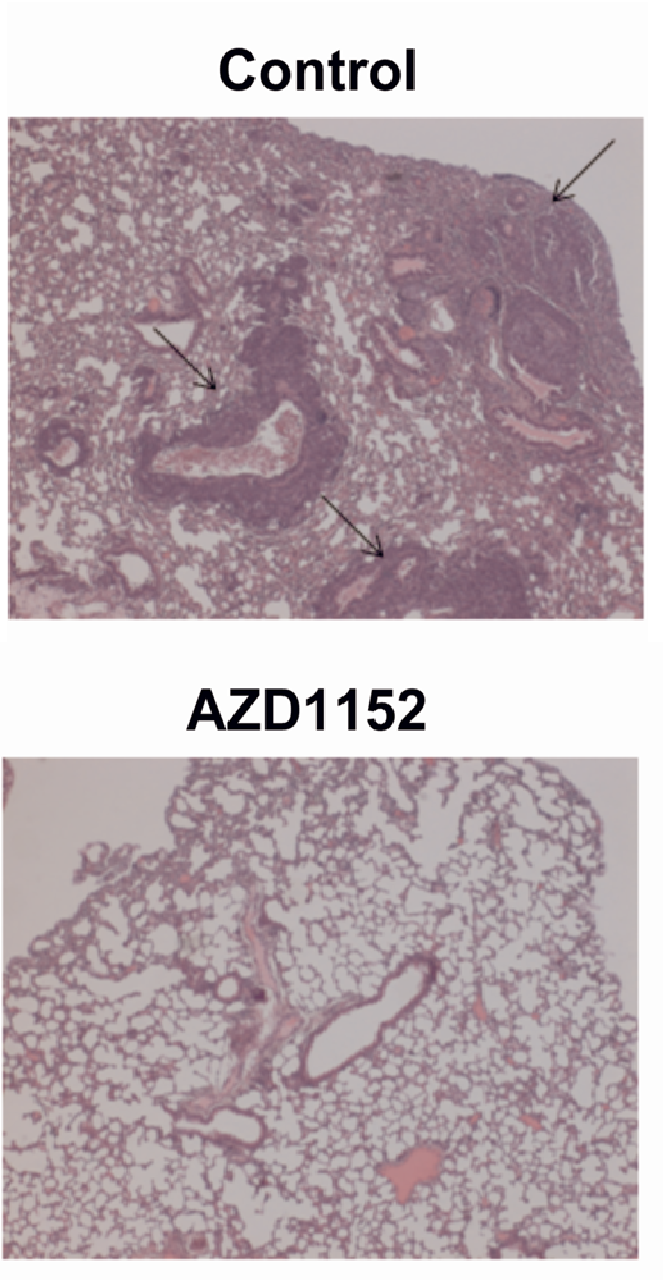

Figure 21. IHC staining of lung tissue from MB-MDA-231 xenografts. H&E staining of lungs from control and drug treated mice are shown at the same magnification. Arrows in the control photomicrograph indicate metastatic tumor nodules.

3.1.6 Poly-ubiquitination and degradation of Aurora B via the proteasome are increased by AZD1152-HQPA

It has been clearly established that AZD1152 can decrease the activity of Aurora B kinase in cells and in animal models but whether this reduction in activity is caused only by competition for the ATP binding pocket is unknown. Further, whether inhibition of the kinase could somehow destabilize it has not been previously investigated. To this end, the steady state level of Aurora B in Her18 cells treated with both increasing exposure and increasing dose of AZD1152-HQPA was investigated. Figure 22 shows that in both cases, the protein level of Aurora B was reduced. Additionally, It appears that the inhibition of the kinase activity, as measured by phospho-Histone H3, precedes the decline in overall protein level of the kinase.

To further investigate the destabilization of Aurora B, the turnover rate in the presence and absence of AZD1152-HQPA was investigated. Her18 cells were treated with drug for 48 hours with an additional 4 hours in the presence of the *de novo* protein synthesis inhibitor, Cycloheximide (CHX). Figure 23 (top panel) shows by immunoblot that the turnover rate of Aurora B is indeed increased in the presence of AZD1152-HQPA. The bands from the top panel were measured by densitometry and the integrated optical density normalized to the Actin control relative to time 0 plotted.

To determine if the turnover rate increase for Aurora B was due to proteasomal degradation, MB-MDA-231 cells were treated with 105 nM

AZD1152-HQPA with and without the proteasome inhibitor, MG132. Figure 24 shows that the reduction in Aurora B levels caused by AZD1152-HQPA was rescued in the presence of MG132 thereby confirming that the proteasome is involved in the degradation.

Next, the ubiquitination of Aurora B in the presence of AZD1152-HQPA was investigated. Her18 cells were transfected with Flag-tagged Aurora B and HA-tagged ubiquitin plasmids. Cell lysates were immunoprecipitated with anti-Flag antibody and immunoblotted with anti-HA antibody. Figure 25 shows that poly-ubiquitinated Aurora B levels were increased in the presence of AZD1152-HQPA. The control lane, without HA-ubiquitin, showed no ubiquitination and only the IgG heavy chain. These results confirm that AZD1152-HQPA increases degradation of Aurora B via the ubiquitin-proteasome system. To determine the E3 ligase responsible for Aurora B ubiquitination, another ubiquitination assay was performed. Figure 25 shows that Aurora B ubiquitination is increased by AZD1152 and can be partially rescued by transfection with either the dominant negative form of CDC20 or Cdh1, which are both substrate recognition subunits of the Anaphase Promoting Complex (APC), the E3 ligase complex responsible for the degradation of Aurora B at the onset of anaphase.

Based on the results from Figures 5 through 24, a model of the regulation of Aurora B by AZD1152 starts to come into focus. Previous studies have shown that AZD1152 can inhibit the activity of Aurora B which interferes with normal mitosis but no studies have shown the consequences of this inhibition for the

kinase itself. Here, we have shown that subsequent to inhibition of Aurora B activity, the level of the kinase itself falls substantially. Cycloheximide assays confirm the increase in turnover of Aurora B and an assay with the proteasome inhibitor MG132 shows that Aurora B turnover is caused at least in part, by the proteasome.

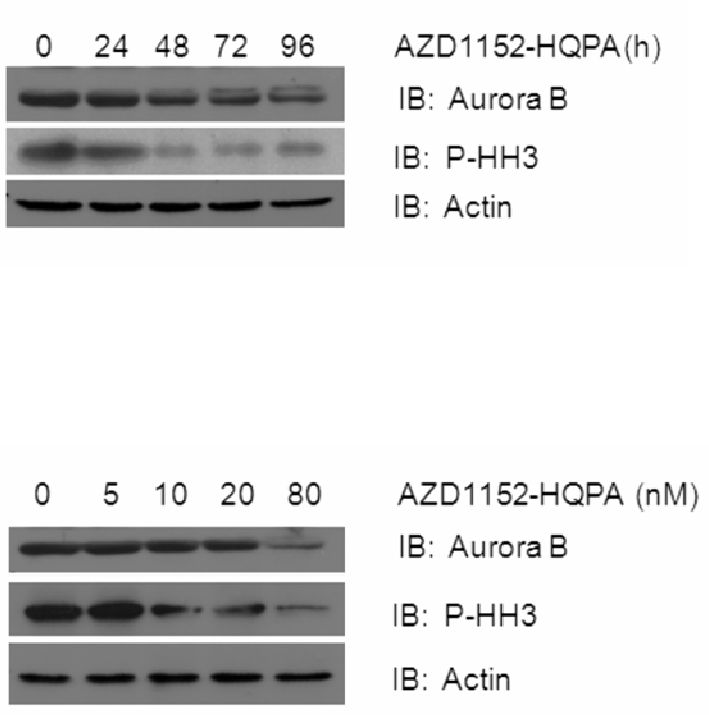

Figure 22. AZD1152 reduces Aurora B protein level in steady state. Her18 cells were treated with increasing exposure time (top panel) and increasing dose (bottom panel) of AZD1152-HQPA and cell lysates analyzed by immunoblot for Aurora B, phospho-Histone H3 and Actin.

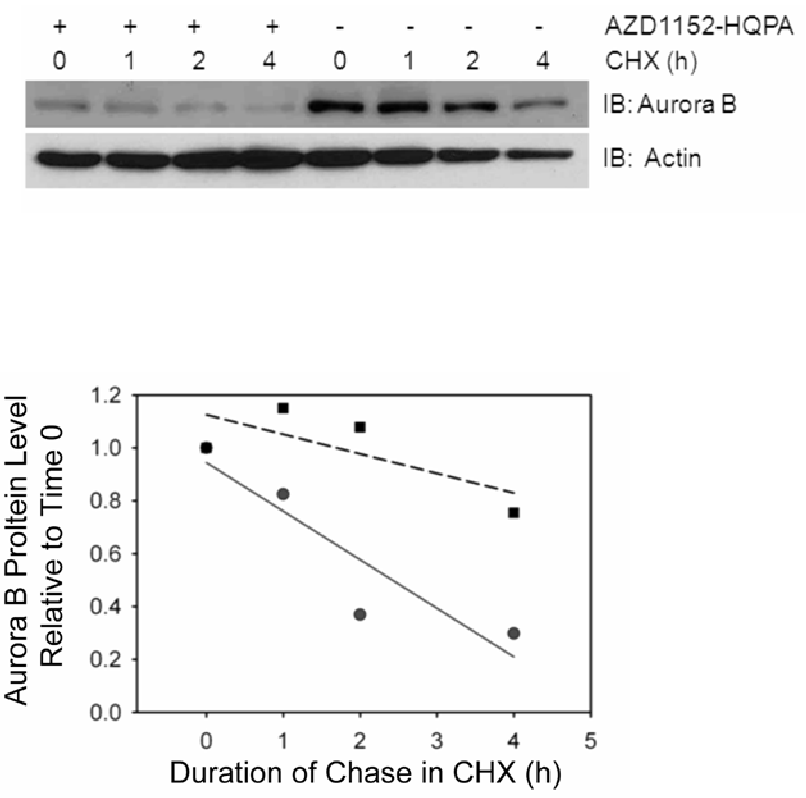

Figure 23. AZD1152 increases the turnover rate of Aurora B kinase. Her18 cells were cultured with and without 20 nM AZD1152-HQPA for 48 hours and then treated for up to 4 hours with cycloheximide. Top, lysates were analyzed by immunoblot for Aurora B and Actin. Bottom, turnover rate of Aurora B from the top panel, is plotted for treated and untreated groups. Plots are the amounts of Aurora B relative to time 0 and are corrected for loading with Actin.

Figure 24

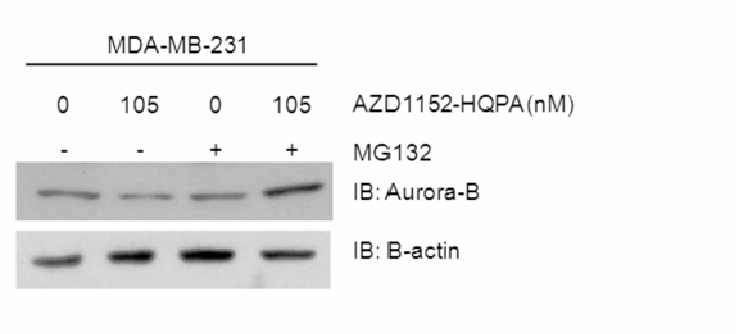

Figure 24. Aurora B degradation via the ubiquitin-proteasome system is increased by AZD1152. MB-MDA-231 cells were treated with 105 nM AZD1152-HQPA for 48 hours in the presence and absence of the proteasome inhibitor MG132. Lysates were immunoblotted for Aurora B and Actin.

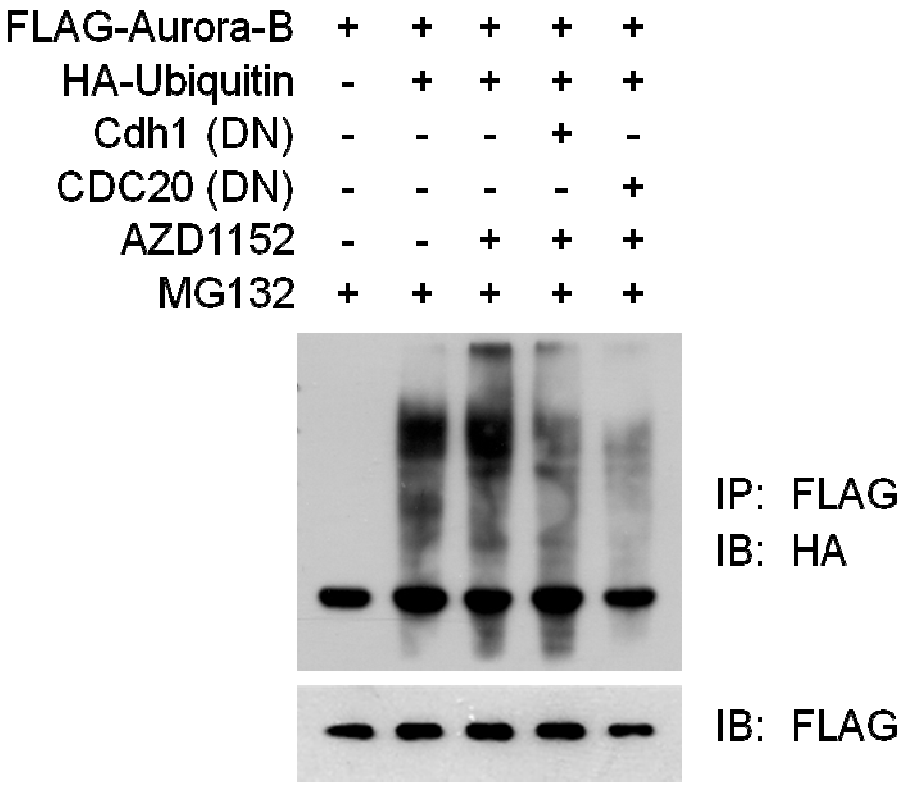

Figure 25. AZD1152 mediated degradation of Aurora B is through the Anaphase Promoting Complex (APC). Her18 cells were co-transfected with Flag tagged Aurora B, HA-Ubiquitin and either the dominant negative form of Cdh1 or CDC20 followed by treatment for 24 hours with 20 nM AZD1152 and the proteasome inhibitor, MG132. Cell lysates were immunoprecipitated with anti-FLAG antibody and immunoblotted with anti-HA antibody.

3.1.7 Inhibition of Aurora B with AZD1152 in human xenografts, increases p53 level.

Upon staining of the Her18 xenografted tumor samples in mice (Figures 15-18), a surprising result was observed. p53 levels had increased dramatically with dose increase of AZD1152 treatment (Figure 26). This observation could be explained in a number of ways since p53 has many sensor pathways that could cause its activation when major perturbations of the genome are occurring as a result of AZD1152. However, the elevations in p53 level could also be explained by a direct interaction of p53 and Aurora B. In the Introduction section of this thesis the phosphorylation of p53 by Aurora A kinase was described. p53 phosphorylation by its close cousin, Aurora B could also be occurring. Thus, with inhibition of Aurora B by AZD1152, any possible negative regulation would be released, and p53 levels would increase. The next section of this thesis focuses on investigation of an Aurora B-p53 interaction and its consequences for p53 level, expression, transcriptional activity and cellular function.

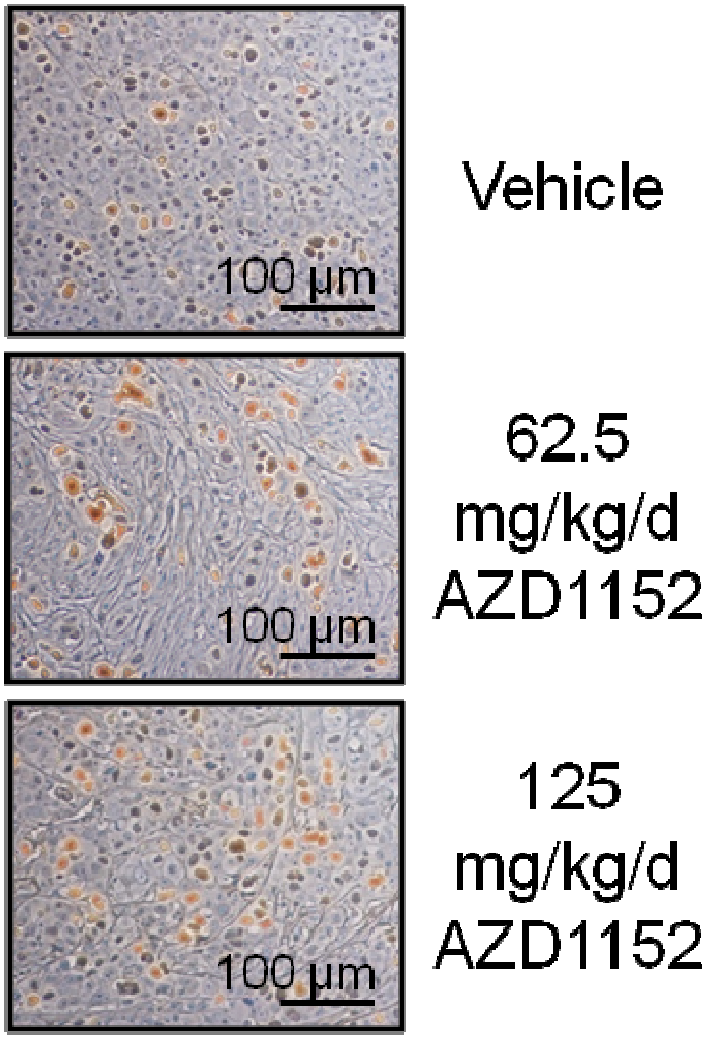

Figure 26. p53 is induced in Her18 xenografts by AZD1152. Her18 xenograft tumor samples (Figure 18) IHC stained for p53 in vehicle, low dose and high dose AZD1152 treatment groups.

3.2 Aurora B downregulates p53 via phosphorylation in the DNA binding domain.

3.2.1 Aurora B and p53 interact *in vitro*.

In our previous findings we showed that the Aurora B kinase inhibitor AZD1152 reduced the steady state levels of Aurora B and that this was concurrent with elevation of p53 levels in the cell. From this we can hypothesize that Aurora B interacts directly with and phosphorylates p53. The first step in proving this hypothesis is to show that Aurora B does associate with p53. To investigate this, a reciprocal co-immunoprecipitation in 293T cells was performed. Figure 27 clearly shows that when Aurora B is IP'd, p53 can be detected, and also the reciprocal. Next, it was determined if the interaction of p53 and Aurora B was direct, by performing an *in vitro* pull down assay. Figure 28 shows that recombinantly produced Aurora B and p53 do associate *in vitro*.

To determine where Aurora B binds to p53, another *in vitro* pull down assay using GST or GST-p53 deletion constructs (Figure 41) was performed (Figure 29). From this result, it can be seen that Aurora B binds to both the DNA binding domain and the C-terminus of p53, hinting at the possibility that the phosphorylation sites for Aurora B could be in the DNA binding domain or close to the C-terminus, as they are for Aurora A.

To understand if the interaction of Aurora B and p53 is cell cycle regulated we synchronized Hct116 cells to S-phase with a double thymidine block. Cells

were released and analyzed every two hours by PI staining and FACS to determine DNA content (Figure 30). Lysates were then immunoprecipitated for Aurora B and immunoblotted for p53. Figure 31 shows that although Aurora B and p53 are present during the whole cell cycle, they only interact during Late S and G2/M phases with a significant drop in their interaction at some point in or just after Mitosis. This corresponds to the reduction seen in Aurora B during mitosis and which is known to be mediated by Anaphase Promoting Complex (APC) in late mitosis.

To determine in which cellular compartment these two proteins interact, a co-localization experiment was performed. Her18 cells were immunostained for endogenous p53 and Aurora B and labeled with secondary antibodies conjugated to Alexa-fluor fluorophores. Since the previous synchronization experiment showed interaction during mitosis, this experiment focused on mitosis. Figure 32 shows that Aurora B is present in late mitosis and shows its typical localization to the midbody while p53 has a diffuse presence in the entire cytoplasm (nuclear envelope not present). It can be said that p53 and Aurora B are co-localizing during mitosis since the merge image shows a yellow color, however, the staining of p53 is not exclusive to the area of staining for Aurora B.

3.2.2 Aurora B and p53 interact during interphase and mitosis.

To determine if the co-localization of Aurora B and p53 described in the last section is real and relevant, a Venus fusion protein system was employed. Figure 33 shows a schematic diagram of this system. The C-terminal end of the

Venus protein (a YFP variant of GFP) is fused to one of the proteins of interest by inserting the cDNA for that protein into the Venus C-term plasmid. The cDNA of the other protein of interest is inserted into the Venus N-term plasmid and both plasmids co-transfected. If the two proteins of interest interact, there is green fluorescence. This process was performed for Aurora B and p53 by inserting their cDNA into Venus plasmids and again in the reverse. The resulting green fluorescence was observed in both the nucleus and cytoplasm of interphase U2OS cells (Figure 34) but not in cells transfected with two empty or one empty and one complete fusion plasmid (Figure 37).

To verify the previous co-localization in mitosis, 293T cells were co-transfected followed by synchronization to prophase with a thymidine-nocodazole block. Figure 35 displays the resulting image of Aurora B-p53 interaction (green) on the condensing chromosomes (Red, RFP-H2B). The interaction localizes to specific points on the DNA which may be the centromeres, a known locale for Aurora B. Figure 34B confirms this in MCF7 cells where the interaction of Aurora B and p53 can be seen in several prophase nuclei localizing to the condensed chromosomes stained by DAPI. An enlargement of a nuclei synchronized to mitosis with a thymidine-nocodazole block is shown in Figure 34C. Several outlying condensed chromosomes can be seen with green fluorescence (Venus) at a distinct point (arrows), which is likely the centromere. Confirmation of the Venus interaction at the centromere is shown in Figure 34C, bottom panel, where 293T cells were synchronized to prophase as before and fluorescence imaged for Venus and Survivin, another member of the CPC. The merge image confirms

that the interaction of p53 and Aurora B is occurring at least partially, at the centromere.

To verify that the observed interaction was not cell-specific, Hct116 cells were also transfected with the Venus plasmids containing Aurora B and p53. Consistent with 293T, localization of interaction was throughout the cells (Figure 36).

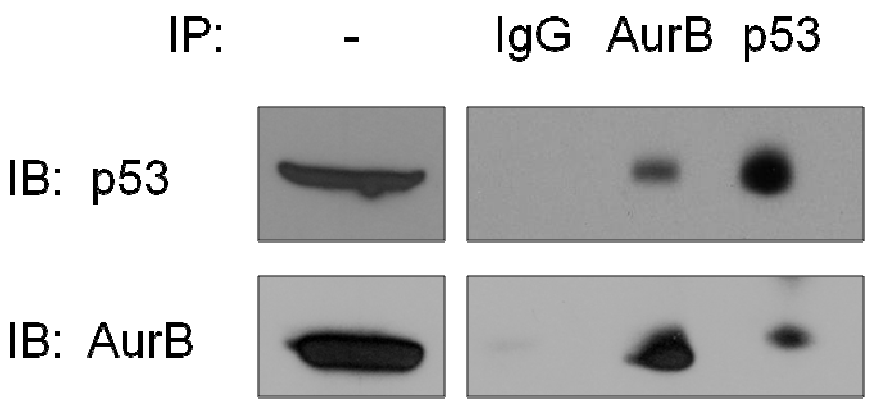

Figure 27. Aurora B and p53 exist in complex. Lysates of 293T cells were immunoprecipitated for endogenous proteins with either anti-Aurora B or anti-p53 antibodies followed by reciprocal immunoblot. Lysates were also IP'd with rabbit IgG as a control.

Figure 28

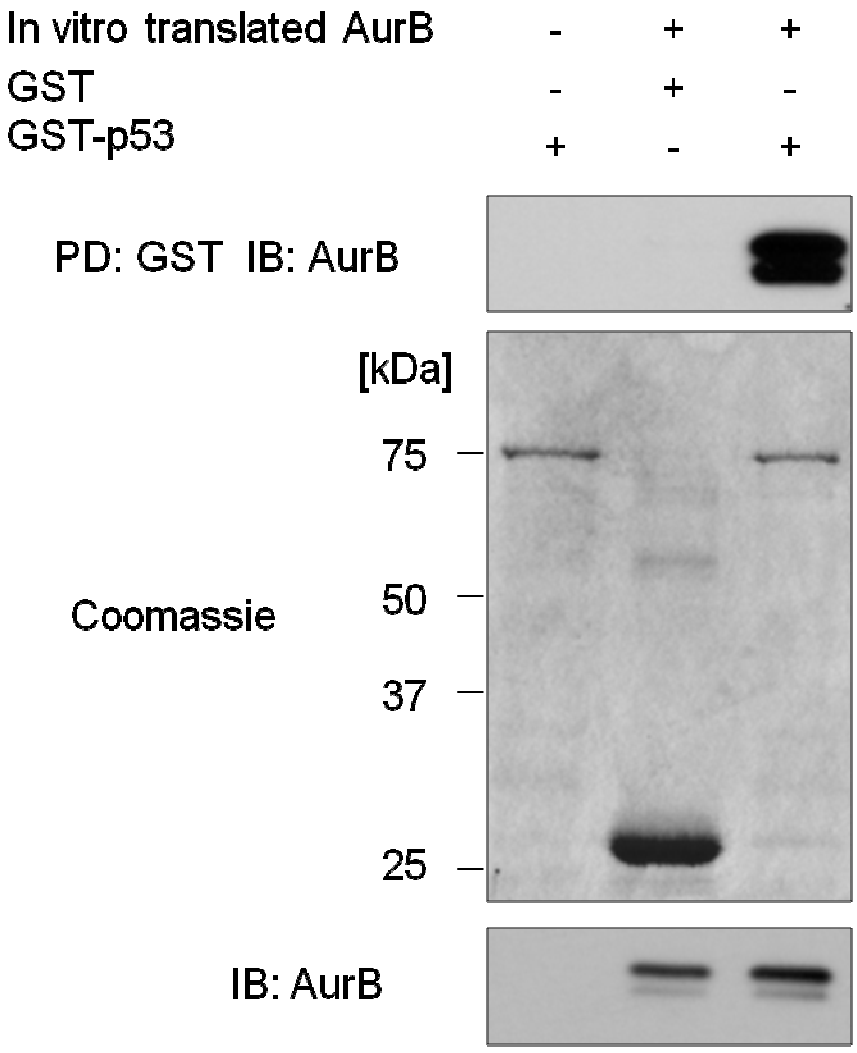

Figure 28. Aurora B and p53 interact directly. *In vitro* translated Aurora B was incubated overnight with recombinantly produced GST or GST-p53 fusion proteins. GST was pulled down with GST beads and precipitates were immunoblotted with anti-Aurora B antibody. GST inputs were analyzed by SDS-PAGE and Coomassie staining. Recombinant Aurora B inputs were immunoblotted directly with anti-Aurora B antibody.

Figure 29.

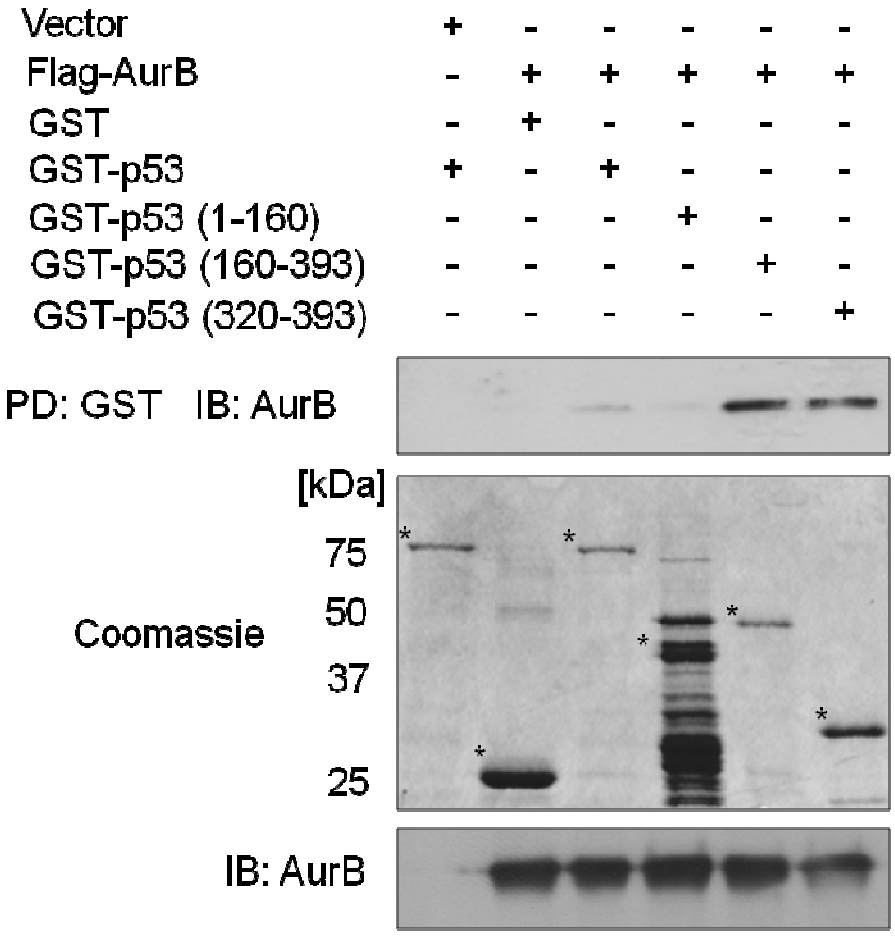

Figure 29. Aurora B binds both the DNA binding domain and C-terminus of p53. Flag-Aurora B plasmid was transfected into 293T cells and lysates immunoprecipitated with anti-Aurora B antibody. IP'd Aurora B was incubated overnight with GST, GST-p53 or GST-p53 deletion constructs that were produced recombinantly in E. coli. GST beads were used to pull down GST and lysates then immunoblotted with anti-Aurora B antibody. Aurora B inputs were analyzed by immunoblot and GST-fusion protein inputs by SDS-PAGE followed by Coomassie stain. * indicates GST-tagged proteins.

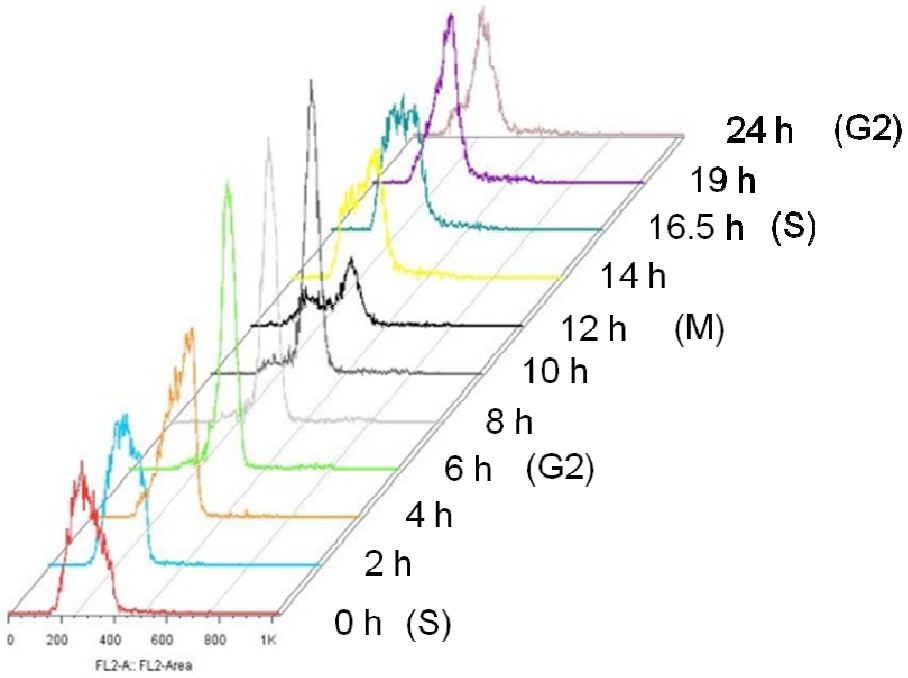

Figure 30. Hct116 cells synchronized with double-thymidine block. Hct116 cells were synchronized to S-phase with a double-thymidine block then released. At two hour intervals, cells were collected and stained with propidium iodide. Cell cycle analysis was done by flow cytometry. Cell cycle phase is indicated at right.

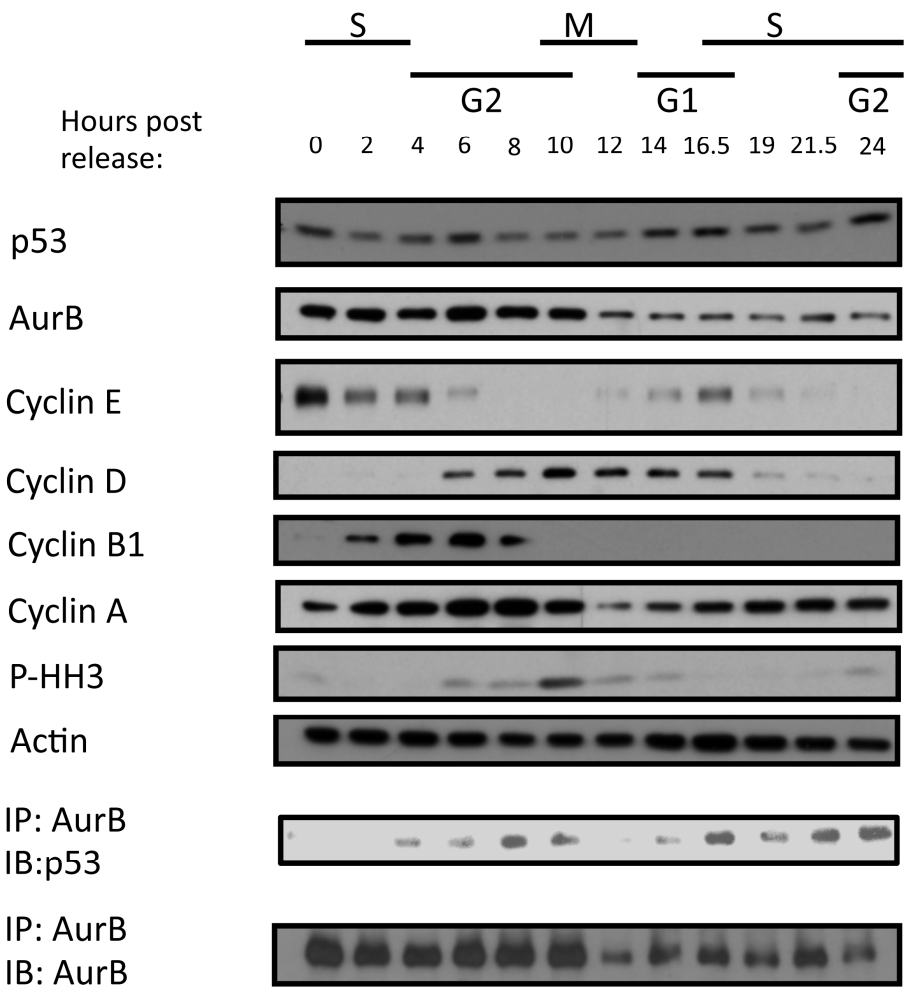

Figure 31. Aurora B and p53 interact during late S and G2/M phases of the cell cycle. Hct116 cell lysates from Figure 30 were immunoblotted for p53, Aurora B, phospho-Histone H3 and Cyclins D, E, A and B1. Lysates were also immunoprecipitated for Aurora B and analyzed by immunoblot for p53 and Aurora B. Hours post release and cell cycle phase are indicated above.

Figure 32

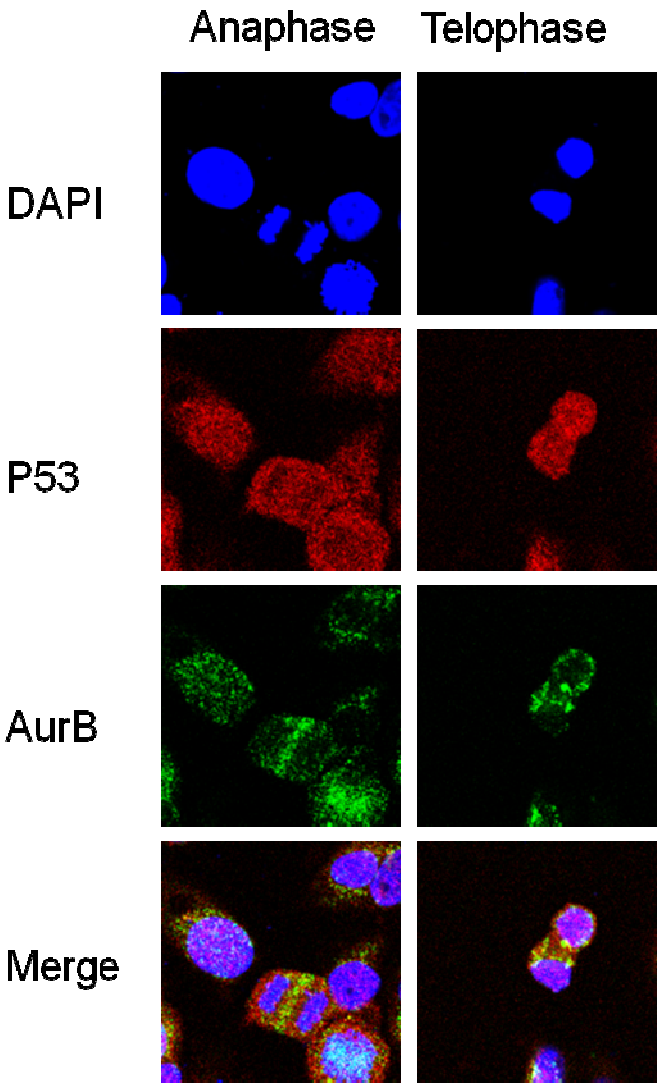

Figure 32. Endogenous p53 and Aurora B colocalize during mitosis. Her18 cells planted in chamber slides were fixed and immunostained for endogenous p53 and Aurora B as well as stained with DAPI. Alexa-fluor 488 and 568 conjugated secondary antibodies were used in the immunostaining. Photomicrographs of cells in anaphase and telophase are shown. Co-localization is displayed as yellow color in the merge image.

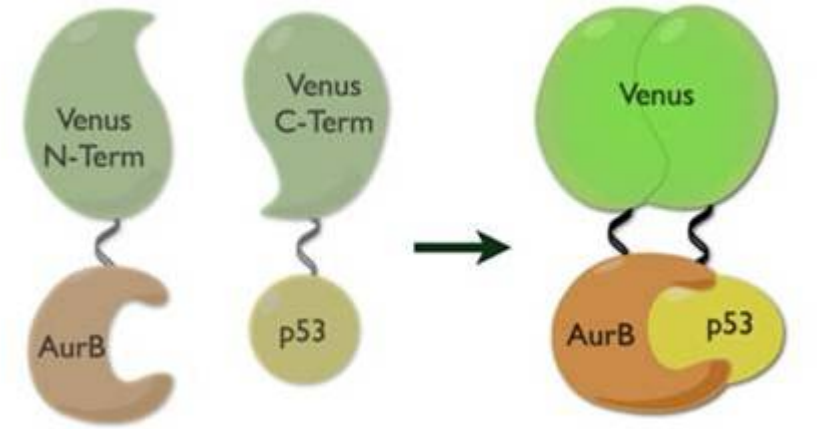

Figure 33. Schematic diagram of the Venus fusion protein system. The Venus (YFP variant) fusion protein interaction system works by inserting the cDNA of a protein of interest in a plasmid containing each half of the Venus protein. Plasmids are then co-transfected and any interaction is observed by fluorescence microscopy.

Figure 34A

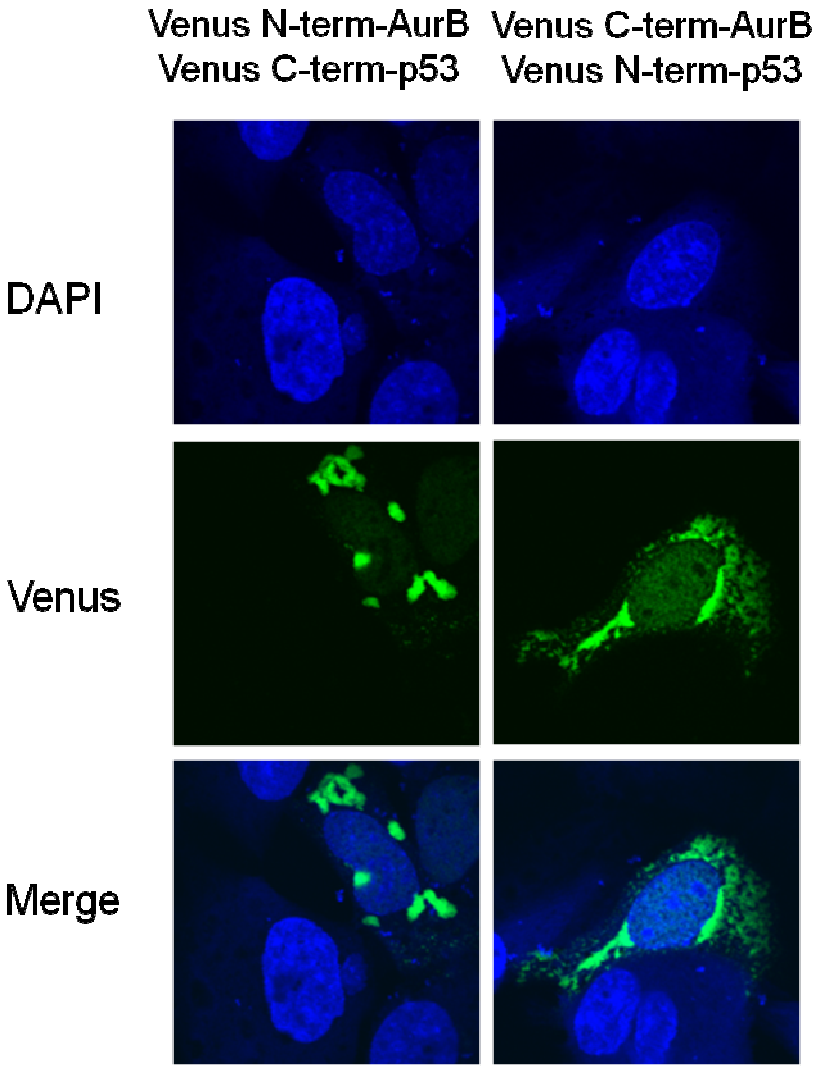

Figure 34B

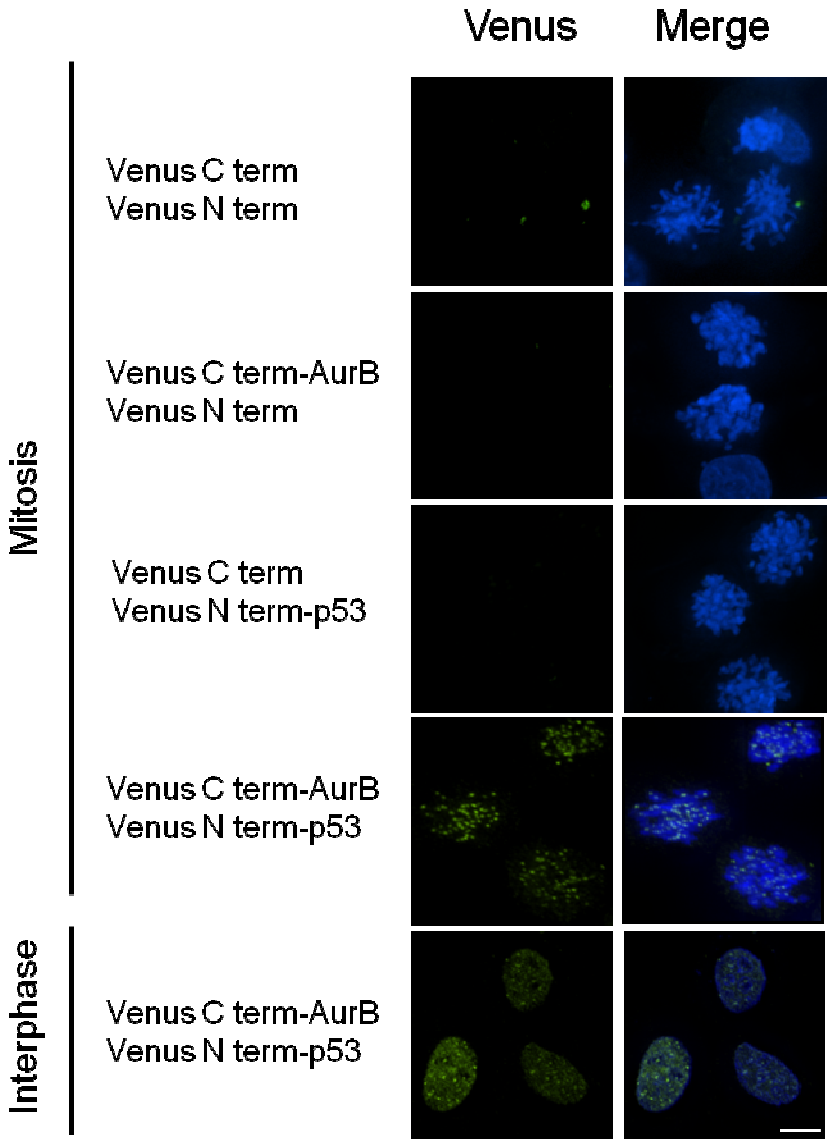

Figure 34C

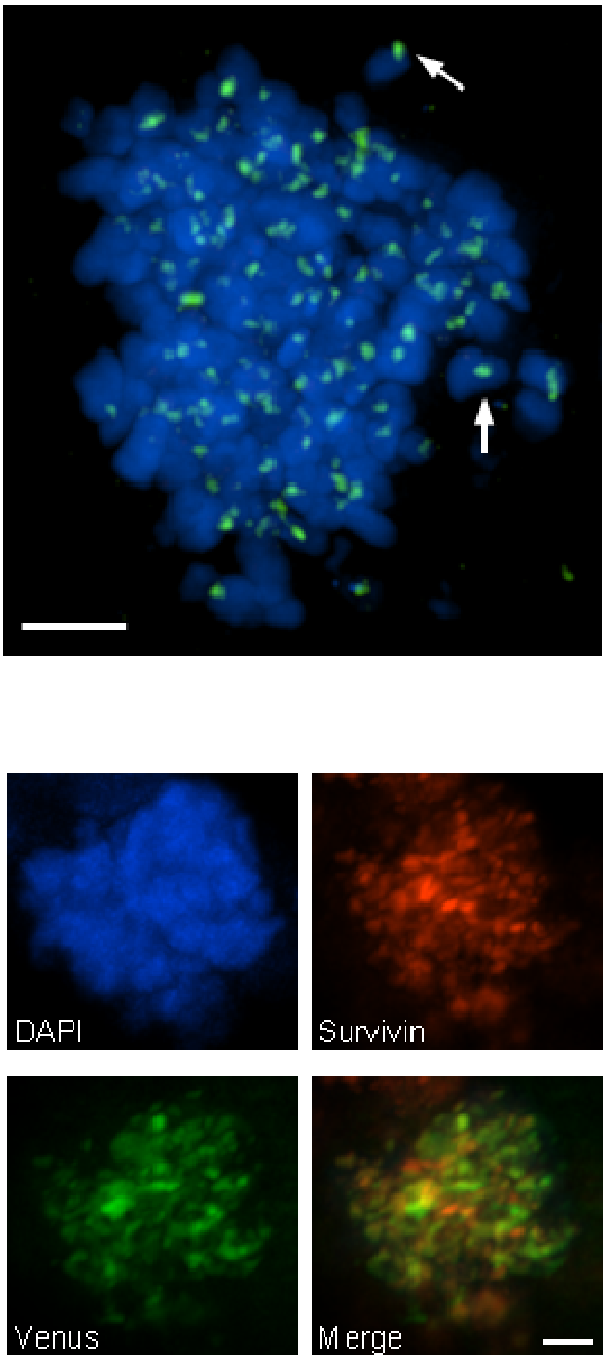

Figure 34. Aurora B and p53 interact directly in both the cytoplasm and nucleus during interphase and mitosis. A Venus N-terminal-Aurora B and Venus C-terminal-p53 plasmids (and the reverse combination) were co-transfected into U2OS cells. Cells were fixed, stained with DAPI and imaged by fluorescence microscopy. Direct interaction of p53 and Aurora B is indicated by green fluorescence. B MCF7 cells were transfected as in A as indicated and synchronized to mitosis using a thymidine-nocodazole block. Scale bar = 10 μm. C Top panel, enlargement of an MCF7 nuclei synchronized as in B to mitosis. Arrows indicate condensed chromosomes with green staining (Venus) at the centromere. Scale bar = 4 μm. Bottom panel, 293T nuclei synchronized to prophase with thymidine-nocodazole block as in B. Immunofluorescence staining for DAPI, Venus (interaction of Aurora B and p53 as in A) Survivin and merge image for red and green channels are shown.

Figure 35

RFP-H2B
Venus C-term-AurB
Venus N-term-p53

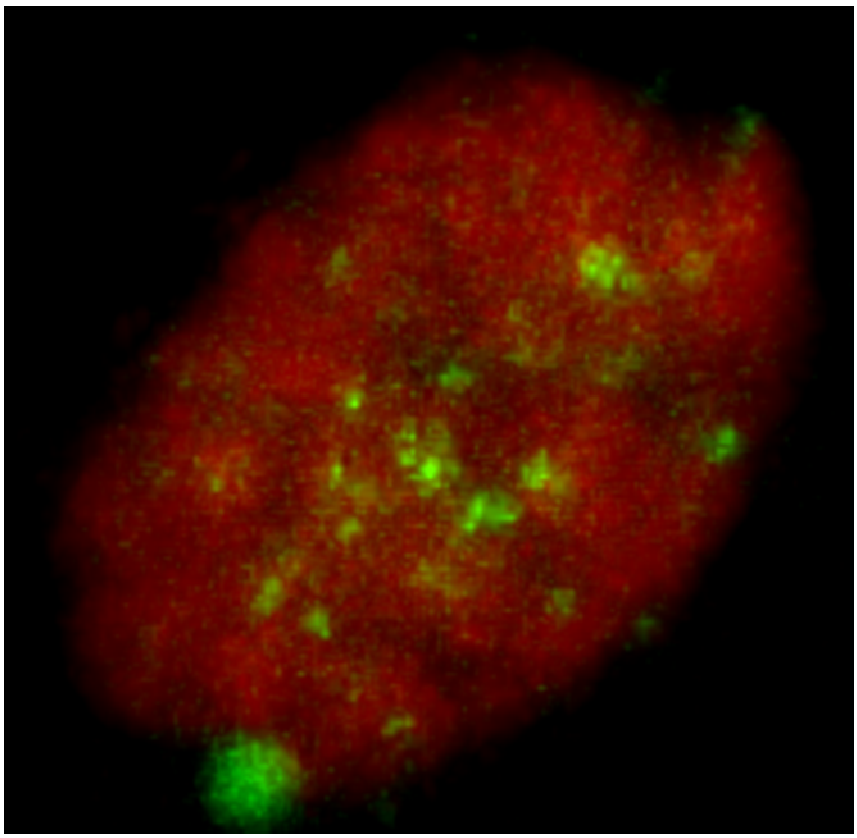

Figure 35. p53 and Aurora B interaction occurs on the DNA during mitosis. 293T cells were transfected with the indicated Venus fusion plasmids and RFP-H2B. Cells were synchronized to prophase with nocodazole and live-imaged by spinning-disk confocal microscopy. Red indicates H2B (DNA) and green indicates direct interaction of Aurora B and p53.

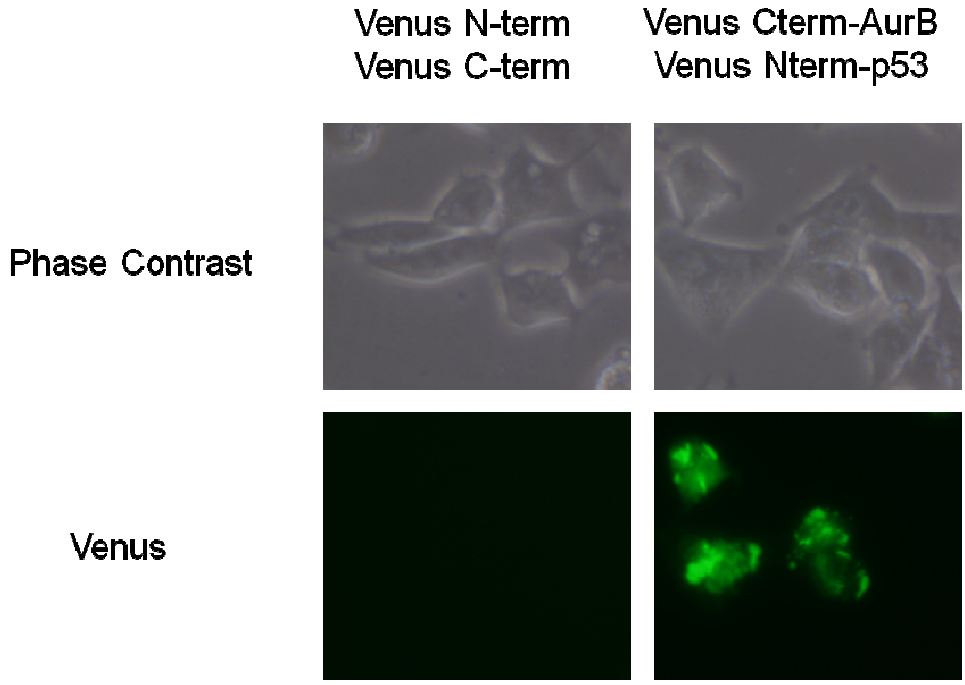

Figure 36. The association between p53 and Aurora B is also present in Hct116 cells. Hct116 cells were transfected with the indicated empty Venus (control) or Venus fusion plasmids and live-imaged by fluorescence microscopy and phase contrast.

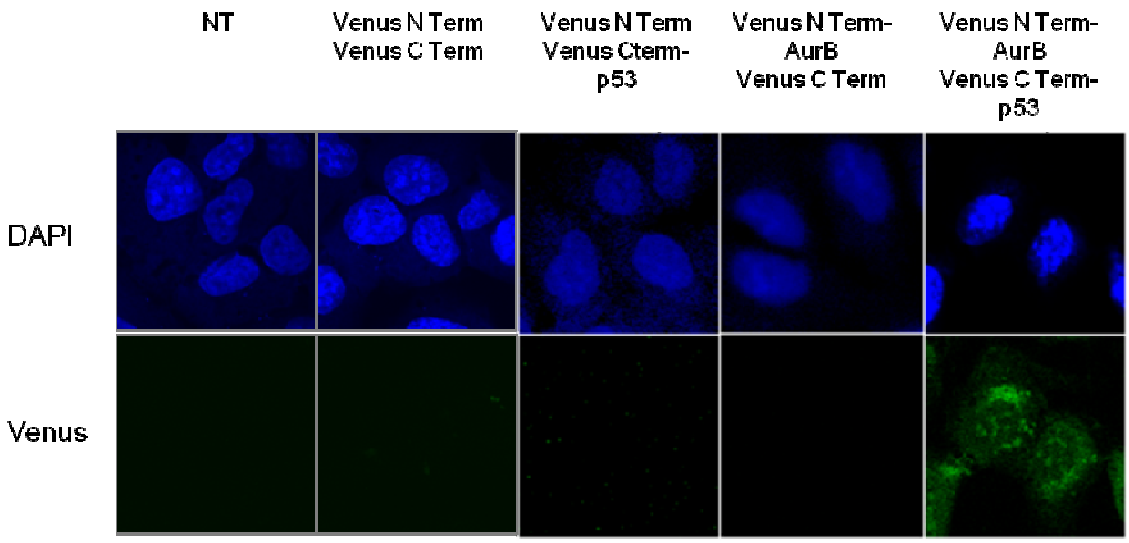

Figure 37. Venus fusion system showing Aurora B and p53 direct colocalization controls. U2OS cells were co-transfected with the indicated control plasmids or Venus fusion plasmids. Cells were fixed, stained with DAPI and imaged via confocal fluorescence microscopy.

3.2.3 Aurora B phosphorylates p53.

Having established that p53 and Aurora B interact directly, investigation of p53 phosphorylation by Aurora B was the logical next step because of Aurora B's kinase activity. To do this, Aurora B immunoprecipitated by 293T cells was incubated with GST or GST-p53 in the presence of ^{32}P labeled ATP in an *in vitro* kinase assay (Figure 38). Aurora B was found to phosphorylate GST-p53 strongly compared to control substrate GST. Kinase reactions where no Aurora B was added did not show p53 phosphorylation.

Once it was established that IP purified Aurora B phosphorylated p53, determination that this was due to Aurora B kinase activity, and not by a contaminating kinase was necessary. This was accomplished through an in vitro kinase assay as before but using IP purified wild type Aurora B or kinase dead Aurora B where lysine 106 was replaced with an arginine (Chen et al., 2003). See Table 5 for primer sequences. Figure 39 shows that wild type Aurora B and not kinase dead Aurora B phosphorylated GST-p53.

Since it was observed in previous results that AZD1152 reduced Aurora B activity and induced p53 level when used in xenografts of breast cancer cells, AZD1152 should be able to reduce the ability of Aurora B to phosphorylate p53. To investigate this, an *in vitro* kinase assay was performed as before but in the presence of increasing dose of AZD1152. Figure 40 clearly shows that 50 nM AZD1152-HQPA inhibited phosphorylation of p53 as well as Aurora B autophosphorylation.

Figure 38

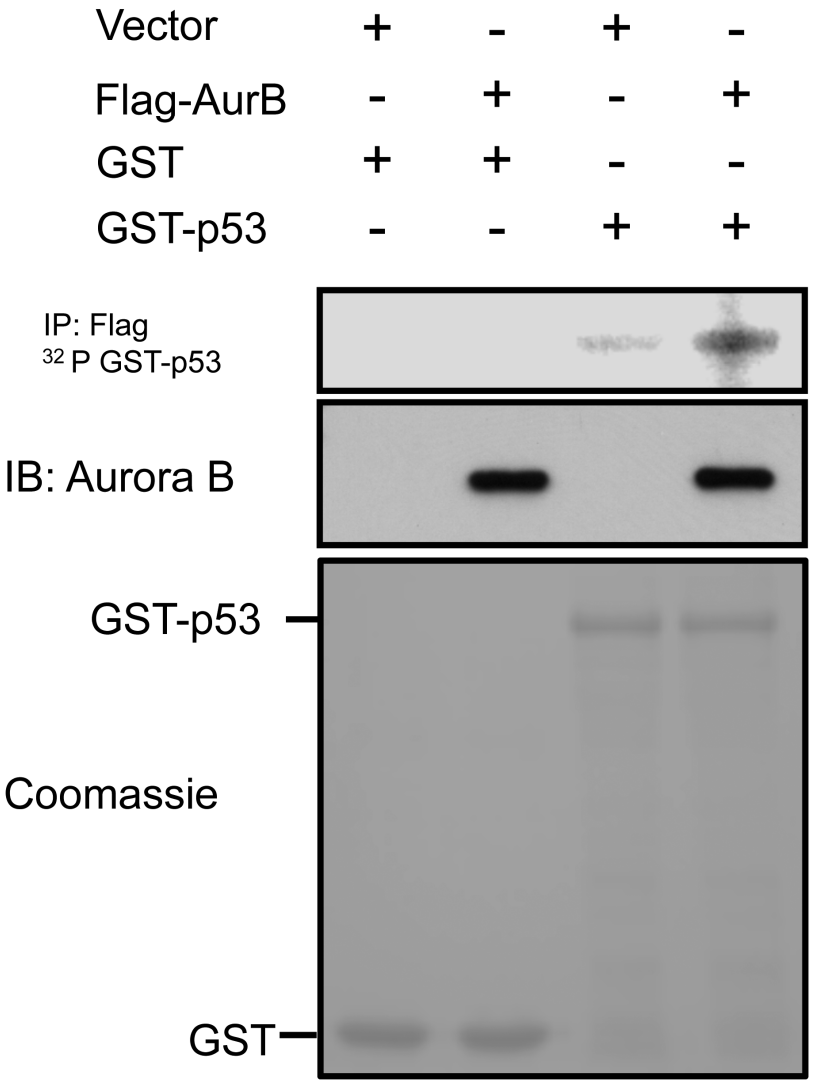

Figure 38. Aurora B phosphorylates p53 *in vitro*. Immunoprecipitated Flag-Aurora B was incubated with GST or GST-p53 substrates in the presence of ^{32}P ATP. Phosphorylated substrates were detected with a phosphoimager. Aurora B inputs were analyzed by immunoblot and GST-tagged substrates by SDS-PAGE and Coomassie staining.

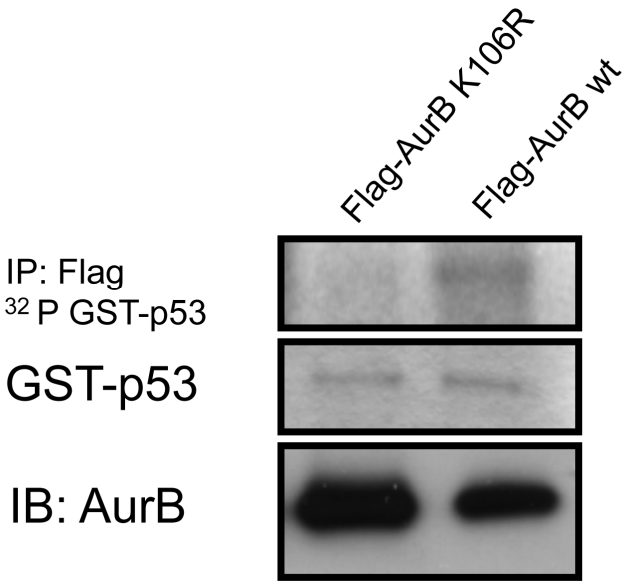

Figure 39. Aurora B but not kinase dead Aurora B phosphorylates p53. Immunoprecipitated Flag-Aurora B or Flag-Aurora B K106R (kinase dead) were incubated with GST-p53 in an *in vitro* kinase assay as in Figure 38. Aurora B and GST-tagged inputs were analyzed by immunoblot.

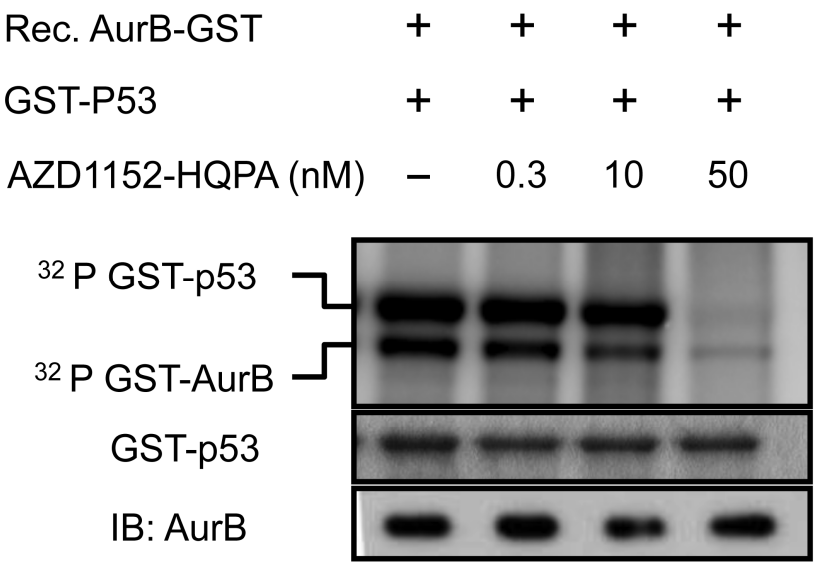

Figure 40. Aurora B mediated phosphorylation of p53 is inhibited by AZD1152-HQPA. Recombinant GST-Aurora B was used in an *in vitro* kinase assay with GST-p53 substrate, as in Figure 38, with increasing dose of AZD1152-HQPA. p53 input was analyzed by SDS-PAGE and Coomassie stain. Recombinant GST-Aurora B input was analyzed by immunoblot for Aurora B.

3.2.4 Aurora B phosphorylates multiple serine/threonine residues in the DNA binding domain of p53.

The next step in further characterizing the phosphorylation of p53 by Aurora B, is to determine where the phosphorylation is occurring. To address this, an *in vitro* kinase assay was performed in which p53 deletion constructs (Figure 41) were used as substrates for Aurora B. Figure 42 shows that Aurora B phosphorylates p53 only in the wild type and the 160-393 construct (indicated by *), while it does not phosphorylate the 320-393 region. This indicates that the phosphorylation occurs between residues 160-320 roughly corresponding to the DNA binding domain of p53. This result is consistent with the *in vitro* binding data in Figure 28 where Aurora B was found to bind the DNA binding domain. A multiple alignment of the p53 DNA binding domain of higher eucaryotes is displayed in Figure 43 and shows that there are five possible phosphorylation sites for Aurora B kinase that match the consensus phosphorylation sequence: $(R/K)_{1.3}X(S/T)$. Further, four of the five sites are fully conserved from Zebra fish to humans with the exception of S183 which is not conserved in Zebra fish only. The evolutionary conservation of these sites lends weight to their importance in the regulation of p53. Figure 44 displays the Netphos scores indicating likely phosphorylation by potential kinases for each of the five sites (Blom et al., 1999). To determine which of the five putative sites in p53's DNA binding domain were phosphorylated, another *in vitro* kinase assay was performed where GST-p53 was mutated in each of the sites to an alanine residue. Recombinant Aurora B was used to phosphorylate each of these mutants as well as wild type p53 and

phosphosubstrates were analyzed for comparison. Figure 45 shows that at least four of the five sites were phosphorylated with S215 being the strongest and T284 not phosphorylated at all. S183, T211 and S269 were also phosphorylated and are listed in order of strength. An alternative interpretation is also possibly. S215 may be the major phosphorylation site with the other sites being required for association of the kinase with p53.

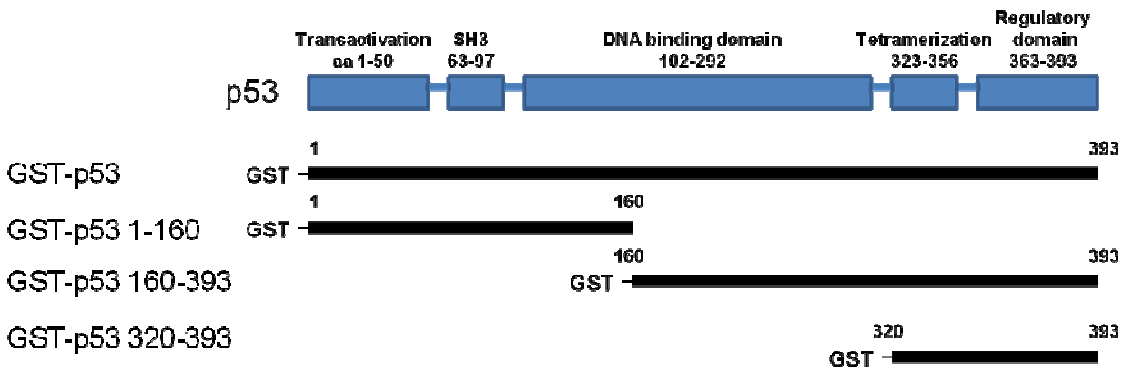

Figure 41. GST-tagged p53 deletion constructs.

Figure 42

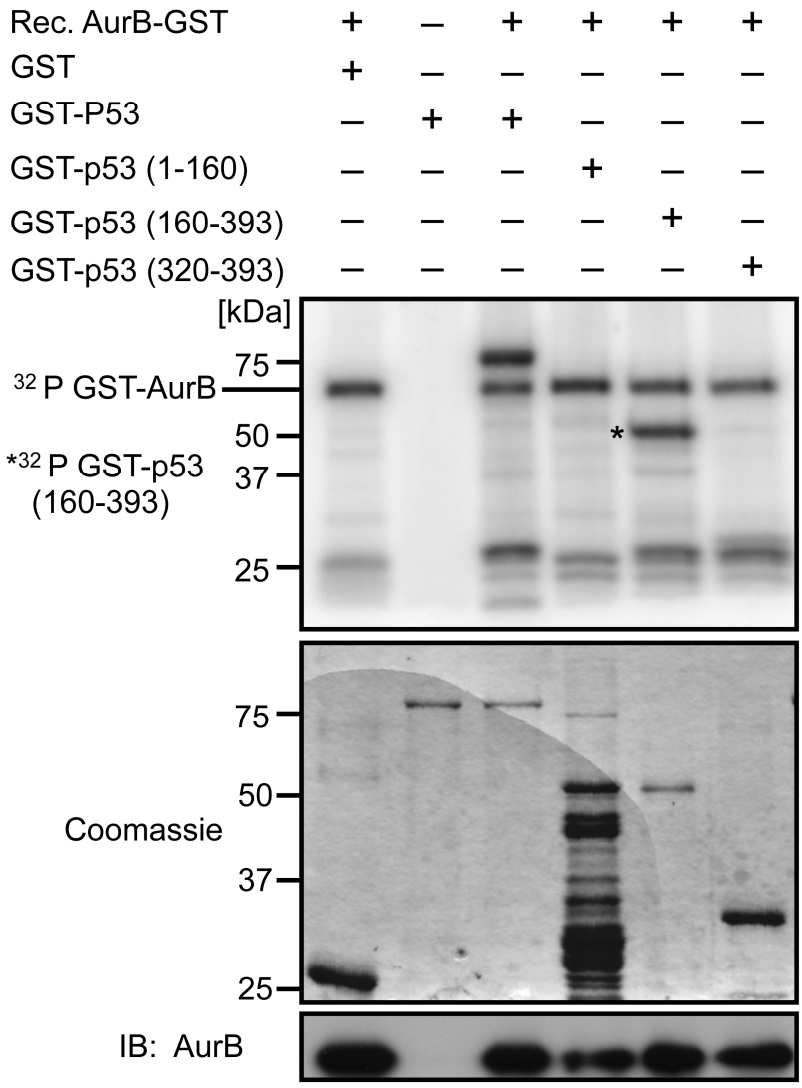

Figure 42. Aurora B phosphorylates p53 in the DNA binding domain. Recombinant Aurora B was incubated with GST, GST-p53 or GST-p53 deletion constructs as substrates in an *in vitro* kinase assay. ^{32}P labeled substrates were detected with a phosphoimager. GST-tagged substrate inputs are shown as Coomassie stained bands, recombinant Aurora B input was analyzed via immunoblot. * indicates phosphorylated GST-p53 (160-393).

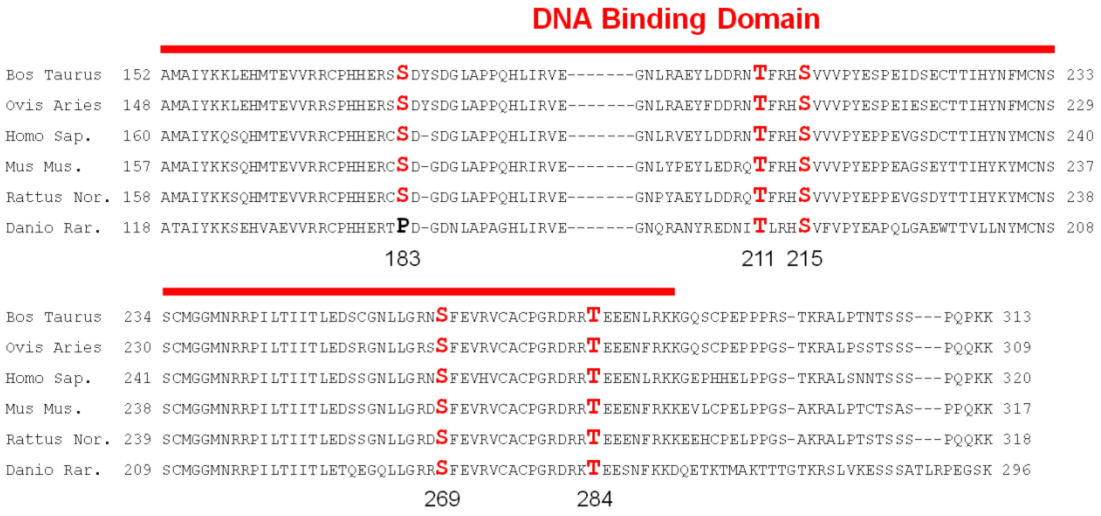

Figure 43. Putative Aurora B phosphorylation sites in the p53 DNA binding domain. Multiple alignment of the p53 DNA binding domain of higher eukaryote species with five putative Aurora B phosphorylation sites shown. Conserved residues are shown in red.

Site	Score
S183	0.993
T211	0.951
S215	0.933
S269	0.957
T284	0.866

Figure 44. Putative Aurora B phosphorylation residues in p53 and their Netphos scores.

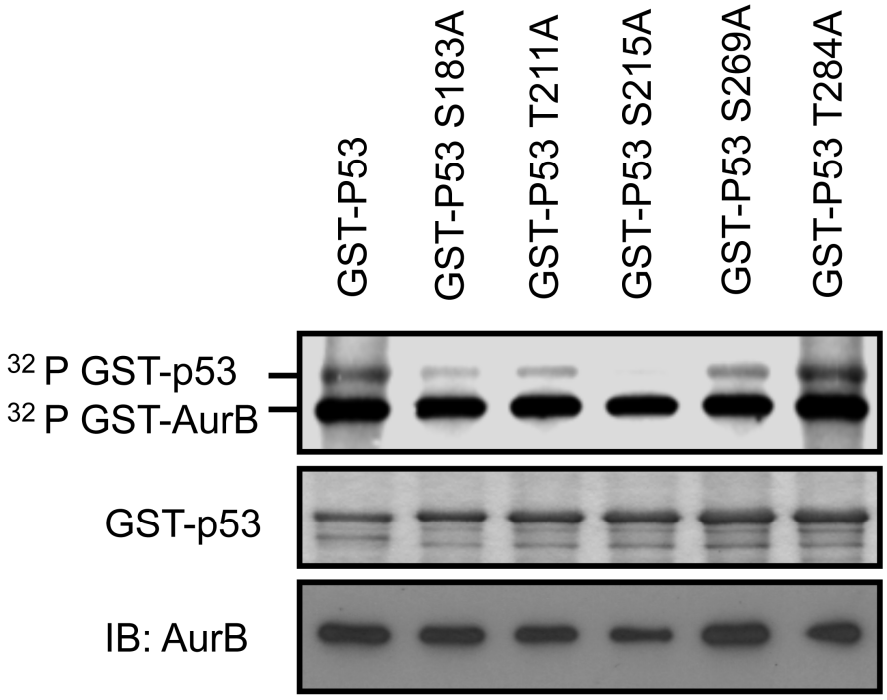

Figure 45. Aurora B phosphorylates four serine/threonine residues in the p53 DNA binding domain. GST-tagged p53 was mutated to contain five separate alanine mutations in the DNA binding domain: S183A, T211A, S215A, S269A and T284A. Wild type and mutated GST substrates were incubated with recombinant Aurora B kinase in an *in vitro* kinase assay. Phosphorylated substrate and Aurora B autophosphorylation were detected with a phosphoimager. GST-p53 substrate inputs were detected by Coomassie stain, Aurora B input was detected by immunoblot.

3.2.5 Aurora B destabilizes p53 via the ubiquitination-proteasome system.

Functional relevance of the phosphorylation of p53 by Aurora B was the next thing investigated in this study. First, the focus was put on whether Aurora B can affect p53 stability or expression. Figure 46 focuses on the steady state level of p53 when Aurora B is overexpressed in increasing dose. The results show that as Aurora B level increased, p53 levels dropped, indicating that Aurora B can effect a change in p53 steady state level. To determine if Aurora B could alter the turnover rate of p53, Flag-Aurora B was transfected into U2OS cells in the presence of cycloheximide (CHX). As Figure 47 shows (top), p53 was degraded faster in the presence of Aurora B versus the control, where no Aurora B was present. To confirm that this result was happening not only in an overexpression system, but also in endogenous p53 levels, 293T cells were infected with lentiviruses containing either control (shRNA luciferase) or Aurora B knockdown shRNA (shRNA 468 AurB), again in the presence of CHX. The result shows that when Aurora B was knocked down, p53 turnover was reduced (Figure 47, bottom panel). These assays confirm that Aurora B affects p53 protein level in both overexpressed and endogenous proteins.

To determine if the increased turnover of p53 observed in the presence of Aurora B is due to proteasomal degradation, p53 null H1299 cells were transfected with GFP-p53 and Flag-Aurora B in the presence of MG341 (Velcade), a proteasome inhibitor. Indeed, MG341 was able to rescue the p53

protein level in the presence of overexpressed Aurora B indicating that Aurora B is mediating the degradation of p53 via the proteasome (Figure 48).

Proteasomal degradation of p53 mediated by ubiquitination of p53 was investigated by performing an ubiquitination assay. 293T cells were transfected with p53, Mdm2 and HA-ubiquitin as indicated in Figure 49. 24 hours prior to harvest, cells were treated with increasing dose of AZD1152-HQPA. Cells were also treated with MG132 five hours prior to harvest. At harvest, cell lysates were immunoprecipitated with anti-HA antibody to isolate ubiquitinated proteins. Ubiquitinated p53 was detected via immunoblot. Figure 49 (top panel) shows that the basal level of p53 ubiquitination in cells was decreased in a dose dependent fashion by the addition of AZD1152-HQPA. This indicates that inhibition of Aurora B increases p53 ubiquitination and agrees with the results in Figure 48 that Aurora B mediates the breakdown of p53 via the proteasome. Of note is that the dosage of AZD1152-HQPA was in the nanomolar range, which is relevant to the IC_{50}s reported for several cell lines in Figures 5 and 6. The bottom panel of Figure 49 also shows that the ubiquitination of p53 is increased by Aurora B with the overexpression of Aurora B itself, and also confirms that Mdm2 is at least partially responsible for the ubiquitination mediated by Aurora B.

It is a possibility that Aurora B could also be affecting the expression level of p53 by regulating genes upstream of p53 or p53 mRNA levels directly. To rule this out, U2OS and Hct116 cells were transfected with Aurora B. mRNA levels of p53 and several p53 target genes were measured by qRT-PCR. In both cases,

p53 mRNA was not affected, however, mRNA levels of p53 target genes Mdm2, p21 and BAX all show reduced levels in the presence of Aurora B (Figure 50). This is confirmation that p53 level is reduced post-translationally by Aurora B and p53 then has a reduced capacity to affected the expression of its target genes.

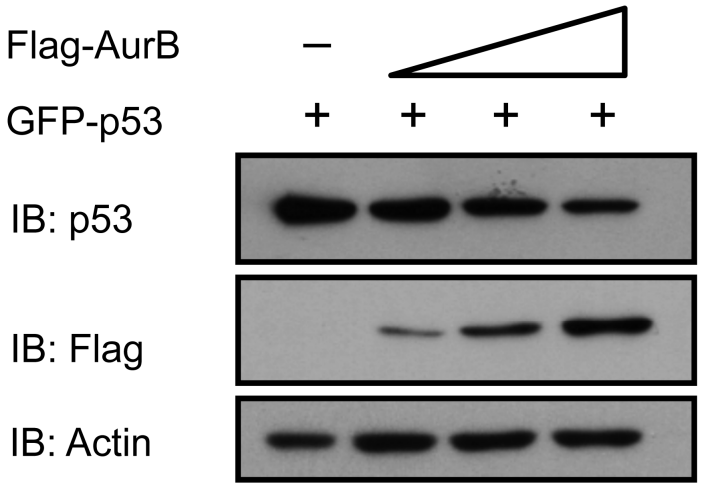

Figure 46. Aurora B reduces p53 steady state level. GFP-p53 and an increasing dose of Flag-Aurora B were transfected in p53 null H1299 cells as indicated. p53, Flag-Aurora B and Actin were detected by immunoblot.

Figure 47

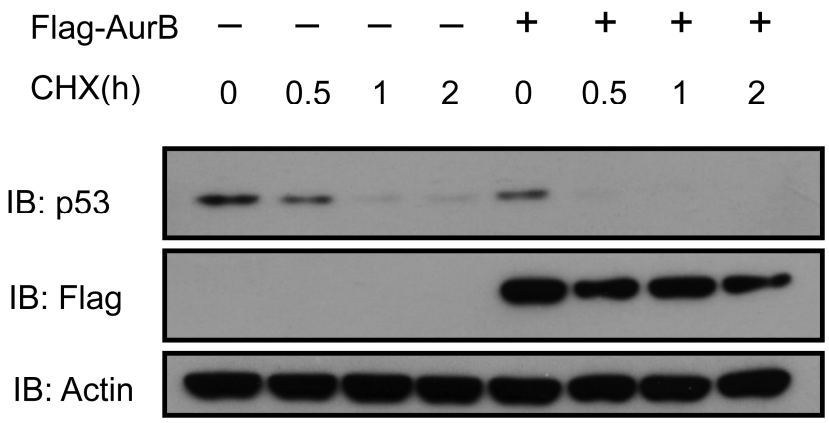

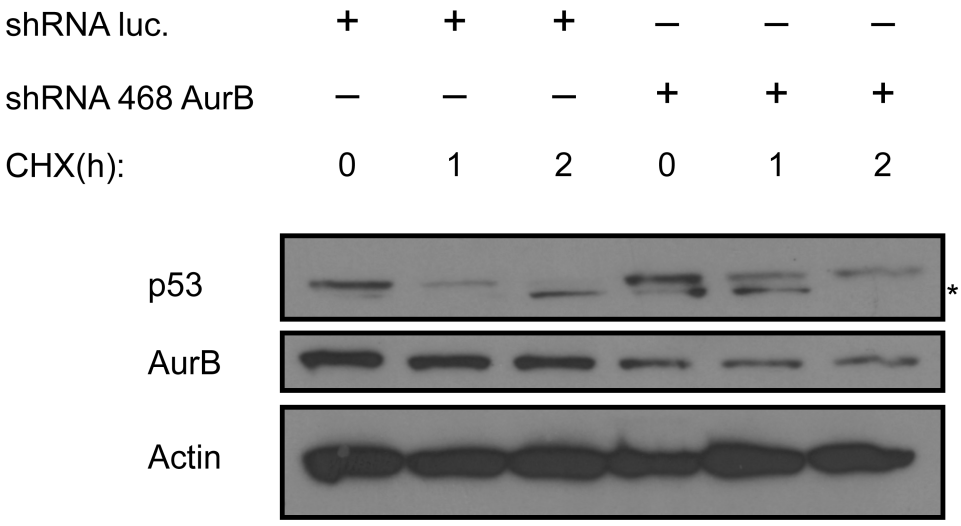

Figure 47. Aurora B increases the turnover rate of p53. Top, U2OS cells were transfected with and without Flag-Aurora B and treated with cycloheximide 2 hours prior to harvest. p53, Flag-Aurora B and Actin were analyzed by immunoblot. Bottom, 293T cells were infected with lentiviruses containing control shRNA-luc. or shRNA 468 AurB. Cells were treated with cycloheximide two hours prior to harvest and lysates analyzed by immunoblot for endogenous p53, Aurora B and Actin. * indicates a non-specific band.

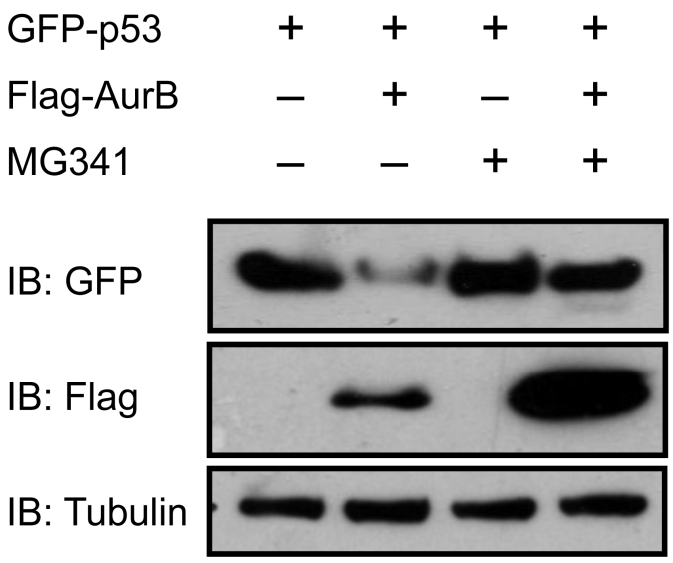

Figure 48. Aurora B mediates turnover of p53 via the proteasome. p53 null H1299 cells were transfected with GFP-p53 and Flag-Aurora B as indicated then treated with MG341 (Velcade), a proteasome inhibitor, for 24 hours prior to harvest. Cell lysates were analyzed by immunoblot for GFP-p53, Flag-Aurora B and Tubulin.

Figure 49

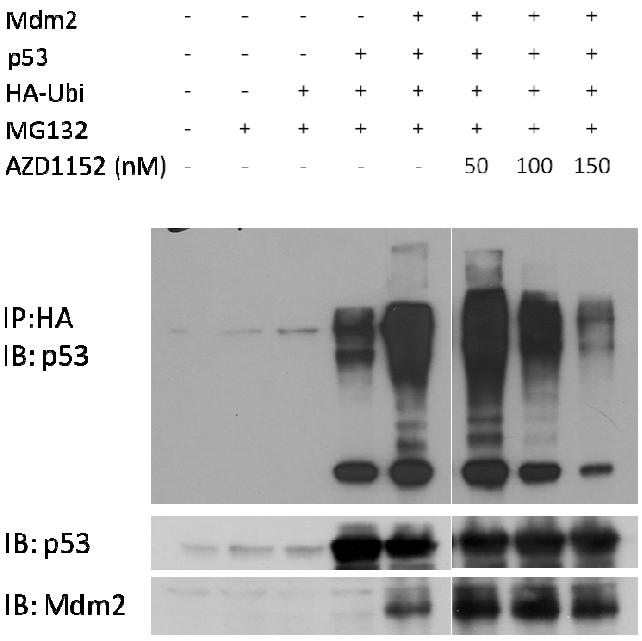

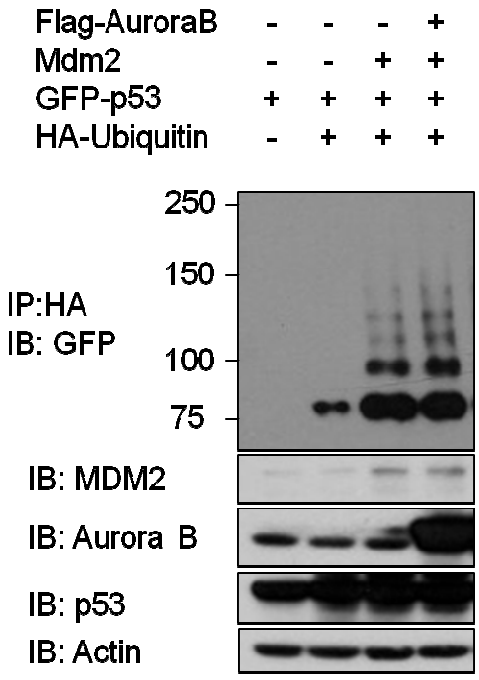

Figure 49. Mdm2 ubiquitination of p53 is increased by Aurora B. Top panel, 293T cells were transfected with p53, Mdm2 and HA-ubiquitin plasmids as indicated. AZD1152-HQPA was applied 24 hours prior to harvest. Five hours prior to harvest, cells were treated with MG132 to accumulate ubiquitinated proteins. Cell lysates were immunoprecipitated with anti-HA antibody and immunoblotted for p53. Bottom Panel, plasmids were transfected as indicated and lysates immunoprecipitated with anti-HA antibody. Ubiquitinated p53 was detected by immunoblot with anti-GFP antibody.

Figure 50

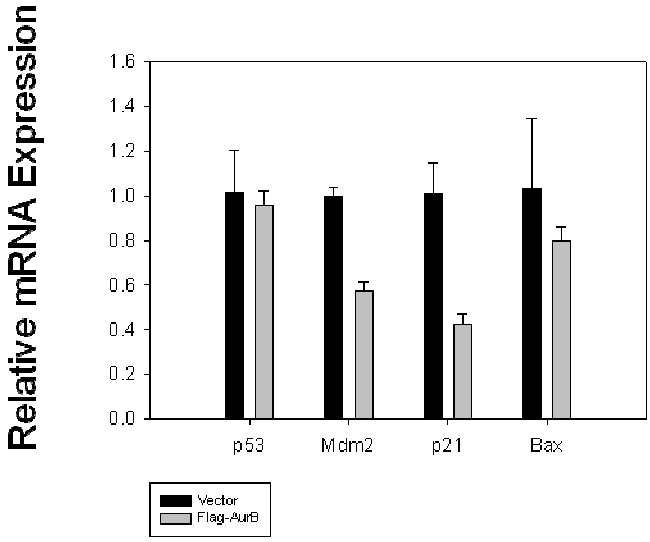

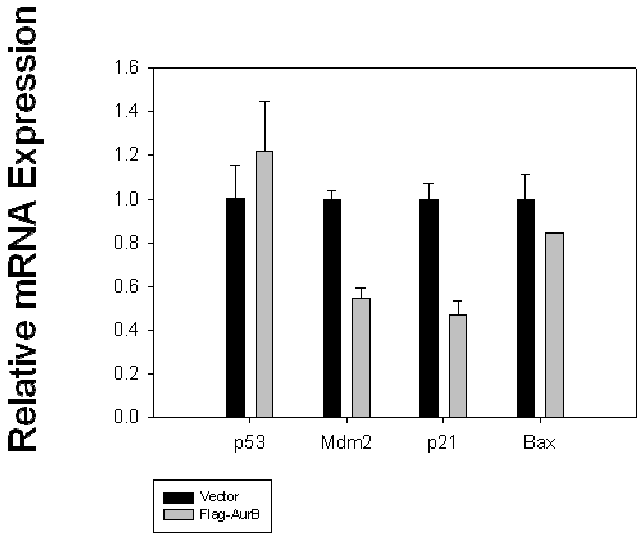

Figure 50. Aurora B affects p53 at the post-transcriptional level. U2OS (top) and Hct116 (bottom) cells were transfected with vector control or Flag-Aurora B kinase and analyzed by qRT-PCR for p53 or p53 target mRNA levels. Error Bars: 95% CI.

3.2.6 p53 transcriptional activity and oligomerization are decreased by Aurora B.

It has been established that the phosphorylation of p53 by Aurora B destabilizes p53 and leads to its degradation via the ubiquitin proteasome system. This should also cause p53 transcriptional activity to be decreased by Aurora B. To investigate this, a dual luciferase reporter system was used in which a p53 reporter luciferase plasmid containing the p53 response elements from the 14-3-3σ promoter were inserted upstream of the firefly luciferase gene. A second luciferase plasmid, Renilla luciferase, is used as a transfection control. In addition to the luciferase reporters, GFP-p53 and increasing dose of GFP-Aurora B plasmids were transfected into 293T cells. p53 transcriptional activity was measured with a luminometer. Figure 51 shows that as Aurora B increased, p53 transcriptional activity dropped. This was confirmed by another luciferase assay where Aurora B was silenced using transfection of an shRNA plasmid (Figure 52, top). Figure 52, bottom panel, shows that as the dose of shRNA 468-AurB plasmid increased, p53 transcriptional activity increased. Together these results indicate that Aurora B can reduce the ability of p53 to bind the p53 response elements in the 14-3-3σ promoter and turn on transcription.

In a further confirmation of the effect of Aurora B on p53 transcriptional activity, a p53 oligomerization assay was performed in the presence of either Flag-Aurora B or the kinase dead Flag-Aurora B K106R. To detect p53 oligomers, cell lysates were treated for 15 minutes with 0.01% glutaraldehyde.

Figure 53 depicts the p53 immunoblot analysis of these cell lysates and shows that in the presence of Aurora B, p53 oligomerization is eliminate,d while K106R Aurora B cannot completely eliminate oligomers. These results confirm and add another layer of regulation to the previous evidence that Aurora B can reduce p53 transcriptional acitivity.

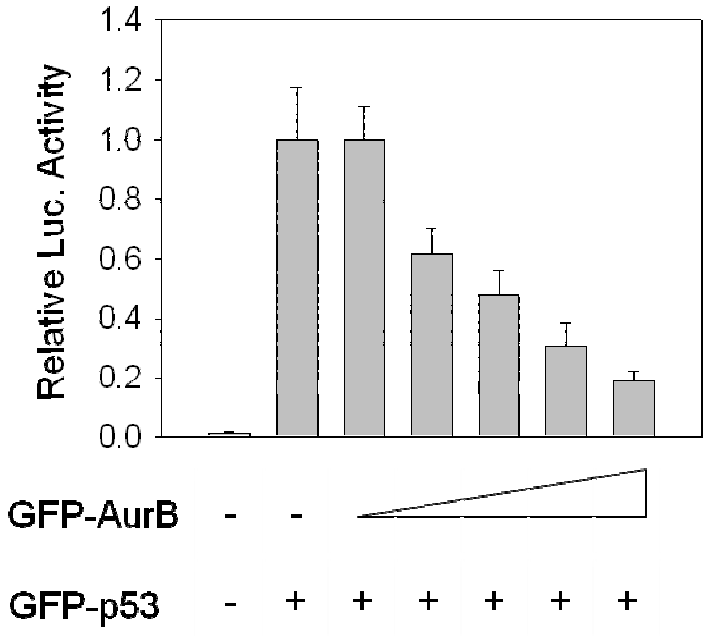

Figure 51. Overexpression of Aurora B decreases p53 transcriptional activity. 293T cells were transfected with GFP-p53 and increasing dose of GFP-Aurora B. p53 transcriptional activity was measured with a dual luciferase reporter system using a p53 luciferase reporter (14-3-3σ promoter) and Renilla luciferase. Baseline p53 transcription was set at 1, error bars are 95% confidence intervals.

Figure 52

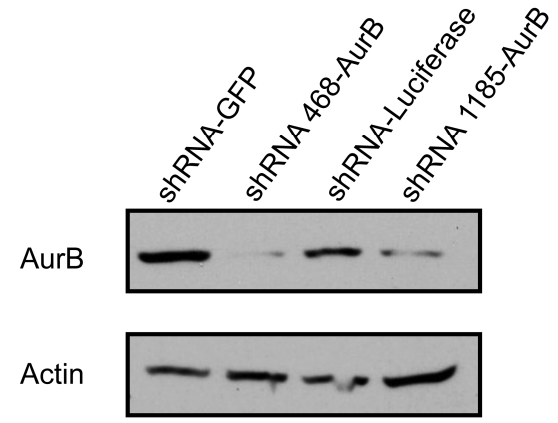

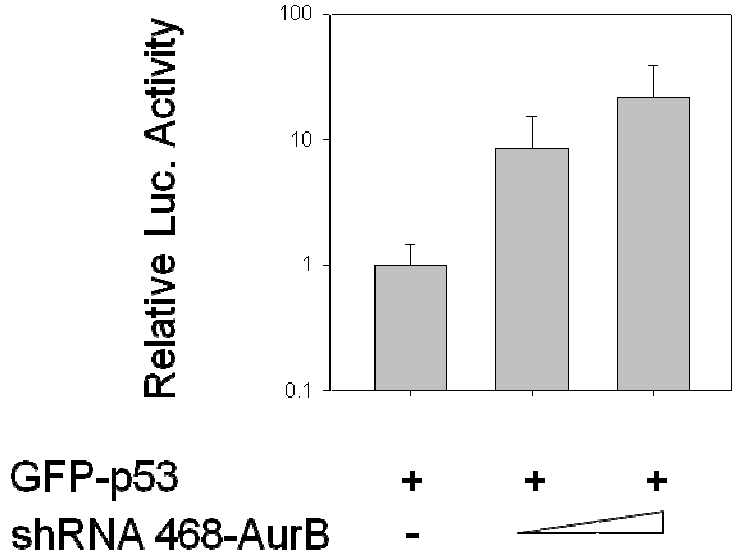

Figure 52. Knockdown of Aurora B increases p53 transcriptional activity. Top panel, 293T cells infected with lentivirus controls, shRNA-GFP or shRNA luciferase, and lentivirus knockdowns of Aurora B, shRNA 468-AurB or shRNA 1185-AurB. Knockdown of Aurora B was detected by immunoblot. Bottom panel, 293T cells were transfected with GFP-p53 and increasing dose of shRNA 468-AurB plasmid. p53 transcriptional activity was measured as in Figure 51. Error bars: 95% CI.

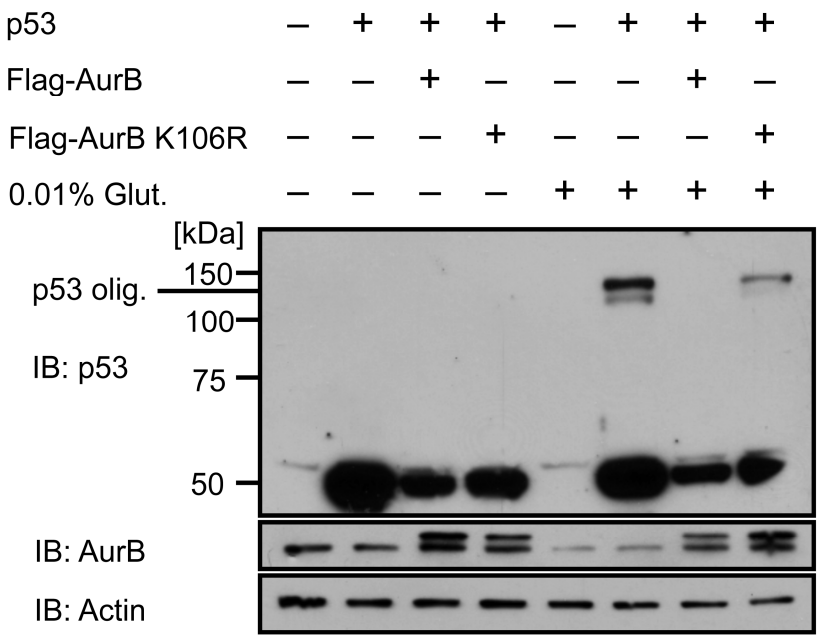

Figure 53. p53 oligomerization is decreased by Aurora B mediated phosphorylation. H1299 cells were transfected with p53 and Flag-Aurora B or Flag-Aurora B K106R with 0.01% glutaraldehyde. p53 oligomers were detected by immunoblot.

3.2.7 Phosphorylation of threonine 211 in p53's DNA binding domain reduces transcriptional activity and increases turnover.

To determine the functional relevance of the Aurora B phosphorylation sites in p53's DNA binding domain, three of these sites were mutated to alanine, which cannot be phosphorylated, and several functional assays carried out. First a luciferase assay was performed to determine which phosphorylation site(s) is important for p53 transcriptional activity. Figure 54 shows the result of this assay where p53 null H1299 cells were transfected with and without Aurora B and various p53 constructs. Control transfection luciferase activity was set at 1 (horizontal bar) and reduction of p53 transcription by Aurora B compared relative to this. By this result, Aurora B expression was able to reduce p53 transcription in all but the threonine 211 mutant. This is corroborated by the inclusion of a triple A mutant in which S183, T211 and S215 were all mutated. It can be seen clearly that Aurora B does not efficiently reduce the transcription of this mutant as well.

Next, the turnover rate of the phosphorylation mutants in the presence of Aurora B was determined. p53 null H1299 cells were transfected with either GFP-p53 or GFP-p53 AAA mutant (S183A, T211A, S215A) in the presence of either Flag-Aurora B or Flag-Aurora B K106R mutant. Two hours prior to harvest, cells were treated with cycloheximide. The turnover rate for p53 was determined by immunoblot (Figure 55). The results show that wild type Aurora B cannot increase the turnover of p53 AAA mutant compared to wild type p53.

Further, kinase dead Aurora B K106R could not turnover wild type p53 as efficiently as wild type Aurora B indicating that the turnover of p53 is mediated by the kinase activity of Aurora B.

To determine if mutation of these DNA binding domain sites could affect the mRNA levels of p53 targets, qRT-PCR was performed for the mRNA levels of p21. Hct116 *p53 -/-* (Figure 56, top panel) or p53 null H1299 cells (Figure 56, bottom panel) were transfected with Flag-Aurora B and either GFP-p53 or GFP-p53 AAA mutant. The result here shows that Aurora B could not efficiently reduce p21 mRNA levels when using the p53 AAA mutant versus the wild type control in both cell lines. The difference in reduction was statistically significant in both cases.

In summary, Figures 54-56 show clearly that mutation of S183, T211 and S215 to alanine, reduces the capacity of Aurora B to inhibit p53 transcriptional activity and mediate its turnover. This demonstrates that one or all of these phosphorylation sites are important in regulation of p53 by Aurora B.

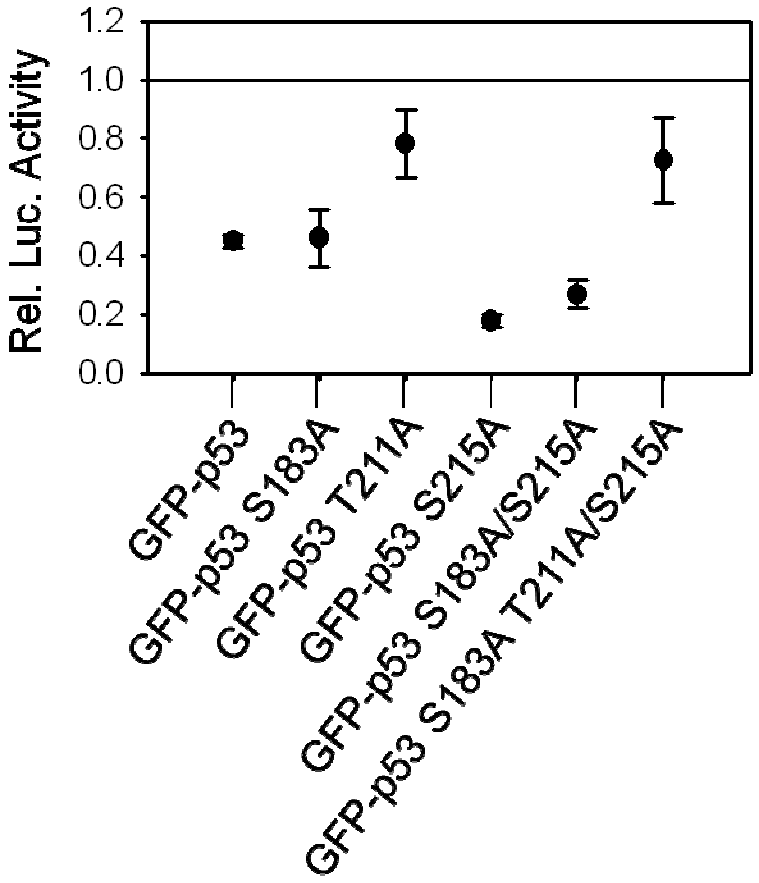

Figure 54. Aurora B reduces p53 transcriptional activity by phosphorylating threonine 211 in p53's DNA binding domain. **p**53 null H1299 cells were transfected with dual luciferase reporters, Aurora B and p53 phosphorylation site alanine mutants. Luciferase activity was measured by luminometer and results plotted relative to control (no Aurora B transfection, horizontal bar). Datapoints represent 3 replicates, error bars: 95% CI.

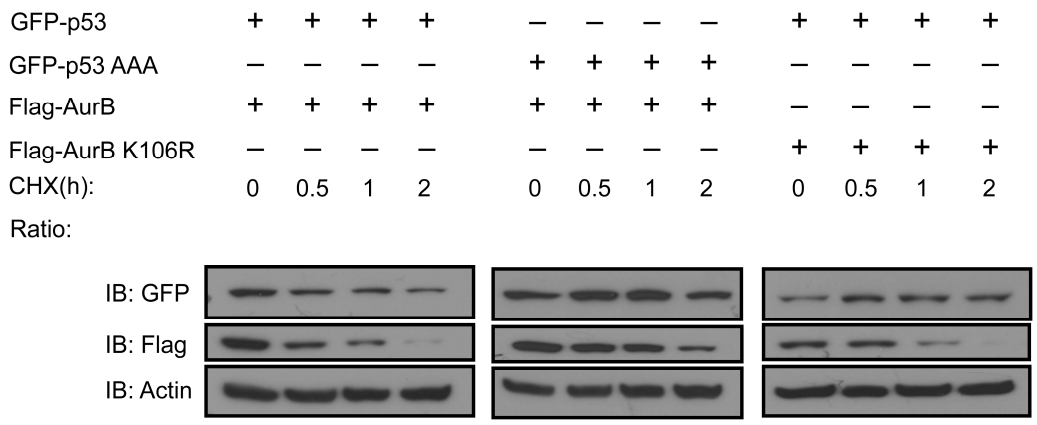

Figure 55. Phosphorylation site mutants are stabilized in the presence of Aurora B. p53 null H1299 cells were transfected with either GFP-p53 or GFP-p53 AAA mutant (S183A, T211A, S215A) in the presence of either Flag-Aurora B or Flag-Aurora B K106R mutant. Two hours prior to harvest, cells were treated with cycloheximide. Lysates were immunoblotted for GFP to determine p53 turnover rate.

Figure 56

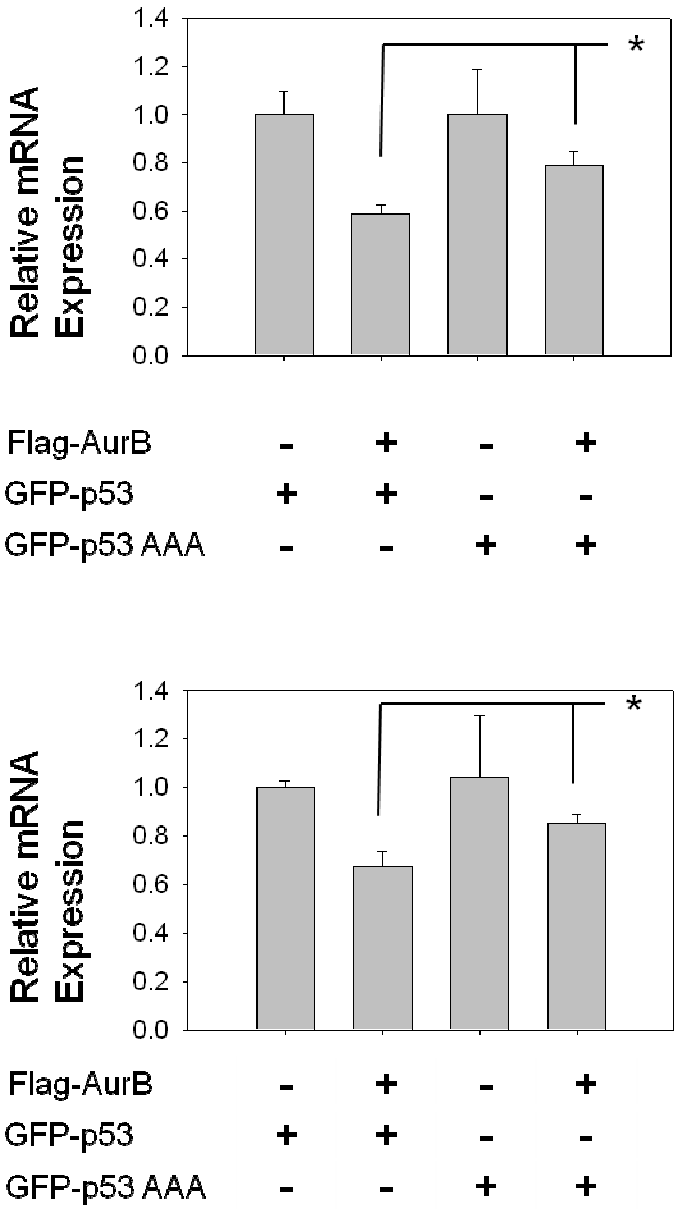

Figure 56. p21 mRNA is not efficiently reduced by Aurora B in the presence of the p53 AAA mutant. Hct116 *p53 -/-* (top panel) or p53 null H1299 cells (bottom panel) were transfected with Flag-Aurora B and either GFP-p53 or GFP-p53 AAA mutant. qRT-PCR was performed to determine p21 mRNA levels. * indicates P<0.05 with a student's t test. Error bars: 95% CI.

3.2.8 Inhibition of Aurora B stabilizes p53 and increases p53 target genes in tumors and tissue culture.

To assess the *in vitro* and *in vivo* effect that the inhibition of Aurora B may cause in tumors or tumor cells, thorough evaluation of p53 and p53 target genes was performed. Her18 xenograft tumors from nude mice (Figures 15-18, 26) were analyzed by immunohistochemistry for p53 in tumors from the three treatment groups: Vehicle, low dose (62.5 mg/kg/day) and high dose (125 mg/kg/day) AZD1152. Figure 26 showed clearly that p53 staining was increased in both drug treated groups. Figure 57 shows quantification of the measurement of percent positive p53 and intensity of staining on these slides. In both drug treated groups percent positive and intensity of p53 staining was significantly increased versus control indicating that inhibition of Aurora B *in vivo* stabilizes p53 effectively.

As confirmation that p53 is stabilized by Aurora B inhibition *in vivo*, tumor proteins were extracted after snap-freezing of tumor tissues and analyzed for p53 and p53 target protein levels. Figure 58 shows that in three representative tumors with use of AZD1152, p53 and p53 target genes Mdm2, Bax and Puma were all increased versus the control. To confirm this in tissue culture, Her18 cells were treated for 48 hours with an increasing dose of AZD1152-HQPA and p53 and its targets analyzed by immunoblot. Figure 59 shows clearly that as in the case of tumor cells, tissue culture also responds the same way and p53 and its target protein levels all increase with dose of AZD1152-HQPA.

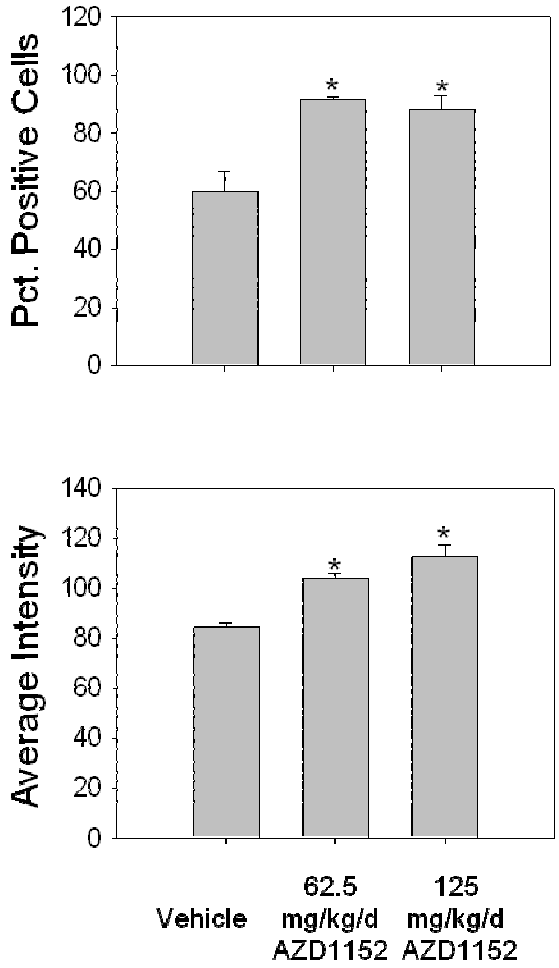

Figure 57. AZD1152 increases p53 level in Her18 human xenografts. Top, Human Her18 xenograft tumors from Figure 26 were scanned for p53 positive cells and are plotted at percentage for vehicle, low dose (62.5 mg/kg/day) and high dose (125 mg/kg/day) AZD1152. Bottom, p53 intensity was scanned and plotted for 3 treatment groups as before. * P<0.05. Error bars: 95% CI.

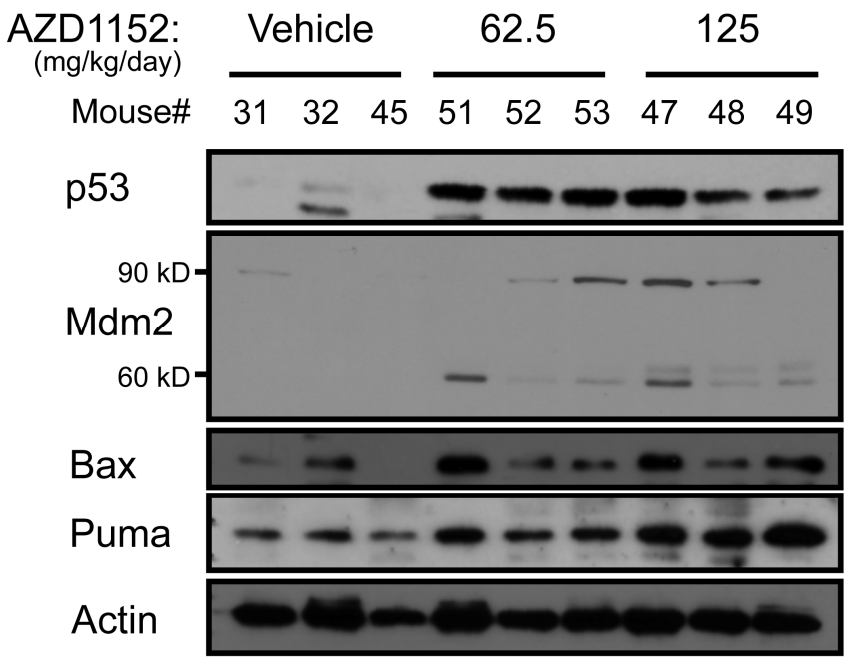

Figure 58. p53 and p53 targets are induced in vivo by AZD1152. Three representative mice bearing Her18 xenograft tumors (from Figure 26) were selected from each treatment group (vehicle, low and high dose AZD1152) and tumor proteins extracted. Lysates were immunoblotted for p53 and the p53 targets: Mdm2, Bax and Puma.

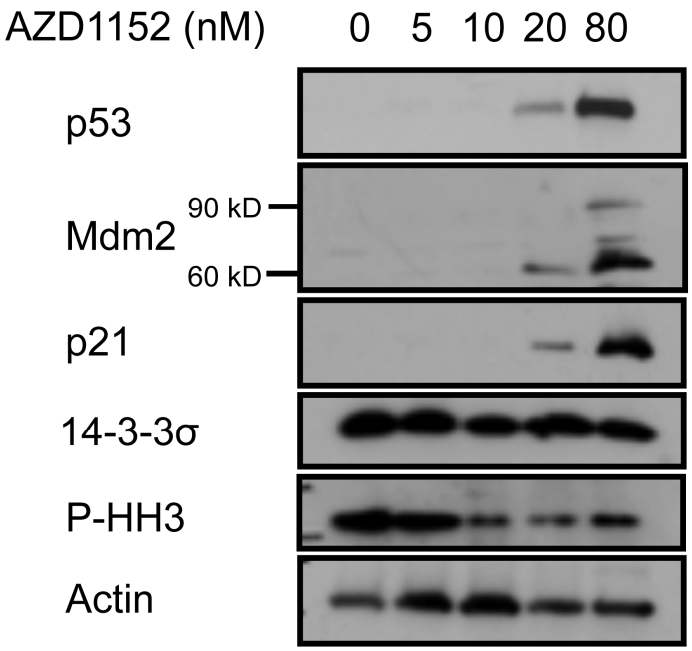

Figure 59. AZD1152-HQPA stabilizes p53 and induces p53 targets *in vitro*. Her18 cells were treated for 48 hours with an increasing dose of AZD1152-HQPA up to 80 nM. Cell lysates were immunoblotted for p53 and the p53 target genes: Mdm2, p21 and 14-3-3σ. Aurora B activity was assessed by immunoblot for phospho-Histone H3.

3.2.9 Aurora B reduces p53 mediated apoptosis.

Previously it was shown that Aurora B could reduce p53 level and downregulate its transcriptional activity. To determine if Aurora B could have an effect on p53's overall function, an apoptosis assay was performed. Hct116 cells were transfected with Flag-Aurora B and treated with 20 μM Cisplatin to induce DNA damage and induce the p53 DNA damage response. To measure this response, p53 mediated apoptosis was assayed by propidium iodide staining and sub G1 cell population determined. Figure 60 shows the result of sub G1 analysis from three replicates. In Cisplatin treated cells, Aurora B was able to reduce sub G1 cells significantly while no reduction was observed in non-treated cells. Representative individual flow cytometry histograms are shown in Figure 61. This data proves conclusively that Aurora B can affect p53's apoptotic function when induced by a DNA damage agent.

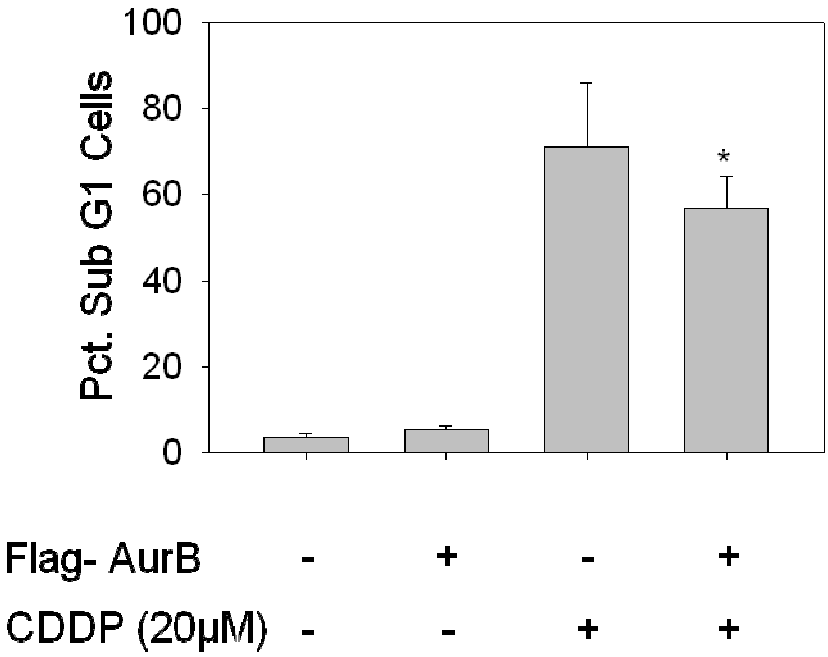

Figure 60. Aurora B reduces p53 mediated apoptosis. Hct116 cells were transfected with Flag-Aurora B followed by treatment with 20 μM Cisplatin (CDDP) for 24 hours. Percentage Sub G1 cells were determined by propidium iodide staining and flow cytometry analysis. * $P<0.05$ by Student's t test. Error Bar: 95% CI.

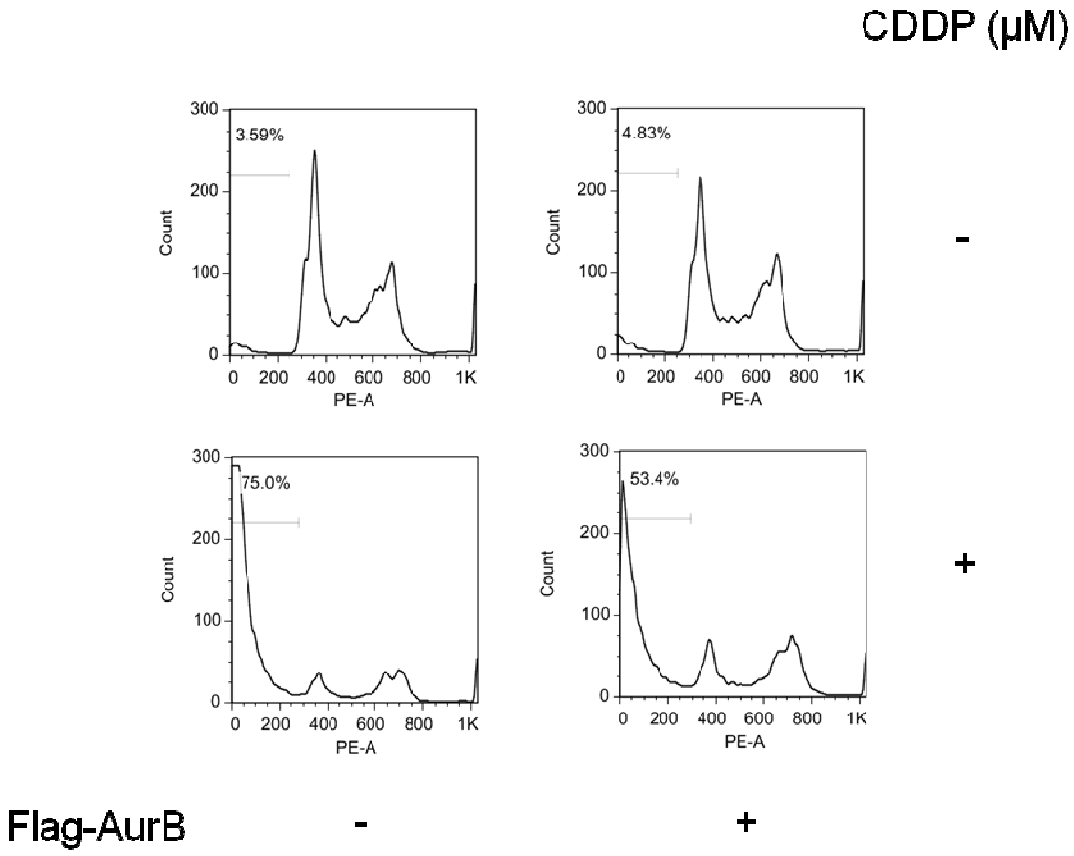

Figure 61. Aurora B reduces p53 mediated apoptosis – representative samples. Representative Hct116 samples from Figure 60. Gating: Sub G1 cells.

Chapter 4. Discussion

The data outlined in this thesis show that inhibition of Aurora B kinase by the specific inhibitor, AZD1152, is sufficient to reduce breast cancer cell growth and may indicate clinical relevance in the treatment of breast cancer. Inhibition of Aurora B was also shown to increase p53 levels in the cell, hinting at a previously unknown negative regulation of p53 by Aurora B. Indeed, it was shown that Aurora B phosphorylates p53 in the DNA binding domain and decreases p53 transcriptional activity. This relationship is of special interest, not only because of the importance of p53 as the genome guardian or because of Aurora B's oncogenic status in many cancer types, but because the function of p53 and Aurora B were previously thought to be temporally exclusive during the cell cycle.

This exclusivity revolves around the fact that Aurora B is thought to have function only during mitosis and that p53 has been presumed to have function outside mitosis, due to shutdown of global transcription during cell division. These data show that p53 and Aurora B interact in both interphase and mitotic phases of the cell cycle, indicating that an important new function for both proteins may be present.

The major findings of this thesis are that inhibition of Aurora B kinase has significant impact on breast cancer tumorigenesis and brings to light a previously unknown pathway for the regulation of p53 by mitotic kinase Aurora B. In several previous studies, it was shown that AZD1152 was able to specifically inhibit the

kinase activity of Aurora B and kill several cancer cell types. This study adds breast cancer to the list of cancers in which AZD1152 is shown to be effective via inhibition of Aurora B kinase. The data clearly shows that AZD1152 inhibits the growth of breast cancer cells regardless of Her2 status (Figures 6, 7, APPENDIX A), can cause mitotic catastrophe (Figure 8) with subsequent apoptosis (Figures 10, 11) and can decrease the tumorigenicity of breast cancer cells (Figures 13, 14, APPENDIX C). AZD1152 was also shown effective in reducing both tumor growth and tumor weight in orthotopic and metastatic xenograft murine models of human breast cancer (Figures 15, 16, 19, 20).

Upon investigation of the outcome for Aurora B kinase in the presence of AZD1152, this study found that protein levels of Aurora B were reduced, and that ubiquitination of Aurora B was increased via the Anaphase Promoting Complex (Figures 22-25). Figure 62 displays a model for these observations. The left pathway was described previously in several reports which showed that AZD1152 inhibits Aurora B activity, as measured by phosphorylated Histone H3. This leads to aberrant and reduced mitosis (Evans et al., 2008; Wilkinson et al., 2007; Yang et al., 2007). These observations are confirmed by the present study in breast cancer. The right model shows the proposed pathway that AZD1152 can also lead to ubiquitination of Aurora B by the APC complex and leads to its subsequent degradation. This, in turn, also led to mitotic blockade or aberrant mitosis.

As a consequence of inhibition of Aurora B by AZD1152, p53 levels were increased in two xenograft murine models (Figure 26). This hinted at a possible direct interaction between p53 and Aurora B. Indeed, it was found that p53 and Aurora B exist in complex and interact directly in a cell cycle dependent fashion (Figures 27-31). Further, Aurora B was shown to phosphorylate p53 at several serine/threonine residues in the DNA binding domain and that these events caused downregulation of p53 levels via ubiquitination mediated by Mdm2 (Figures 38-42, 49). Phosphorylation of T211 was shown to reduce p53's transcriptional activity while phosphorylation at S183 or S215 was unable to do this (Figure 54). Inhibition of Aurora B was also shown to increase p53 levels in tumors and in tissue culture which led to increased levels of p53 target genes (Figures 57, 58). Functionally, Aurora B was shown to reduce p53's capacity to mediate apoptosis in response to the DNA damaging agent, cisplatin (Figures 60, 61).

Figure 63 outlines the proposed regulation of p53 by Aurora B and shows that Aurora B can phosphorylate the p53 DNA binding domain, which results in the degradation of p53 and reduction of p53's transcriptional function.

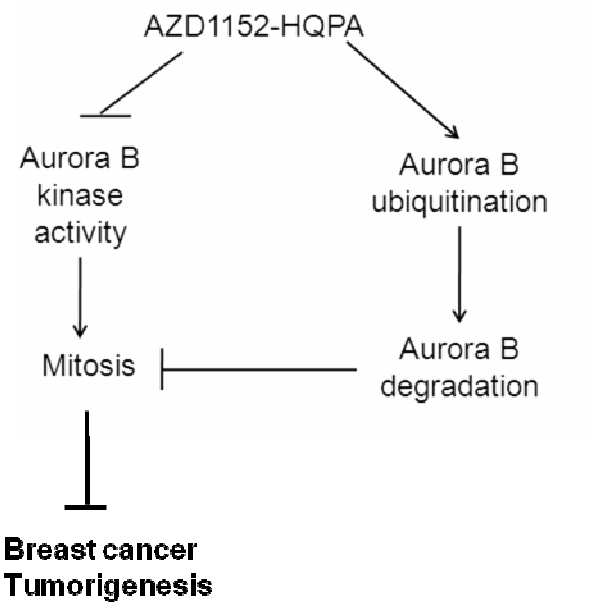

Figure 62. Model of regulation of Aurora B kinase by AZD1152. AZD1152 is known to negatively impact Aurora B activity by reducing phospho-HH3 levels. Reduced p-HH3 levels block chromatin condensation and thereby inhibit mitosis. New data from this study shows that AZD1152 also increases Aurora B ubiquitination and destabilizes Aurora B leading to activation of the spindle assembly checkpoint and mitotic blockade thereby decreasing breast cancer tumorigenesis.

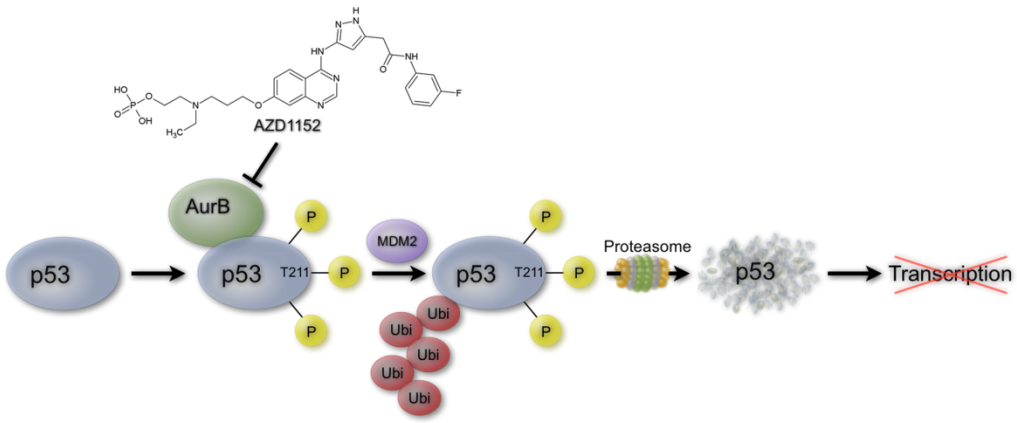

Figure 63. Model of regulation of p53 by Aurora B kinase. Mitotic kinase Aurora B phosphorylates p53 in the DNA binding domain at four sites. Phosphorylation of one of these sites, threonine 211, was shown to be an important negative regulatory event for the transcriptional activity of p53. This site, together with two others, serines 183 and 215, were also shown to be important in the degradation of p53 via the proteasome ubiquitin pathway resulting in reduced p53 transcriptional activity and reduced p53 mediated apoptosis.

The findings of this thesis are important for many reasons and have broad implications in both understanding the mechanisms of regulation by Aurora B as well as significant clinical relevance of Aurora B inhibition. AZD1152 was shown to be an effective treatment in breast cancer, thus adding breast cancer to the list of cancers evaluated for treatment with inhibitors of Aurora kinases. Mitotic defects, polyploidy and apoptosis were confirmed in breast cancer as a result of treatment with AZD1152, in agreement with several other reports that observed these phenotypes in other cancer cells (Evans et al., 2008; Wilkinson et al., 2007; Yang et al., 2007). Further, this study adds another dimension to the inhibition of Aurora B kinase itself in that inhibition was shown to cause Aurora B's ubiquitination and degradation. This observation is very important to the understanding of how AZD1152 is able to control the activity of Aurora B and shows that it is not only doing this by competing for ATP binding but by actually causing the degradation of the kinase and leading to decreased kinase activity. This observation also agrees with observations for many other kinases- that the inactive form may be unstable due to ubiquitination and degradation. Through this mechanism, AZD1152 is likely preventing Aurora B's auto-ubiquitination which keeps Aurora B in the inactive form leading to its breakdown.

This study also made the important discovery that inhibition of Aurora B led to increased p53 levels in breast cancer cells and gave the impetus for investigation of the interaction between Aurora B and p53 (Figure 26). Indeed, an interaction between these two proteins was found and p53 was found to be a novel substrate for Aurora B, indicating that some mitotic regulation of p53 may

be occurring. This result is intriguing in the sense that p53 has never been found to have a mitotic function, although one report described p53 at the centrosome during mitosis but no functional mechanism was given (Tritarelli et al., 2004). This observation is consistent with another report that p53 is a substrate of Aurora A kinase, a known centrosome protein and mitotic regulator (Katayama et al., 2004). Similar to this, Aurora B is not known to have a function outside mitosis with the exception of a report that described Aurora B in late S phase as co-localizing with foci of phospho-HH3 in the nucleus. The role of Aurora B during interphase was not well characterized in this study and the issue of Aurora B function outside mitosis remains unresolved. Our data show clearly that p53 and Aurora B interact both during mitosis and during interphase (Figure 31) and that during the mitotic interaction, p53 is located at the centromere during prophase. We have also confirmed recently that the interaction of Aurora B and p53 at the centromere co-localizes with Survivin (Figure 34C), another centromere protein and member of the CPC. Our findings that Aurora B and p53 interact during late S and G2 shed some light on the subject and are interesting clues to a possible non-mitotic role for Aurora B.

Most important and central to the findings of this thesis is that p53 was found to be a substrate of Aurora B and adds yet another kinase to the list of proteins that regulate the already heavily dictated p53 protein. Regulation of p53 in a positive fashion is well known by phosphorylation in the N-teminal transactivating domain, however, our results show that p53 is phosphorylated in the DNA binding domain and has an overall negative effect on p53 regulation. It

was also shown that phosphorylation leads to ubiquitination of p53 by Mdm2, reduction in oligomerization and ultimately, a decrease in p53's transcriptional activity.

This work focused on at least three major phosphorylation sites in p53's DNA binding domain: S183, T211 and S215. Of these, T211 was shown to be most important in reducing p53's transcriptional activity though the others may play an important role as well since mutation of S215 was shown to nearly completely block p53 phosphorylation by Aurora B in vitro. An alternative interpretation of this data is that S215 may be the major Aurora B phosphorylation site with the other sites being required for association between the kinase and p53. The functional relevance of the regulation of p53 by Aurora B was described by an experiment that investigated the ability of Aurora B to block p53's apoptotic function in the presence of DNA damage. Cisplatin was shown to cause apoptosis in breast cancer cells at a high percentage while introduction of Aurora B was able to reduce apoptosis effectively. This shows that Aurora B is able to regulate one of the global functions of p53 in response to DNA damage and is a significant new regulator of p53.

Evaluation of AZD1152 provided confirmation that this drug could be effective in treating breast cancer as in other reported cancer types. These findings also show that breast cancer was controlled at a similar or lower nanomolar range. Additionally, the finding that inhibition of Aurora B caused an increase in p53 protein level was unexpected and highly significant. This

increase in p53 levels was due to phosphoregulation by Aurora B and is similar to several previous reports that found that another Aurora kinase family member, Aurora A, can also phosphorylate p53.

Phosphorylation of p53 by Aurora A has been observed at two sites in the DNA binding domain, S315 (Blaydes et al., 2001; Katayama et al., 2004) and S215 (Liu et al., 2004), both of which were claimed to be the more important site for regulation of p53. These sites are located in the DNA binding domain and the studies make the conflicting observations that phosphorylation of S315 is both a positive and negative regulatory event for p53 transcription (Blaydes et al., 2001; Katayama et al., 2004). Further, there is a report that S215 is the phosphorylation site responsible for p53 negative regulation and not S315 (Liu et al., 2004). These inconsistent observations make the picture unclear for the phosphoregulation of p53 by Aurora A.

The observations presented in this thesis also confirm S215 as a major phosphorylation site for p53, but do not confirm its regulatory importance. We found that Aurora B phosphorylates this site but that there was no major impact on p53 transcriptional activity. Instead, we found that T211, albeit a modest phosphorylation site as far as amount, was the major site for regulation of p53 transcriptional activity (Figures 45, 54).

Our results show clearly that Aurora B and p53 are interacting in both interphase and mitotic cells and that during mitosis, p53 is located with Aurora B at the centromere, as confirmed by the co-localization of Survivin staining (Figure

34C). Only one other report has shown that p53 is present at a specific locale during mitosis and was found at the centrosome, where it is presumed to be phosphorylated by Aurora A (Tritarelli et al., 2004). No other findings have shown that p53 localizes to the centromere during mitosis but one report hinted at a possible role for p53 in the spindle assembly checkpoint. Cross et al found that the spindle assembly checkpoint in several murine models was dependent on p53 status, as shown using p53 null MEF cells (Cross et al., 1995). These results are in line with our finding that p53 resides at the centromere during mitosis and points at a possible transcription independent function for p53 in chromosome segregation.

Though it is possible that p53 does indeed have a transcription independent function at the centromere and plays some role in the spindle assembly checkpoint, there is an alternate view of how this data could be interpreted. Blagosklonny describes the induction and accumulation of p53 protein during mitosis through global inhibition of transcription due to depletion of the major negative regulators of p53 such as Mdm2, COP1 and Pirh2 (Blagosklonny, 2007) . These regulators are depleted when global transcription is turned off during mitosis causing p53 to accumulate due to its long-lived mRNA (Blagosklonny et al., 2002). Therefore, during mitosis p53 is still being translated and produced from mRNA while global transcription of its negative regulators is turned off. Following mitosis, transcription restarts and accumulated p53 can then transactivate its target genes leading to post-mitotic arrest and apoptosis. Given that p53 may be accumulating during mitosis and could cause the cell to

die in G1, there is another way to explain why Aurora B may be phosphorylating p53. It is possible that Aurora B maintains negative phosphoregulatory control of p53 during mitosis to prevent p53 from activating a post-mitotic checkpoint and causing cell death. Aurora B phosphorylating p53 at S183, T211 and S215 could be reducing its ability to turn on target genes thereby bypassing cell cycle arrest and apoptosis in G1.

Another alternate view of Aurora B phosphoregulation of p53 is that Aurora B may be functioning in interphase to prevent p53 cell cycle arrest, apoptosis and DNA damage inducing functions. As yet, there is no known function for Aurora B in interphase but our data show that Aurora B is present throughout the cell cycle, interacts with p53 during S phase and G2, and co-localizes with p53 in interphase cells. While the data presented in this study for an Aurora B interphase function is not conclusive, the possibility remains that cells overexpressing Aurora B could have a function to inactivate p53 outside mitosis.

As with all studies involving chemotherapeutics, clinical relevance is a central consideration in the design of these experiments. It was observed that AZD1152 was effective not only in a model of primary breast cancer but also in a model of breast cancer that was metastatic, a major complicating factor in this disease. Tumor size was reduced by 50% in solid malignancy and metastases were completely eliminated in treated mice versus control. Relevant to dosage, AZD1152 was shown effective in low nanomolar ranges for all breast cancer cell

lines treated (Figures 5, 6) and similarly, was shown effective in nearly the same range in Skov3, PC3, Hct116, MB-MDA-435 and MiaPaCa-2 (IC_{50}<150nM, APPENDIX A). Of note, breast cancer cell lines were sensitive to AZD1152 regardless of Her2 status and was effective in tissue culture and the metatstatic model of a triple negative, especially aggressive breast cancer cell line, MB-MDA-231.

Important in the area of cancer treatment regimens, Yang et al found that AZD1152 showed synergism with topoisomerase II inhibitors in leukemia cells *in vitro* (Yang et al., 2007). Our results confirm a similar observation where synergy between AZD1152 and etoposide (Vp-16) was noted over a broad range of fractional effect in both Her18 and the parent line, MCF7 (APPENDIX D).

The effect of AZD1152 on p53 holds special clinical relevance since p53 is lost or mutated in 50% of all cancers and because of p53's role as the master tumor suppressor. The use of an Aurora B inhibitor showed dramatic induction of p53 in both tissue culture and *in vivo* models and should be considered as a possible contraindication in patients with mutant p53 status.

The results reported in this thesis have covered a large amount of territory, from the use of AZD1152 in breast cancer, to the regulation of p53 by Aurora B. While these discoveries are significant and important, they inevitably lead to more questions and future experiments. One example, is that we reported that phosphorylation of p53 by Aurora B leads to p53 ubiquitination and degradation, but the exact mechanism of how this occurs has not been

investigated. A future study in this area should focus on determining if the phosphorylation sites mentioned earlier (Figure 42), form a recognition motif for Mdm2 or other E3 ubiquitination ligases to enhance their binding. Another possibility is that the phosphorylation of p53 simply prevents p53 from binding DNA or oligomerizing, which leads to ubiquitination since the unbound monomer is more readily degraded. Further, examination of the p53 localization would shed light on whether phosphorylated p53 has differential compartment localization. For example, Aurora B phosphorylation could facilitate the shuttling of p53 to the cytoplasm where it is subsequently degraded.

Future studies could also focus on the individual phosphorylation sites themselves and their contribution, independent of each other, in p53's degradation, transcriptional activity, oligomerization or DNA binding. In this study the triple AAA mutant of p53 was used, but with the exception of transcriptional activity, we do not report differential effects by site. One site or a combination of sites could serve as a code for varying effects on p53.

Important for any future consideration of the temporal interaction of Aurora B and p53, is to determine if the most important regulation occurs during interphase or mitosis. We show that Aurora B and p53 interact in both dividing and non-dividing cells, but when during the cell cycle the major impact of phosphorylation is occurring, remains an open question. Should the major regulation be found interphase, p53 could be negatively regulated by Aurora B in order to block the negative transcriptional effect on Cyclin B1 and Cdk2, thus

driving the cell cycle forward. An even more interesting proposition is that p53 could have a function in mitosis. As mentioned earlier, Cross et al found that p53 was required for proper spindle assembly checkpoint and investigation of this necessity would also be a central consideration in future experiments centering on mitosis.

Relevant to the clinical importance of this study, future animal and human trials involving the use of AZD1152 in p53 wild type cancers should be investigated. Since AZD1152 has the ability to increase p53 protein level and turn on its target genes, use of this drug could be important in turning on the tumor killing activity of p53. Specifically, cancers that overexpress Aurora B (Table 2) or Aurora A would be good candidates for such a trial since their aberrant control of p53 may be contributing to the tumor phenotype without actually having lost p53 expression. With this in mind, inhibiting Aurora B could help to not only reduce the growth of tumor cells but could turn on the tumor killing activity of the p53 tumor suppressor. Conversely, mutant p53 status could aggravate the tumor phenotype and cause increased cancer growth. Careful consideration of p53 status would be needed in any future animal or human trials.

In summary, this study has shown that inhibition of Aurora B kinase has significant impact on breast cancer tumorigenesis and brings to light a previously unknown pathway for the regulation of p53 by mitotic kinase Aurora B. Further, this study adds breast cancer to the list of cancers in which AZD1152 is shown to

be effective via inhibition of Aurora B kinase. The data clearly show that AZD1152 inhibits the growth of breast cancer cells regardless of Her2 status and can cause mitotic catastrophe with subsequent apoptosis thus decreasing the tumorigenicity of breast cancer cells. Importantly, it was also shown that inhibition of Aurora B with AZD1152 led to ubiquitination and degradation of Aurora B by the APC complex, an observation not previously seen with use of Aurora B inhibitors.

With downregulation of Aurora B it was observed that p53 was induced. This hinted at a possible direct interaction between p53 and Aurora B. Indeed, it was found that p53 associates with Aurora B in a cell cycle dependent fashion. Further, Aurora B was shown to phosphorylate p53 at several serine/threonine residues in the DNA binding domain and that these events caused downregulation of p53 levels via ubiquitination mediated by Mdm2. The phosphorylation of one site, T211, was shown to reduce p53's transcriptional activity while this was not observed for phosphorylation at S183 or S215. Functionally, Aurora B was shown to reduce p53's capacity to mediate apoptosis in response to the DNA damaging agent, cisplatin. Of special note, it was observed that p53 localizes to the centromere with Aurora B and may play a role in mitosis, especially, the spindle assembly checkpoint.

Together these data show that the mitotic kinase Aurora B is an important target in breast cancer and an important regulator of p53 function. Consideration

of these interactions must be given in future clinical trials which focus on Aurora B inhibition since there is a major impact on the master tumor suppressor, p53.

Chapter 5. APPENDICES

APPENDIX A

AZD1152-HQPA dose response curves for SKOV3, PC3, Hct116, MB-MDA-435 and Miapaca-2 cell lines.

SKOV3 Cells- 96 Hour Incubation

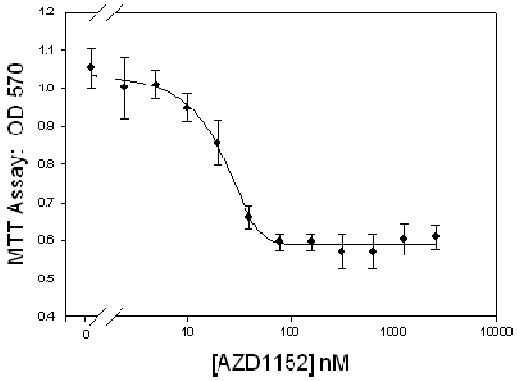

PC3 Cells- 96 Hour Incubation

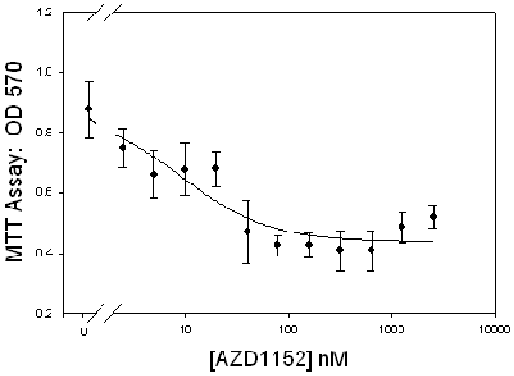

Hct116 Cells- 96 Hour Incubation

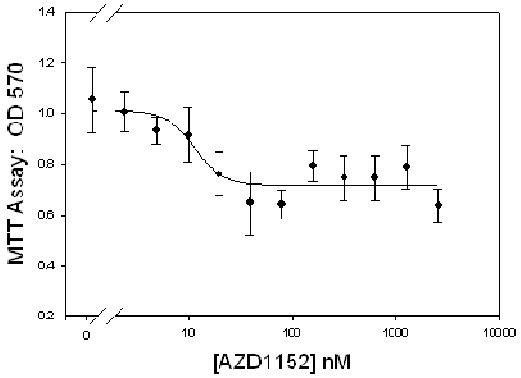

MB-MDA-435 Cells- 5 Day Incubation

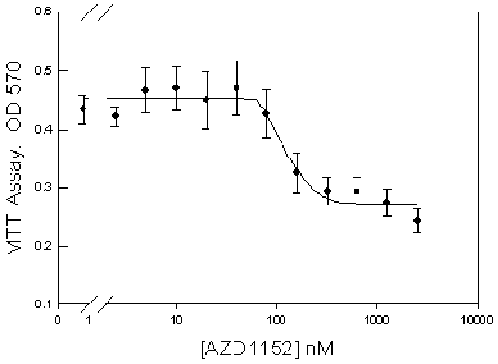

Miapaca-2 Cells- 96 Hour Incubation

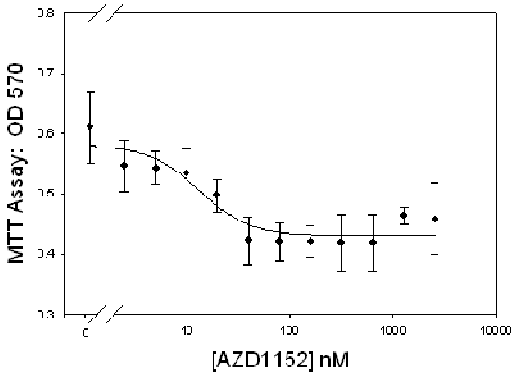

APPENDIX B

Cell cycle FACS analysis for Mcf7 breast cancer cells treated with 300 nM AZD1152 for up to 48 hours.

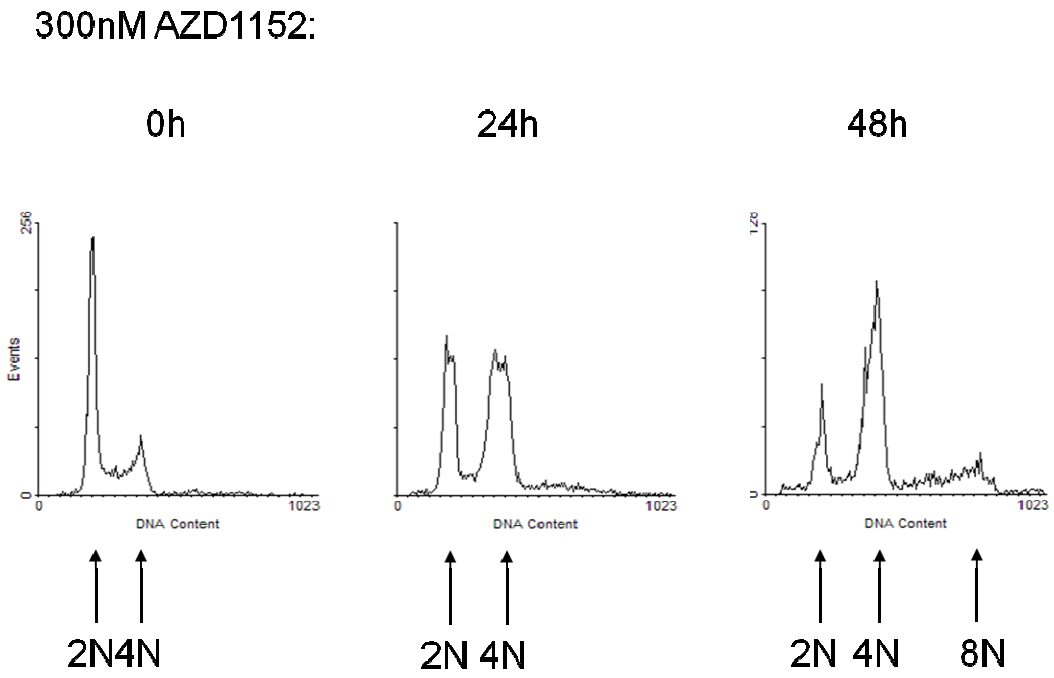

APPENDIX C

Colony forming and soft agar colony forming assays for MCF7 cells treated with AZD1152-HQPA.

MCF7

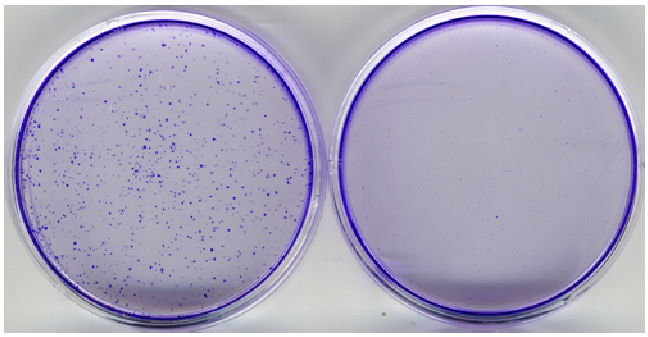

DMSO 40 nM AZD1152

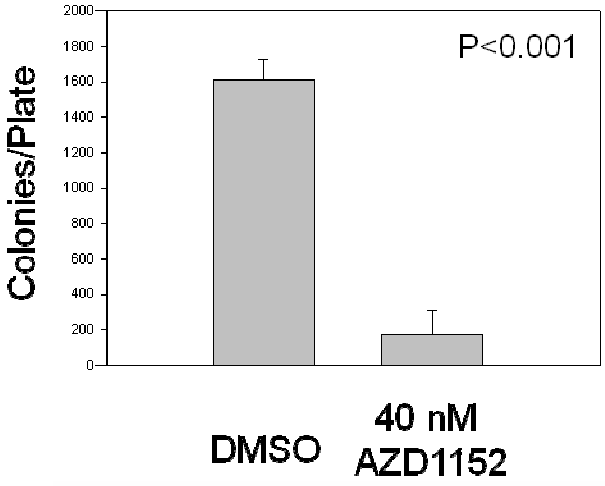

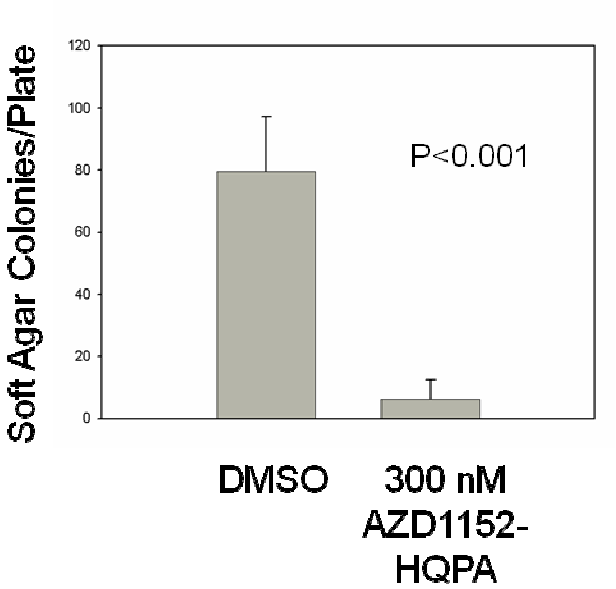

APPENDIX D

Analysis of synergism between AZD1152 and etoposide (VP-16) in MCF7 and Her18 breast cancer cells.

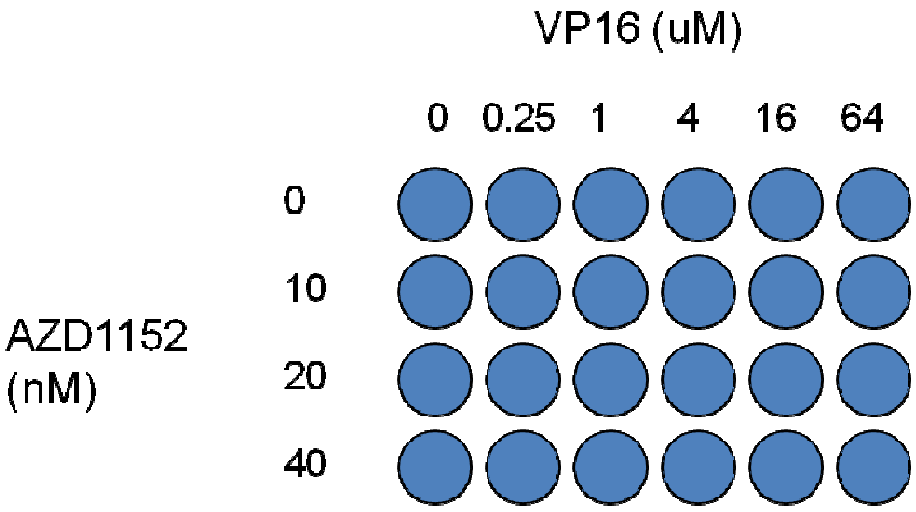

24-Well Plate Layout

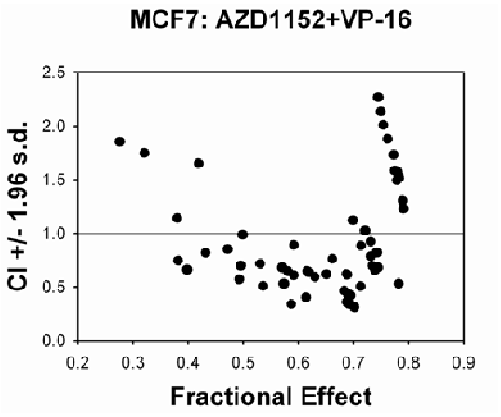

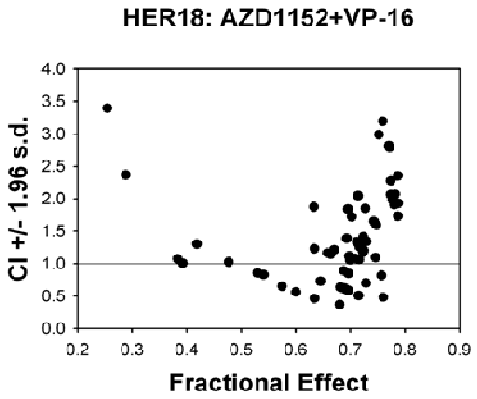

APPENDIX E

Cell line List

Cell Line	ATCC#	Cancer Type	Reference
MCF7	HTB-22	Breast	(Sugarman et al., 1985)
Her18		Breast	(Laronga et al., 2000)
MB-MDA-231	HTB-26	Breast	(Brinkley et al., 1980)
293T	CRL-11268	Human Embryo Kidney	(Sena-Esteves et al., 1999)
U2OS	HTB-96	Osteosarcoma	(Heldin et al., 1986)
H1299	CRL-5803	Lung	(Giaccone et al., 1992)
Hct116	CCL-247	Colorectal	(Brattain et al., 1981)
Hct116 p53-/-		Colorectal	(Bunz et al., 1998)
SKOV3	HTB-77	Ovarian	(Fogh et al., 1977)
PC3	CRL-1435	Prostate	(Kaighn et al., 1979)
MIA PaCa-2	CRL-1420	Pancreatic	(Wu et al., 1977)
MB-MDA-468	HTB-132	Breast	(Brinkley et al., 1980)
MB-MDA-435	HTB-129	Melanoma	(Brinkley et al., 1980; Chambers, 2009)
BT474	HTB-20	Breast	(Lasfargues et al., 1978)

Chapter 6. References

Adams, R.R., M. Carmena, and W.C. Earnshaw. 2001. Chromosomal passengers and the (aurora) ABCs of mitosis. *Trends Cell Biol* 11(2):49-54.

Adams, R.R., S.P. Wheatley, A.M. Gouldsworthy, S.E. Kandels-Lewis, M. Carmena, C. Smythe, D.L. Gerloff, and W.C. Earnshaw. 2000. INCENP binds the Aurora-related kinase AIRK2 and is required to target it to chromosomes, the central spindle and cleavage furrow. *Curr Biol* 10(17):1075-1078.

Adimoolam, S., and J.M. Ford. 2002. p53 and DNA damage-inducible expression of the xeroderma pigmentosum group C gene. *Proc Natl Acad Sci U S A* 99(20):12985-12990.

Agami, R., G. Blandino, M. Oren, and Y. Shaul. 1999. Interaction of c-Abl and p73alpha and their collaboration to induce apoptosis. *Nature* 399(6738):809-813.

Andersson, S., D.L. Davis, H. Dahlback, H. Jornvall, and D.W. Russell. 1989. Cloning, structure, and expression of the mitochondrial cytochrome P-450 sterol 26-hydroxylase, a bile acid biosynthetic enzyme. *J Biol Chem* 264(14):8222-8229.

Andrews, P.D., Y. Ovechkina, N. Morrice, M. Wagenbach, K. Duncan, L. Wordeman, and J.R. Swedlow. 2004. Aurora B regulates MCAK at the mitotic centromere. *Dev Cell* 6(2):253-268.

Araki, K., K. Nozaki, T. Ueba, M. Tatsuka, and N. Hashimoto. 2004. High expression of Aurora-B/Aurora and Ipll-like midbody-associated protein (AIM-1) in astrocytomas. *J Neurooncol* 67(1-2):53-64.

Baker, S.J., E.R. Fearon, J.M. Nigro, S.R. Hamilton, A.C. Preisinger, J.M. Jessup, P. vanTuinen, D.H. Ledbetter, D.F. Barker, Y. Nakamura, R. White, and B. Vogelstein. 1989. Chromosome 17 deletions and p53 gene mutations in colorectal carcinomas. *Science* 244(4901):217-221.

Baptiste, N., P. Friedlander, X. Chen, and C. Prives. 2002. The proline-rich domain of p53 is required for cooperation with anti-neoplastic agents to promote apoptosis of tumor cells. *Oncogene* 21(1):9-21.

Bartkova, J., Z. Horejsi, K. Koed, A. Kramer, F. Tort, K. Zieger, P. Guldberg, M. Sehested, J.M. Nesland, C. Lukas, T. Orntoft, J. Lukas, and J. Bartek. 2005. DNA damage response as a candidate anti-cancer barrier in early human tumorigenesis. *Nature* 434(7035):864-870.

Beardmore, V.A., L.J. Ahonen, G.J. Gorbsky, and M.J. Kallio. 2004. Survivin dynamics increases at centromeres during G2/M phase transition and is regulated by microtubule-attachment and Aurora B kinase activity. *J Cell Sci* 117(Pt 18):4033-4042.

Bement, W.M., H.A. Benink, and G. von Dassow. 2005. A microtubule-dependent zone of active RhoA during cleavage plane specification. *J Cell Biol* 170(1):91-101.

Bensaad, K., A. Tsuruta, M.A. Selak, M.N. Vidal, K. Nakano, R. Bartrons, E. Gottlieb, and K.H. Vousden. 2006. TIGAR, a p53-inducible regulator of glycolysis and apoptosis. *Cell* 126(1):107-120.

Bernard, M., P. Sanseau, C. Henry, A. Couturier, and C. Prigent. 1998. Cloning of STK13, a third human protein kinase related to Drosophila aurora and budding yeast Ipl1 that maps on chromosome 19q13.3-ter. *Genomics* 53(3):406-409.

Biggins, S., and A.W. Murray. 2001. The budding yeast protein kinase Ipl1/Aurora allows the absence of tension to activate the spindle checkpoint. *Genes Dev* 15(23):3118-3129.

Bischoff, J.R., L. Anderson, Y. Zhu, K. Mossie, L. Ng, B. Souza, B. Schryver, P. Flanagan, F. Clairvoyant, C. Ginther, C.S. Chan, M. Novotny, D.J. Slamon, and G.D. Plowman. 1998. A homologue of Drosophila aurora kinase is oncogenic and amplified in human colorectal cancers. *Embo J* 17(11):3052-3065.

Bishop, J.D., and J.M. Schumacher. 2002. Phosphorylation of the carboxyl terminus of inner centromere protein (INCENP) by the Aurora B Kinase stimulates Aurora B kinase activity. *J Biol Chem* 277(31):27577-27580.

Blagosklonny, M.V. 2007. Mitotic arrest and cell fate: why and how mitotic inhibition of transcription drives mutually exclusive events. *Cell Cycle* 6(1):70-74.

Blagosklonny, M.V., Z.N. Demidenko, and T. Fojo. 2002. Inhibition of transcription results in accumulation of Wt p53 followed by delayed outburst of p53-inducible proteins: p53 as a sensor of transcriptional integrity. *Cell Cycle* 1(1):67-74.

Blaydes, J.P., M.G. Luciani, S. Pospisilova, H.M. Ball, B. Vojtesek, and T.R. Hupp. 2001. Stoichiometric phosphorylation of human p53 at Ser315 stimulates p53-dependent transcription. *J Biol Chem* 276(7):4699-4708.

Blom, N., S. Gammeltoft, and S. Brunak. 1999. Sequence and structure-based prediction of eukaryotic protein phosphorylation sites. *J Mol Biol* 294(5):1351-1362.

Bode, A.M., and Z. Dong. 2004. Post-translational modification of p53 in tumorigenesis. *Nat Rev Cancer* 4(10):793-805.

Boss, D.S., P.O. Witteveen, J. van der Sar, M.P. Lolkema, E.E. Voest, P.K. Stockman, O. Ataman, D. Wilson, S. Das, and J.H. Schellens. Clinical evaluation of AZD1152, an i.v. inhibitor of Aurora B kinase, in patients with solid malignant tumors. *Ann Oncol*.

Bourdon, J.C., V. Deguin-Chambon, J.C. Lelong, P. Dessen, P. May, B. Debuire, and E. May. 1997. Further characterisation of the p53 responsive element--identification of new candidate genes for trans-activation by p53. *Oncogene* 14(1):85-94.

Bourdon, J.C., K. Fernandes, F. Murray-Zmijewski, G. Liu, A. Diot, D.P. Xirodimas, M.K. Saville, and D.P. Lane. 2005. p53 isoforms can regulate p53 transcriptional activity. *Genes Dev* 19(18):2122-2137.

Brattain, M.G., W.D. Fine, F.M. Khaled, J. Thompson, and D.E. Brattain. 1981. Heterogeneity of malignant cells from a human colonic carcinoma. *Cancer Res* 41(5):1751-1756.

Brinkley, B.R., P.T. Beall, L.J. Wible, M.L. Mace, D.S. Turner, and R.M. Cailleau. 1980. Variations in cell form and cytoskeleton in human breast carcinoma cells in vitro. *Cancer Res* 40(9):3118-3129.

Bunz, F., A. Dutriaux, C. Lengauer, T. Waldman, S. Zhou, J.P. Brown, J.M. Sedivy, K.W. Kinzler, and B. Vogelstein. 1998. Requirement for p53 and p21 to sustain G2 arrest after DNA damage. *Science* 282(5393):1497-1501.

Carmena, M., and W.C. Earnshaw. 2003. The cellular geography of aurora kinases. *Nat Rev Mol Cell Biol* 4(11):842-854.

Carmena, M., S. Ruchaud, and W.C. Earnshaw. 2009. Making the Auroras glow: regulation of Aurora A and B kinase function by interacting proteins. *Curr Opin Cell Biol* 21(6):796-805.

Cazales, M., E. Schmitt, E. Montembault, C. Dozier, C. Prigent, and B. Ducommun. 2005. CDC25B phosphorylation by Aurora-A occurs at the G2/M transition and is inhibited by DNA damage. *Cell Cycle* 4(9):1233-1238.

Chambers, A.F. 2009. MDA-MB-435 and M14 cell lines: identical but not M14 melanoma? *Cancer Res* 69(13):5292-5293.

Cheeseman, I.M., J.S. Chappie, E.M. Wilson-Kubalek, and A. Desai. 2006. The conserved KMN network constitutes the core microtubule-binding site of the kinetochore. *Cell* 127(5):983-997.

Chen, I.T., M.L. Smith, P.M. O'Connor, and A.J. Fornace, Jr. 1995. Direct interaction of Gadd45 with PCNA and evidence for competitive interaction of Gadd45 and p21Waf1/Cip1 with PCNA. *Oncogene* 11(10):1931-1937.

Chen, J., S. Jin, S.K. Tahir, H. Zhang, X. Liu, A.V. Sarthy, T.P. McGonigal, Z. Liu, S.H. Rosenberg, and S.C. Ng. 2003. Survivin enhances Aurora-B kinase activity and localizes Aurora-B in human cells. *J Biol Chem* 278(1):486-490.

Cheung, C.H., M.S. Coumar, H.P. Hsieh, and J.Y. Chang. 2009. Aurora kinase inhibitors in preclinical and clinical testing. *Expert Opin Investig Drugs* 18(4):379-398.

Chieffi, P., G. Troncone, A. Caleo, S. Libertini, S. Linardopoulos, D. Tramontano, and G. Portella. 2004. Aurora B expression in normal testis and seminomas. *J Endocrinol* 181(2):263-270.

Chin, P.L., J. Momand, and G.P. Pfeifer. 1997. In vivo evidence for binding of p53 to consensus binding sites in the p21 and GADD45 genes in response to ionizing radiation. *Oncogene* 15(1):87-99.

Cimini, D., X. Wan, C.B. Hirel, and E.D. Salmon. 2006. Aurora kinase promotes turnover of kinetochore microtubules to reduce chromosome segregation errors. *Curr Biol* 16(17):1711-1718.

Cox, D.G., S.E. Hankinson, and D.J. Hunter. 2006. Polymorphisms of the AURKA (STK15/Aurora Kinase) Gene and Breast Cancer Risk (United States). *Cancer Causes Control* 17(1):81-83.

Crosio, C., G.M. Fimia, R. Loury, M. Kimura, Y. Okano, H. Zhou, S. Sen, C.D. Allis, and P. Sassone-Corsi. 2002. Mitotic phosphorylation of histone H3: spatio-temporal regulation by mammalian Aurora kinases. *Mol Cell Biol* 22(3):874-885.

Cross, S.M., C.A. Sanchez, C.A. Morgan, M.K. Schimke, S. Ramel, R.L. Idzerda, W.H. Raskind, and B.J. Reid. 1995. A p53-dependent mouse spindle checkpoint. *Science* 267(5202):1353-1356.

Dai, Q., Q.Y. Cai, X.O. Shu, A. Ewart-Toland, W.Q. Wen, A. Balmain, Y.T. Gao, and W. Zheng. 2004. Synergistic effects of STK15 gene polymorphisms and endogenous estrogen exposure in the risk of breast cancer. *Cancer Epidemiol Biomarkers Prev* 13(12):2065-2070.

DeLeo, A.B., G. Jay, E. Appella, G.C. Dubois, L.W. Law, and L.J. Old. 1979. Detection of a transformation-related antigen in chemically induced sarcomas and other transformed cells of the mouse. *Proc Natl Acad Sci U S A* 76(5):2420-2424.

DeLuca, J.G., W.E. Gall, C. Ciferri, D. Cimini, A. Musacchio, and E.D. Salmon. 2006. Kinetochore microtubule dynamics and attachment stability are regulated by Hec1. *Cell* 127(5):969-982.

Ding, Z., J. Liang, Y. Lu, Q. Yu, Z. Songyang, S.Y. Lin, and G.B. Mills. 2006. A retrovirus-based protein complementation assay screen reveals functional AKT1-binding partners. *Proc Natl Acad Sci U S A* 103(41):15014-15019.

Ditchfield, C., V.L. Johnson, A. Tighe, R. Ellston, C. Haworth, T. Johnson, A. Mortlock, N. Keen, and S.S. Taylor. 2003. Aurora B couples chromosome alignment with anaphase by targeting BubR1, Mad2, and Cenp-E to kinetochores. *J Cell Biol* 161(2):267-280.

Ducat, D., and Y. Zheng. 2004. Aurora kinases in spindle assembly and chromosome segregation. *Exp Cell Res* 301(1):60-67.

Dumaz, N., D.M. Milne, and D.W. Meek. 1999. Protein kinase CK1 is a p53-threonine 18 kinase which requires prior phosphorylation of serine 15. *FEBS Lett* 463(3):312-316.

Dutertre, S., M. Cazales, M. Quaranta, C. Froment, V. Trabut, C. Dozier, G. Mirey, J.P. Bouche, N. Theis-Febvre, E. Schmitt, B. Monsarrat, C. Prigent, and B. Ducommun. 2004. Phosphorylation of CDC25B by Aurora-A at the centrosome contributes to the G2-M transition. *J Cell Sci* 117(Pt 12):2523-2531.

el-Deiry, W.S., S.E. Kern, J.A. Pietenpol, K.W. Kinzler, and B. Vogelstein. 1992. Definition of a consensus binding site for p53. *Nat Genet* 1(1):45-49.

Emanuele, M.J., W. Lan, M. Jwa, S.A. Miller, C.S. Chan, and P.T. Stukenberg. 2008. Aurora B kinase and protein phosphatase 1 have opposing roles in modulating kinetochore assembly. *J Cell Biol* 181(2):241-254.

Espinosa, J.M., and B.M. Emerson. 2001. Transcriptional regulation by p53 through intrinsic DNA/chromatin binding and site-directed cofactor recruitment. *Mol Cell* 8(1):57-69.

Evans, R.P., C. Naber, T. Steffler, T. Checkland, C.A. Maxwell, J.J. Keats, A.R. Belch, L.M. Pilarski, R. Lai, and T. Reiman. 2008. The selective Aurora B

kinase inhibitor AZD1152 is a potential new treatment for multiple myeloma. *Br J Haematol* 140(3):295-302.

Eyers, P.A., and J.L. Maller. 2004. Regulation of Xenopus Aurora A activation by TPX2. *J Biol Chem* 279(10):9008-9015.

Feng, Z., H. Zhang, A.J. Levine, and S. Jin. 2005. The coordinate regulation of the p53 and mTOR pathways in cells. *Proc Natl Acad Sci U S A* 102(23):8204-8209.

Fletcher, O., N. Johnson, C. Palles, I. dos Santos Silva, V. McCormack, J. Whittaker, A. Ashworth, and J. Peto. 2006. Inconsistent association between the STK15 F31I genetic polymorphism and breast cancer risk. *J Natl Cancer Inst* 98(14):1014-1018.

Fogh, J., W.C. Wright, and J.D. Loveless. 1977. Absence of HeLa cell contamination in 169 cell lines derived from human tumors. *J Natl Cancer Inst* 58(2):209-214.

Fu, J., M. Bian, Q. Jiang, and C. Zhang. 2007. Roles of Aurora kinases in mitosis and tumorigenesis. *Mol Cancer Res* 5(1):1-10.

Fu, J., M. Bian, J. Liu, Q. Jiang, and C. Zhang. 2009. A single amino acid change converts Aurora-A into Aurora-B-like kinase in terms of partner specificity and cellular function. *Proc Natl Acad Sci U S A* 106(17):6939-6944.

Funk, W.D., D.T. Pak, R.H. Karas, W.E. Wright, and J.W. Shay. 1992. A transcriptionally active DNA-binding site for human p53 protein complexes. *Mol Cell Biol* 12(6):2866-2871.

Gaiddon, C., M. Lokshin, I. Gross, D. Levasseur, Y. Taya, J.P. Loeffler, and C. Prives. 2003. Cyclin-dependent kinases phosphorylate p73 at threonine 86 in a cell cycle-dependent manner and negatively regulate p73. *J Biol Chem* 278(30):27421-27431.

Gassmann, R., A. Carvalho, A.J. Henzing, S. Ruchaud, D.F. Hudson, R. Honda, E.A. Nigg, D.L. Gerloff, and W.C. Earnshaw. 2004. Borealin: a novel chromosomal passenger required for stability of the bipolar mitotic spindle. *J Cell Biol* 166(2):179-191.

Gatti, A., H.H. Li, J.A. Traugh, and X. Liu. 2000. Phosphorylation of human p53 on Thr-55. *Biochemistry* 39(32):9837-9842.

Giaccone, G., J. Battey, A.F. Gazdar, H. Oie, M. Draoui, and T.W. Moody. 1992. Neuromedin B is present in lung cancer cell lines. *Cancer Res* 52(9 Suppl):2732s-2736s.

Gibbs, E., Z. Kelman, J.M. Gulbis, M. O'Donnell, J. Kuriyan, P.M. Burgers, and J. Hurwitz. 1997. The influence of the proliferating cell nuclear antigen-interacting domain of p21(CIP1) on DNA synthesis catalyzed by the human and Saccharomyces cerevisiae polymerase delta holoenzymes. *J Biol Chem* 272(4):2373-2381.

Glover, D.M., M.H. Leibowitz, D.A. McLean, and H. Parry. 1995. Mutations in aurora prevent centrosome separation leading to the formation of monopolar spindles. *Cell* 81(1):95-105.

Gonfloni, S., L. Di Tella, S. Caldarola, S.M. Cannata, F.G. Klinger, C. Di Bartolomeo, M. Mattei, E. Candi, M. De Felici, G. Melino, and G. Cesareni. 2009. Inhibition of the c-Abl-TAp63 pathway protects mouse oocytes from chemotherapy-induced death. *Nat Med* 15(10):1179-1185.

Gong, J.G., A. Costanzo, H.Q. Yang, G. Melino, W.G. Kaelin, Jr., M. Levrero, and J.Y. Wang. 1999. The tyrosine kinase c-Abl regulates p73 in apoptotic response to cisplatin-induced DNA damage. *Nature* 399(6738):806-809.

Gonzalez, S., C. Prives, and C. Cordon-Cardo. 2003. p73alpha regulation by Chk1 in response to DNA damage. *Mol Cell Biol* 23(22):8161-8171.

Gorgoulis, V.G., L.V. Vassiliou, P. Karakaidos, P. Zacharatos, A. Kotsinas, T. Liloglou, M. Venere, R.A. Ditullio, Jr., N.G. Kastrinakis, B. Levy, D. Kletsas, A. Yoneta, M. Herlyn, C. Kittas, and T.D. Halazonetis. 2005. Activation of the DNA damage checkpoint and genomic instability in human precancerous lesions. *Nature* 434(7035):907-913.

Goto, H., T. Kiyono, Y. Tomono, A. Kawajiri, T. Urano, K. Furukawa, E.A. Nigg, and M. Inagaki. 2006. Complex formation of Plk1 and INCENP required for metaphase-anaphase transition. *Nat Cell Biol* 8(2):180-187.

Goto, H., Y. Yasui, A. Kawajiri, E.A. Nigg, Y. Terada, M. Tatsuka, K. Nagata, and M. Inagaki. 2003. Aurora-B regulates the cleavage furrow-specific vimentin phosphorylation in the cytokinetic process. *J Biol Chem* 278(10):8526-8530.

Goto, H., Y. Yasui, E.A. Nigg, and M. Inagaki. 2002. Aurora-B phosphorylates Histone H3 at serine28 with regard to the mitotic chromosome condensation. *Genes Cells* 7(1):11-17.

Gu, W., X.L. Shi, and R.G. Roeder. 1997. Synergistic activation of transcription by CBP and p53. *Nature* 387(6635):819-823.

Han, Z., G.M. Riefler, J.R. Saam, S.E. Mango, and J.M. Schumacher. 2005. The C. elegans Tousled-like kinase contributes to chromosome segregation as a substrate and regulator of the Aurora B kinase. *Curr Biol* 15(10):894-904.

Hans, F., D.A. Skoufias, S. Dimitrov, and R.L. Margolis. 2009. Molecular distinctions between Aurora A and B: a single residue change transforms Aurora A into correctly localized and functional Aurora B. *Mol Biol Cell* 20(15):3491-3502.

Harrington, E.A., D. Bebbington, J. Moore, R.K. Rasmussen, A.O. Ajose-Adeogun, T. Nakayama, J.A. Graham, C. Demur, T. Hercend, A. Diu-Hercend, M. Su, J.M. Golec, and K.M. Miller. 2004. VX-680, a potent and

selective small-molecule inhibitor of the Aurora kinases, suppresses tumor growth in vivo. *Nat Med* 10(3):262-267.

Harris, S.L., and A.J. Levine. 2005. The p53 pathway: positive and negative feedback loops. *Oncogene* 24(17):2899-2908.

Hauf, S., R.W. Cole, S. LaTerra, C. Zimmer, G. Schnapp, R. Walter, A. Heckel, J. van Meel, C.L. Rieder, and J.M. Peters. 2003. The small molecule Hesperadin reveals a role for Aurora B in correcting kinetochore-microtubule attachment and in maintaining the spindle assembly checkpoint. *J Cell Biol* 161(2):281-294.

Heldin, C.H., A. Johnsson, S. Wennergren, C. Wernstedt, C. Betsholtz, and B. Westermark. 1986. A human osteosarcoma cell line secretes a growth factor structurally related to a homodimer of PDGF A-chains. *Nature* 319(6053):511-514.

Hirota, T., J.J. Lipp, B.H. Toh, and J.M. Peters. 2005. Histone H3 serine 10 phosphorylation by Aurora B causes HP1 dissociation from heterochromatin. *Nature* 438(7071):1176-1180.

Hollander, M.C., I. Alamo, J. Jackman, M.G. Wang, O.W. McBride, and A.J. Fornace, Jr. 1993. Analysis of the mammalian gadd45 gene and its response to DNA damage. *J Biol Chem* 268(32):24385-24393.

Horvath, M.M., X. Wang, M.A. Resnick, and D.A. Bell. 2007. Divergent evolution of human p53 binding sites: cell cycle versus apoptosis. *PLoS Genet* 3(7):e127.

Huang, Y., T. Sen, J. Nagpal, S. Upadhyay, B. Trink, E. Ratovitski, and D. Sidransky. 2008. ATM kinase is a master switch for the Delta Np63 alpha phosphorylation/degradation in human head and neck squamous cell carcinoma cells upon DNA damage. *Cell Cycle* 7(18):2846-2855.

Hupp, T.R., and D.P. Lane. 1994. Allosteric activation of latent p53 tetramers. *Curr Biol* 4(10):865-875.

Hussain, S.P., P. Amstad, P. He, A. Robles, S. Lupold, I. Kaneko, M. Ichimiya, S. Sengupta, L. Mechanic, S. Okamura, L.J. Hofseth, M. Moake, M. Nagashima, K.S. Forrester, and C.C. Harris. 2004. p53-induced up-regulation of MnSOD and GPx but not catalase increases oxidative stress and apoptosis. *Cancer Res* 64(7):2350-2356.

Hwang, B.J., J.M. Ford, P.C. Hanawalt, and G. Chu. 1999. Expression of the p48 xeroderma pigmentosum gene is p53-dependent and is involved in global genomic repair. *Proc Natl Acad Sci U S A* 96(2):424-428.

Jelluma, N., A.B. Brenkman, N.J. van den Broek, C.W. Cruijsen, M.H. van Osch, S.M. Lens, R.H. Medema, and G.J. Kops. 2008. Mps1 phosphorylates Borealin to control Aurora B activity and chromosome alignment. *Cell* 132(2):233-246.

Jerome, L., N. Alami, S. Belanger, V. Page, Q. Yu, J. Paterson, L. Shiry, M. Pegram, and B. Leyland-Jones. 2006. Recombinant human insulin-like growth factor binding protein 3 inhibits growth of human epidermal growth factor receptor-2-overexpressing breast tumors and potentiates herceptin activity in vivo. *Cancer Res* 66(14):7245-7252.

Jones, E.V., M.J. Dickman, and A.J. Whitmarsh. 2007. Regulation of p73-mediated apoptosis by c-Jun N-terminal kinase. *Biochem J* 405(3):617-623.

Kaghad, M., H. Bonnet, A. Yang, L. Creancier, J.C. Biscan, A. Valent, A. Minty, P. Chalon, J.M. Lelias, X. Dumont, P. Ferrara, F. McKeon, and D. Caput. 1997. Monoallelically expressed gene related to p53 at 1p36, a region frequently deleted in neuroblastoma and other human cancers. *Cell* 90(4):809-819.

Kaighn, M.E., K.S. Narayan, Y. Ohnuki, J.F. Lechner, and L.W. Jones. 1979. Establishment and characterization of a human prostatic carcinoma cell line (PC-3). *Invest Urol* 17(1):16-23.

Kaitna, S., P. Pasierbek, M. Jantsch, J. Loidl, and M. Glotzer. 2002. The aurora B kinase AIR-2 regulates kinetochores during mitosis and is required for separation of homologous Chromosomes during meiosis. *Curr Biol* 12(10):798-812.

Kallio, M.J., M.L. McCleland, P.T. Stukenberg, and G.J. Gorbsky. 2002. Inhibition of aurora B kinase blocks chromosome segregation, overrides the spindle checkpoint, and perturbs microtubule dynamics in mitosis. *Curr Biol* 12(11):900-905.

Kanda, A., H. Kawai, S. Suto, S. Kitajima, S. Sato, T. Takata, and M. Tatsuka. 2005. Aurora-B/AIM-1 kinase activity is involved in Ras-mediated cell transformation. *Oncogene* 24(49):7266-7272.

Kastan, M.B., O. Onyekwere, D. Sidransky, B. Vogelstein, and R.W. Craig. 1991. Participation of p53 protein in the cellular response to DNA damage. *Cancer Res* 51(23 Pt 1):6304-6311.

Katayama, H., W.R. Brinkley, and S. Sen. 2003. The Aurora kinases: role in cell transformation and tumorigenesis. *Cancer Metastasis Rev* 22(4):451-464.

Katayama, H., T. Ota, F. Jisaki, Y. Ueda, T. Tanaka, S. Odashima, F. Suzuki, Y. Terada, and M. Tatsuka. 1999. Mitotic kinase expression and colorectal cancer progression. *J Natl Cancer Inst* 91(13):1160-1162.

Katayama, H., K. Sasai, H. Kawai, Z.M. Yuan, J. Bondaruk, F. Suzuki, S. Fujii, R.B. Arlinghaus, B.A. Czerniak, and S. Sen. 2004. Phosphorylation by aurora kinase A induces Mdm2-mediated destabilization and inhibition of p53. *Nat Genet* 36(1):55-62.

Kawajiri, A., Y. Yasui, H. Goto, M. Tatsuka, M. Takahashi, K. Nagata, and M. Inagaki. 2003. Functional significance of the specific sites phosphorylated in desmin at cleavage furrow: Aurora-B may phosphorylate and regulate type III intermediate filaments during cytokinesis coordinatedly with Rho-kinase. *Mol Biol Cell* 14(4):1489-1500.

Kawashima, S.A., T. Tsukahara, M. Langegger, S. Hauf, T.S. Kitajima, and Y. Watanabe. 2007. Shugoshin enables tension-generating attachment of kinetochores by loading Aurora to centromeres. *Genes Dev* 21(4):420-435.

Keen, N., and S. Taylor. 2004. Aurora-kinase inhibitors as anticancer agents. *Nat Rev Cancer* 4(12):927-936.

Kelly, A.E., S.C. Sampath, T.A. Maniar, E.M. Woo, B.T. Chait, and H. Funabiki. 2007. Chromosomal enrichment and activation of the aurora B pathway are coupled to spatially regulate spindle assembly. *Dev Cell* 12(1):31-43.

Kim, E.J., J.S. Park, and S.J. Um. 2002. Identification and characterization of HIPK2 interacting with p73 and modulating functions of the p53 family in vivo. *J Biol Chem* 277(35):32020-32028.

Kimura, M., Y. Matsuda, T. Yoshioka, N. Sumi, and Y. Okano. 1998. Identification and characterization of STK12/Aik2: a human gene related to aurora of Drosophila and yeast IPL1. *Cytogenet Cell Genet* 82(3-4):147-152.

Kitzen, J.J., M.J. de Jonge, and J. Verweij. Aurora kinase inhibitors. *Crit Rev Oncol Hematol* 73(2):99-110.

Knowlton, A.L., W. Lan, and P.T. Stukenberg. 2006. Aurora B is enriched at merotelic attachment sites, where it regulates MCAK. *Curr Biol* 16(17):1705-1710.

Koida, N., T. Ozaki, H. Yamamoto, S. Ono, T. Koda, K. Ando, R. Okoshi, T. Kamijo, K. Omura, and A. Nakagawara. 2008. Inhibitory role of Plk1 in the regulation of p73-dependent apoptosis through physical interaction and phosphorylation. *J Biol Chem* 283(13):8555-8563.

Kress, M., E. May, R. Cassingena, and P. May. 1979. Simian virus 40-transformed cells express new species of proteins precipitable by anti-simian virus 40 tumor serum. *J Virol* 31(2):472-483.

Lampson, M.A., and T.M. Kapoor. 2005. The human mitotic checkpoint protein BubR1 regulates chromosome-spindle attachments. *Nat Cell Biol* 7(1):93-98.

Lampson, M.A., K. Renduchitala, A. Khodjakov, and T.M. Kapoor. 2004. Correcting improper chromosome-spindle attachments during cell division. *Nat Cell Biol* 6(3):232-237.

Lan, W., X. Zhang, S.L. Kline-Smith, S.E. Rosasco, G.A. Barrett-Wilt, J. Shabanowitz, D.F. Hunt, C.E. Walczak, and P.T. Stukenberg. 2004.

Aurora B phosphorylates centromeric MCAK and regulates its localization and microtubule depolymerization activity. *Curr Biol* 14(4):273-286.

Lane, D.P. 1992. Cancer. p53, guardian of the genome. *Nature* 358(6381):15-16.

Lane, D.P., and L.V. Crawford. 1979. T antigen is bound to a host protein in SV40-transformed cells. *Nature* 278(5701):261-263.

Laronga, C., H.Y. Yang, C. Neal, and M.H. Lee. 2000. Association of the cyclin-dependent kinases and 14-3-3 sigma negatively regulates cell cycle progression. *J Biol Chem* 275(30):23106-23112.

Lasfargues, E.Y., W.G. Coutinho, and E.S. Redfield. 1978. Isolation of two human tumor epithelial cell lines from solid breast carcinomas. *J Natl Cancer Inst* 61(4):967-978.

Lavin, M.F., and N. Gueven. 2006. The complexity of p53 stabilization and activation. *Cell Death Differ* 13(6):941-950.

Lens, S.M., and R.H. Medema. 2003. The survivin/Aurora B complex: its role in coordinating tension and attachment. *Cell Cycle* 2(6):507-510.

Lens, S.M., R.M. Wolthuis, R. Klompmaker, J. Kauw, R. Agami, T. Brummelkamp, G. Kops, and R.H. Medema. 2003. Survivin is required for a sustained spindle checkpoint arrest in response to lack of tension. *Embo J* 22(12):2934-2947.

Levine, A.J., W. Hu, and Z. Feng. 2006. The P53 pathway: what questions remain to be explored? *Cell Death Differ* 13(6):1027-1036.

Lin, Z.Z., Y.M. Jeng, F.C. Hu, H.W. Pan, H.W. Tsao, P.L. Lai, P.H. Lee, A.L. Cheng, and H.C. Hsu. Significance of Aurora B overexpression in hepatocellular carcinoma. Aurora B Overexpression in HCC. *BMC Cancer* 10:461.

Linzer, D.I., and A.J. Levine. 1979. Characterization of a 54K dalton cellular SV40 tumor antigen present in SV40-transformed cells and uninfected embryonal carcinoma cells. *Cell* 17(1):43-52.

Liu, D., G. Vader, M.J. Vromans, M.A. Lampson, and S.M. Lens. 2009. Sensing chromosome bi-orientation by spatial separation of aurora B kinase from kinetochore substrates. *Science* 323(5919):1350-1353.

Liu, Q., S. Kaneko, L. Yang, R.I. Feldman, S.V. Nicosia, J. Chen, and J.Q. Cheng. 2004. Aurora-A abrogation of p53 DNA binding and transactivation activity by phosphorylation of serine 215. *J Biol Chem* 279(50):52175-52182.

Macurek, L., A. Lindqvist, D. Lim, M.A. Lampson, R. Klompmaker, R. Freire, C. Clouin, S.S. Taylor, M.B. Yaffe, and R.H. Medema. 2008. Polo-like kinase-1 is activated by aurora A to promote checkpoint recovery. *Nature* 455(7209):119-123.

Maltzman, W., and L. Czyzyk. 1984. UV irradiation stimulates levels of p53 cellular tumor antigen in nontransformed mouse cells. *Mol Cell Biol* 4(9):1689-1694.

Mantovani, F., F. Tocco, J. Girardini, P. Smith, M. Gasco, X. Lu, T. Crook, and G. Del Sal. 2007. The prolyl isomerase Pin1 orchestrates p53 acetylation and dissociation from the apoptosis inhibitor iASPP. *Nat Struct Mol Biol* 14(10):912-920.

Matoba, S., J.G. Kang, W.D. Patino, A. Wragg, M. Boehm, O. Gavrilova, P.J. Hurley, F. Bunz, and P.M. Hwang. 2006. p53 regulates mitochondrial respiration. *Science* 312(5780):1650-1653.

McKenzie, T., Y. Liu, M. Fanale, S.G. Swisher, S. Chada, and K.K. Hunt. 2004. Combination therapy of Ad-mda7 and trastuzumab increases cell death in Her-2/neu-overexpressing breast cancer cells. *Surgery* 136(2):437-442.

Meek, D.W., and C.W. Anderson. 2009. Posttranslational modification of p53: cooperative integrators of function. *Cold Spring Harb Perspect Biol* 1(6):a000950.

Melero, J.A., D.T. Stitt, W.F. Mangel, and R.B. Carroll. 1979. Identification of new polypeptide species (48-55K) immunoprecipitable by antiserum to purified large T antigen and present in SV40-infected and -transformed cells. *Virology* 93(2):466-480.

Mihara, M., S. Erster, A. Zaika, O. Petrenko, T. Chittenden, P. Pancoska, and U.M. Moll. 2003. p53 has a direct apoptogenic role at the mitochondria. *Mol Cell* 11(3):577-590.

Millau, J.F., N. Bastien, and R. Drouin. 2009. P53 transcriptional activities: a general overview and some thoughts. *Mutat Res* 681(2-3):118-133.

Minoshima, Y., T. Kawashima, K. Hirose, Y. Tonozuka, A. Kawajiri, Y.C. Bao, X. Deng, M. Tatsuka, S. Narumiya, W.S. May, Jr., T. Nosaka, K. Semba, T. Inoue, T. Satoh, M. Inagaki, and T. Kitamura. 2003. Phosphorylation by aurora B converts MgcRacGAP to a RhoGAP during cytokinesis. *Dev Cell* 4(4):549-560.

Mishima, M., S. Kaitna, and M. Glotzer. 2002. Central spindle assembly and cytokinesis require a kinesin-like protein/RhoGAP complex with microtubule bundling activity. *Dev Cell* 2(1):41-54.

Miyoshi, Y., K. Iwao, C. Egawa, and S. Noguchi. 2001. Association of centrosomal kinase STK15/BTAK mRNA expression with chromosomal instability in human breast cancers. *Int J Cancer* 92(3):370-373.

Morrison, C., A.J. Henzing, O.N. Jensen, N. Osheroff, H. Dodson, S.E. Kandels-Lewis, R.R. Adams, and W.C. Earnshaw. 2002. Proteomic analysis of human metaphase chromosomes reveals topoisomerase II alpha as an Aurora B substrate. *Nucleic Acids Res* 30(23):5318-5327.

Morrow, C.J., A. Tighe, V.L. Johnson, M.I. Scott, C. Ditchfield, and S.S. Taylor. 2005. Bub1 and aurora B cooperate to maintain BubR1-mediated inhibition of APC/CCdc20. *J Cell Sci* 118(Pt 16):3639-3652.

Mortlock, A.A., K.M. Foote, N.M. Heron, F.H. Jung, G. Pasquet, J.J. Lohmann, N. Warin, F. Renaud, C. De Savi, N.J. Roberts, T. Johnson, C.B. Dousson, G.B. Hill, D. Perkins, G. Hatter, R.W. Wilkinson, S.R. Wedge, S.P. Heaton, R. Odedra, N.J. Keen, C. Crafter, E. Brown, K. Thompson, S. Brightwell, L. Khatri, M.C. Brady, S. Kearney, D. McKillop, S. Rhead, T. Parry, and S. Green. 2007. Discovery, synthesis, and in vivo activity of a new class of pyrazoloquinazolines as selective inhibitors of aurora B kinase. *J Med Chem* 50(9):2213-2224.

Murray-Zmijewski, F., D.P. Lane, and J.C. Bourdon. 2006. p53/p63/p73 isoforms: an orchestra of isoforms to harmonise cell differentiation and response to stress. *Cell Death Differ* 13(6):962-972.

Nadler, Y., R.L. Camp, C. Schwartz, D.L. Rimm, H.M. Kluger, and Y. Kluger. 2008. Expression of Aurora A (but not Aurora B) is predictive of survival in breast cancer. *Clin Cancer Res* 14(14):4455-4462.

Nakano, K., and K.H. Vousden. 2001. PUMA, a novel proapoptotic gene, is induced by p53. *Mol Cell* 7(3):683-694.

Nguyen, H.G., D. Chinnappan, T. Urano, and K. Ravid. 2005. Mechanism of Aurora-B degradation and its dependency on intact KEN and A-boxes:

identification of an aneuploidy-promoting property. *Mol Cell Biol* 25(12):4977-4992.

Nicholls, C.D., K.G. McLure, M.A. Shields, and P.W. Lee. 2002. Biogenesis of p53 involves cotranslational dimerization of monomers and posttranslational dimerization of dimers. Implications on the dominant negative effect. *J Biol Chem* 277(15):12937-12945.

Nigg, E.A. 2001. Mitotic kinases as regulators of cell division and its checkpoints. *Nat Rev Mol Cell Biol* 2(1):21-32.

Oda, E., R. Ohki, H. Murasawa, J. Nemoto, T. Shibue, T. Yamashita, T. Tokino, T. Taniguchi, and N. Tanaka. 2000. Noxa, a BH3-only member of the Bcl-2 family and candidate mediator of p53-induced apoptosis. *Science* 288(5468):1053-1058.

Ohi, R., T. Sapra, J. Howard, and T.J. Mitchison. 2004. Differentiation of cytoplasmic and meiotic spindle assembly MCAK functions by Aurora B-dependent phosphorylation. *Mol Biol Cell* 15(6):2895-2906.

Oltvai, Z.N., C.L. Milliman, and S.J. Korsmeyer. 1993. Bcl-2 heterodimerizes in vivo with a conserved homolog, Bax, that accelerates programmed cell death. *Cell* 74(4):609-619.

Oren, M. 2003. Decision making by p53: life, death and cancer. *Cell Death Differ* 10(4):431-442.

Osborne, C.K., K. Hobbs, and G.M. Clark. 1985. Effect of estrogens and antiestrogens on growth of human breast cancer cells in athymic nude mice. *Cancer Res* 45(2):584-590.

Ota, T., S. Suto, H. Katayama, Z.B. Han, F. Suzuki, M. Maeda, M. Tanino, Y. Terada, and M. Tatsuka. 2002. Increased mitotic phosphorylation of histone H3 attributable to AIM-1/Aurora-B overexpression contributes to chromosome number instability. *Cancer Res* 62(18):5168-5177.

Papoutsaki, M., F. Moretti, M. Lanza, B. Marinari, V. Sartorelli, L. Guerrini, S. Chimenti, M. Levrero, and A. Costanzo. 2005. A p38-dependent pathway regulates DeltaNp63 DNA binding to p53-dependent promoters in UV-induced apoptosis of keratinocytes. *Oncogene* 24(46):6970-6975.

Patturajan, M., S. Nomoto, M. Sommer, A. Fomenkov, K. Hibi, R. Zangen, N. Poliak, J. Califano, B. Trink, E. Ratovitski, and D. Sidransky. 2002. DeltaNp63 induces beta-catenin nuclear accumulation and signaling. *Cancer Cell* 1(4):369-379.

Petersen, J., and I.M. Hagan. 2003. S. pombe aurora kinase/survivin is required for chromosome condensation and the spindle checkpoint attachment response. *Curr Biol* 13(7):590-597.

Pinsky, B.A., C.V. Kotwaliwale, S.Y. Tatsutani, C.A. Breed, and S. Biggins. 2006. Glc7/protein phosphatase 1 regulatory subunits can oppose the

Ipl1/aurora protein kinase by redistributing Glc7. *Mol Cell Biol* 26(7):2648-2660.

Pouwels, J., A.M. Kukkonen, W. Lan, J.R. Daum, G.J. Gorbsky, T. Stukenberg, and M.J. Kallio. 2007. Shugoshin 1 plays a central role in kinetochore assembly and is required for kinetochore targeting of Plk1. *Cell Cycle* 6(13):1579-1585.

Qi, G., I. Ogawa, Y. Kudo, M. Miyauchi, B.S. Siriwardena, F. Shimamoto, M. Tatsuka, and T. Takata. 2007. Aurora-B expression and its correlation with cell proliferation and metastasis in oral cancer. *Virchows Arch* 450(3):297-302.

Rogers, E., J.D. Bishop, J.A. Waddle, J.M. Schumacher, and R. Lin. 2002. The aurora kinase AIR-2 functions in the release of chromosome cohesion in Caenorhabditis elegans meiosis. *J Cell Biol* 157(2):219-229.

Ruchaud, S., M. Carmena, and W.C. Earnshaw. 2007. Chromosomal passengers: conducting cell division. *Nat Rev Mol Cell Biol* 8(10):798-812.

Ruiz-Cortes, Z.T., S. Kimmins, L. Monaco, K.H. Burns, P. Sassone-Corsi, and B.D. Murphy. 2005. Estrogen mediates phosphorylation of histone H3 in ovarian follicle and mammary epithelial tumor cells via the mitotic kinase, Aurora B. *Mol Endocrinol* 19(12):2991-3000.

Sakaguchi, K., S. Saito, Y. Higashimoto, S. Roy, C.W. Anderson, and E. Appella. 2000. Damage-mediated phosphorylation of human p53 threonine 18 through a cascade mediated by a casein 1-like kinase. Effect on Mdm2 binding. *J Biol Chem* 275(13):9278-9283.

Sakamuro, D., P. Sabbatini, E. White, and G.C. Prendergast. 1997. The polyproline region of p53 is required to activate apoptosis but not growth arrest. *Oncogene* 15(8):887-898.

Sasai, K., H. Katayama, D.L. Stenoien, S. Fujii, R. Honda, M. Kimura, Y. Okano, M. Tatsuka, F. Suzuki, E.A. Nigg, W.C. Earnshaw, W.R. Brinkley, and S. Sen. 2004. Aurora-C kinase is a novel chromosomal passenger protein that can complement Aurora-B kinase function in mitotic cells. *Cell Motil Cytoskeleton* 59(4):249-263.

Satinover, D.L., D.L. Brautigan, and P.T. Stukenberg. 2006. Aurora-A kinase and inhibitor-2 regulate the cyclin threshold for mitotic entry in Xenopus early embryonic cell cycles. *Cell Cycle* 5(19):2268-2274.

Seki, A., J.A. Coppinger, C.Y. Jang, J.R. Yates, and G. Fang. 2008. Bora and the kinase Aurora a cooperatively activate the kinase Plk1 and control mitotic entry. *Science* 320(5883):1655-1658.

Sena-Esteves, M., Y. Saeki, S.M. Camp, E.A. Chiocca, and X.O. Breakefield. 1999. Single-step conversion of cells to retrovirus vector producers with

herpes simplex virus-Epstein-Barr virus hybrid amplicons. *J Virol* 73(12):10426-10439.

Sessa, F., M. Mapelli, C. Ciferri, C. Tarricone, L.B. Areces, T.R. Schneider, P.T. Stukenberg, and A. Musacchio. 2005. Mechanism of Aurora B activation by INCENP and inhibition by hesperadin. *Mol Cell* 18(3):379-391.

Shaulsky, G., N. Goldfinger, A. Ben-Ze'ev, and V. Rotter. 1990. Nuclear accumulation of p53 protein is mediated by several nuclear localization signals and plays a role in tumorigenesis. *Mol Cell Biol* 10(12):6565-6577.

Smith, S.L., N.L. Bowers, D.C. Betticher, O. Gautschi, D. Ratschiller, P.R. Hoban, R. Booton, M.F. Santibanez-Koref, and J. Heighway. 2005. Overexpression of aurora B kinase (AURKB) in primary non-small cell lung carcinoma is frequent, generally driven from one allele, and correlates with the level of genetic instability. *Br J Cancer* 93(6):719-729.

Sorrentino, R., S. Libertini, P.L. Pallante, G. Troncone, L. Palombini, V. Bavetsias, D. Spalletti-Cernia, P. Laccetti, S. Linardopoulos, P. Chieffi, A. Fusco, and G. Portella. 2005. Aurora B overexpression associates with the thyroid carcinoma undifferentiated phenotype and is required for thyroid carcinoma cell proliferation. *J Clin Endocrinol Metab* 90(2):928-935.

Soussi, T., and K.G. Wiman. 2007. Shaping genetic alterations in human cancer: the p53 mutation paradigm. *Cancer Cell* 12(4):303-312.

Stommel, J.M., N.D. Marchenko, G.S. Jimenez, U.M. Moll, T.J. Hope, and G.M. Wahl. 1999. A leucine-rich nuclear export signal in the p53 tetramerization domain: regulation of subcellular localization and p53 activity by NES masking. *Embo J* 18(6):1660-1672.

Stommel, J.M., and G.M. Wahl. 2004. Accelerated MDM2 auto-degradation induced by DNA-damage kinases is required for p53 activation. *Embo J* 23(7):1547-1556.

Sugarman, B.J., B.B. Aggarwal, P.E. Hass, I.S. Figari, M.A. Palladino, Jr., and H.M. Shepard. 1985. Recombinant human tumor necrosis factor-alpha: effects on proliferation of normal and transformed cells in vitro. *Science* 230(4728):943-945.

Sugiyama, K., K. Sugiura, T. Hara, K. Sugimoto, H. Shima, K. Honda, K. Furukawa, S. Yamashita, and T. Urano. 2002. Aurora-B associated protein phosphatases as negative regulators of kinase activation. *Oncogene* 21(20):3103-3111.

Sun, L., J. Gao, X. Dong, M. Liu, D. Li, X. Shi, J.T. Dong, X. Lu, C. Liu, and J. Zhou. 2008. EB1 promotes Aurora-B kinase activity through blocking its inactivation by protein phosphatase 2A. *Proc Natl Acad Sci U S A* 105(20):7153-7158.

Tan, M., S. Li, M. Swaroop, K. Guan, L.W. Oberley, and Y. Sun. 1999. Transcriptional activation of the human glutathione peroxidase promoter by p53. *J Biol Chem* 274(17):12061-12066.

Tan, T., and G. Chu. 2002. p53 Binds and activates the xeroderma pigmentosum DDB2 gene in humans but not mice. *Mol Cell Biol* 22(10):3247-3254.

Tanaka, T., M. Kimura, K. Matsunaga, D. Fukada, H. Mori, and Y. Okano. 1999. Centrosomal kinase AIK1 is overexpressed in invasive ductal carcinoma of the breast. *Cancer Res* 59(9):2041-2044.

Tanaka, T.U., N. Rachidi, C. Janke, G. Pereira, M. Galova, E. Schiebel, M.J. Stark, and K. Nasmyth. 2002. Evidence that the Ipl1-Sli15 (Aurora kinase-INCENP) complex promotes chromosome bi-orientation by altering kinetochore-spindle pole connections. *Cell* 108(3):317-329.

Tang, J.Y., B.J. Hwang, J.M. Ford, P.C. Hanawalt, and G. Chu. 2000. Xeroderma pigmentosum p48 gene enhances global genomic repair and suppresses UV-induced mutagenesis. *Mol Cell* 5(4):737-744.

Tao, Y., P. Zhang, F. Girdler, V. Frascogna, M. Castedo, J. Bourhis, G. Kroemer, and E. Deutsch. 2008. Enhancement of radiation response in p53-deficient cancer cells by the Aurora-B kinase inhibitor AZD1152. *Oncogene* 27:3244-3255.

Tatsuka, M., H. Katayama, T. Ota, T. Tanaka, S. Odashima, F. Suzuki, and Y. Terada. 1998. Multinuclearity and increased ploidy caused by overexpression of the aurora- and Ipl1-like midbody-associated protein mitotic kinase in human cancer cells. *Cancer Res* 58(21):4811-4816.

Tchatchou, S., M. Wirtenberger, K. Hemminki, C. Sutter, A. Meindl, B. Wappenschmidt, M. Kiechle, P. Bugert, R.K. Schmutzler, C.R. Bartram, and B. Burwinkel. 2007. Aurora kinases A and B and familial breast cancer risk. *Cancer Lett* 247(2):266-272.

Terada, Y., M. Tatsuka, F. Suzuki, Y. Yasuda, S. Fujita, and M. Otsu. 1998. AIM-1: a mammalian midbody-associated protein required for cytokinesis. *Embo J* 17(3):667-676.

Tritarelli, A., E. Oricchio, M. Ciciarello, R. Mangiacasale, A. Palena, P. Lavia, S. Soddu, and E. Cundari. 2004. p53 localization at centrosomes during mitosis and postmitotic checkpoint are ATM-dependent and require serine 15 phosphorylation. *Mol Biol Cell* 15(8):3751-3757.

Uren, A.G., L. Wong, M. Pakusch, K.J. Fowler, F.J. Burrows, D.L. Vaux, and K.H. Choo. 2000. Survivin and the inner centromere protein INCENP show similar cell-cycle localization and gene knockout phenotype. *Curr Biol* 10(21):1319-1328.

Vader, G., and S.M. Lens. 2008. The Aurora kinase family in cell division and cancer. *Biochim Biophys Acta* 1786(1):60-72.

Vagnarelli, P., and W.C. Earnshaw. 2004. Chromosomal passengers: the four-dimensional regulation of mitotic events. *Chromosoma* 113(5):211-222.

Vas, A.C., and D.J. Clarke. 2008. Aurora B kinases restrict chromosome decondensation to telophase of mitosis. *Cell Cycle* 7(3):293-296.

Vigneron, S., S. Prieto, C. Bernis, J.C. Labbe, A. Castro, and T. Lorca. 2004. Kinetochore localization of spindle checkpoint proteins: who controls whom? *Mol Biol Cell* 15(10):4584-4596.

Vousden, K.H., and C. Prives. 2009. Blinded by the Light: The Growing Complexity of p53. *Cell* 137(3):413-431.

Wadsworth, P. 2005. Cytokinesis: Rho marks the spot. *Curr Biol* 15(21):R871-874.

Walker, K.K., and A.J. Levine. 1996. Identification of a novel p53 functional domain that is necessary for efficient growth suppression. *Proc Natl Acad Sci U S A* 93(26):15335-15340.

Wang, L.H., X.Y. Yang, X. Zhang, K. Mihalic, Y.X. Fan, W. Xiao, O.M. Howard, E. Appella, A.T. Maynard, and W.L. Farrar. 2004. Suppression of breast cancer by chemical modulation of vulnerable zinc fingers in estrogen receptor. *Nat Med* 10(1):40-47.

Wang, P., J. Yu, and L. Zhang. 2007. The nuclear function of p53 is required for PUMA-mediated apoptosis induced by DNA damage. *Proc Natl Acad Sci U S A* 104(10):4054-4059.

Wang, X., Y.X. Zhou, W. Qiao, Y. Tominaga, M. Ouchi, T. Ouchi, and C.X. Deng. 2006. Overexpression of aurora kinase A in mouse mammary epithelium induces genetic instability preceding mammary tumor formation. *Oncogene* 25(54):7148-7158.

Warburton, C., W.H. Dragowska, K. Gelmon, S. Chia, H. Yan, D. Masin, T. Denyssevych, A.E. Wallis, and M.B. Bally. 2004. Treatment of HER-2/neu overexpressing breast cancer xenograft models with trastuzumab (Herceptin) and gefitinib (ZD1839): drug combination effects on tumor growth, HER-2/neu and epidermal growth factor receptor expression, and viable hypoxic cell fraction. *Clin Cancer Res* 10(7):2512-2524.

Wei, C.L., Q. Wu, V.B. Vega, K.P. Chiu, P. Ng, T. Zhang, A. Shahab, H.C. Yong, Y. Fu, Z. Weng, J. Liu, X.D. Zhao, J.L. Chew, Y.L. Lee, V.A. Kuznetsov, W.K. Sung, L.D. Miller, B. Lim, E.T. Liu, Q. Yu, H.H. Ng, and Y. Ruan. 2006. A global map of p53 transcription-factor binding sites in the human genome. *Cell* 124(1):207-219.

Wei, Y., L. Yu, J. Bowen, M.A. Gorovsky, and C.D. Allis. 1999. Phosphorylation of histone H3 is required for proper chromosome condensation and segregation. *Cell* 97(1):99-109.

Weinberg, R.L., S.M. Freund, D.B. Veprintsev, M. Bycroft, and A.R. Fersht. 2004. Regulation of DNA binding of p53 by its C-terminal domain. *J Mol Biol* 342(3):801-811.

Wheatley, S.P., A. Carvalho, P. Vagnarelli, and W.C. Earnshaw. 2001. INCENP is required for proper targeting of Survivin to the centromeres and the anaphase spindle during mitosis. *Curr Biol* 11(11):886-890.

Wheatley, S.P., A.J. Henzing, H. Dodson, W. Khaled, and W.C. Earnshaw. 2004. Aurora-B phosphorylation in vitro identifies a residue of survivin that is essential for its localization and binding to inner centromere protein (INCENP) in vivo. *J Biol Chem* 279(7):5655-5660.

Wilkinson, R.W., R. Odedra, S.P. Heaton, S.R. Wedge, N.J. Keen, C. Crafter, J.R. Foster, M.C. Brady, A. Bigley, E. Brown, K.F. Byth, N.C. Barrass, K.E. Mundt, K.M. Foote, N.M. Heron, F.H. Jung, A.A. Mortlock, F.T. Boyle, and S. Green. 2007. AZD1152, a selective inhibitor of Aurora B kinase, inhibits human tumor xenograft growth by inducing apoptosis. *Clin Cancer Res* 13(12):3682-3688.

Wu, M., G.K. Arimura, and A.A. Yunis. 1977. Purification and characterization of a plasminogen activator secreted by cultured human pancreatic carcinoma cells. *Biochemistry* 16(9):1908-1913.

Yang, A., M. Kaghad, D. Caput, and F. McKeon. 2002. On the shoulders of giants: p63, p73 and the rise of p53. *Trends Genet* 18(2):90-95.

Yang, J., T. Ikezoe, C. Nishioka, T. Tasaka, A. Taniguchi, Y. Kuwayama, N. Komatsu, K. Bandobashi, K. Togitani, H.P. Koeffler, H. Taguchi, and A. Yokoyama. 2007. AZD1152, a novel and selective aurora B kinase inhibitor, induces growth arrest, apoptosis, and sensitization for tubulin depolymerizing agent or topoisomerase II inhibitor in human acute leukemia cells in vitro and in vivo. *Blood* 110(6):2034-2040.

Yu, J., Z. Wang, K.W. Kinzler, B. Vogelstein, and L. Zhang. 2003. PUMA mediates the apoptotic response to p53 in colorectal cancer cells. *Proc Natl Acad Sci U S A* 100(4):1931-1936.

Yuan, Z.M., H. Shioya, T. Ishiko, X. Sun, J. Gu, Y.Y. Huang, H. Lu, S. Kharbanda, R. Weichselbaum, and D. Kufe. 1999. p73 is regulated by tyrosine kinase c-Abl in the apoptotic response to DNA damage. *Nature* 399(6738):814-817.

Zachos, G., E.J. Black, M. Walker, M.T. Scott, P. Vagnarelli, W.C. Earnshaw, and D.A. Gillespie. 2007. Chk1 is required for spindle checkpoint function. *Dev Cell* 12(2):247-260.

Zeitlin, S.G., C.M. Barber, C.D. Allis, and K.F. Sullivan. 2001a. Differential regulation of CENP-A and histone H3 phosphorylation in G2/M. *J Cell Sci* 114(Pt 4):653-661.

Zeitlin, S.G., R.D. Shelby, and K.F. Sullivan. 2001b. CENP-A is phosphorylated by Aurora B kinase and plays an unexpected role in completion of cytokinesis. *J Cell Biol* 155(7):1147-1157.

Zhou, H., J. Kuang, L. Zhong, W.L. Kuo, J.W. Gray, A. Sahin, B.R. Brinkley, and S. Sen. 1998. Tumour amplified kinase STK15/BTAK induces centrosome amplification, aneuploidy and transformation. *Nat Genet* 20(2):189-193.

Zhu, J., J. Jiang, W. Zhou, K. Zhu, and X. Chen. 1999. Differential regulation of cellular target genes by p53 devoid of the PXXP motifs with impaired apoptotic activity. *Oncogene* 18(12):2149-2155.

Chapter 7. Vita

Christopher Patrick Gully was born in Salisbury, Maryland on August 25th, 1969, the son of Frank E. and Margaret L. Gully. Upon graduating from Delmar, High School in Delmar, Delaware (1987), he entered the Henson School of Science at Salisbury University and earned a Bachelor of Science with a major in Biology and a minor in Chemistry (1992). In August 2003, he enrolled in the Zanvyl Krieger School of Arts and Sciences at Johns Hopkins University and graduated with a Master of Science degree in Biotechnology and a concentration in Bioinformatics (2006). In September of 2006 he enrolled in The University of Texas Health Science Center, Graduate School of Biomedical Sciences, where he conducted his doctoral studies under the guidance of Dr. Mong-Hong Ph.D., Department of Molecular and Cellular Oncology, The University of Texas MD Anderson Cancer Center. He was awarded the degree of Doctor of Philosophy in May 2011.

Publications:

Gully C., E. Fuentes-Mattei, J.H. Shin, G. Velazquez-Torres, C. Carlock, E. Wang, D. Rothenberg, J. Chen, S. Guma, HH. Choi, CH. Su, B. Chou, F. Zhang, H. Adams, S.C. Yeung, M.H. Lee. Mitotic kinase Aurora B regulates p53 by direct phosphorylation of the DNA binding domain. *Submitted.*

Gully C., F. Zhang, J. Chen, J.A. yeung, G. Velazquez-Torres, e. Wang, S.C. Yeung, and M.H. Lee. 2010. Antineoplastic effects of an Aurora B kinase inhibitor in breast cancer. *Mol Cancer* (9):42.